



Eidgenössische Technische Hochschule Zürich  
Swiss Federal Institute of Technology Zurich



Swiss Federal Institute for Forest,  
Snow and Landscape Research WSL

Department of  
Environmental Systems Science  
ETH Zürich

Research Unit  
Biodiversity and Conservation Biology  
WSL Birmensdorf

Master thesis

# **Challenging the predictive power of flight corridor models for bats**

**Tina Meier**

12-474-771

28<sup>th</sup> October 2019

Supervisor: Prof. Dr. Rolf Holderegger, WSL, ETH

Supervisor: Dr. Martin K. Obrist, WSL

Co-Supervisor: Dr. Klaus Ecker, WSL

## ABSTRACT

Increasing human pressure on landscapes and natural environments in the last century led to severe alterations of habitats and to a decline of many native species. Bats are among the most affected species of this development. In summer, females of Greater mouse-eared bats (*Myotis myotis*) and Lesser horseshoe bats (*Rhinolophus hipposideros*) form maternity roosts under roofs of churches, barns or large houses within settlements. For foraging, they commute to forests presumably following a commuting corridor. To predict these corridors, a numeric model based on circuit-theory was established at WSL (Swiss Federal Institute for Forest, Snow and Landscape Research). Three slightly different versions of this model were delivered to be compared: *current\_advanced*, *current\_subaverag* and *current\_submaximum*. To test the quality of these models, predicted corridors were compared to experimentally measured bat activity at 18 roost locations in Switzerland (9 *M. myotis* roosts and 9 *R. hipposideros* roosts). 16 Batloggers devices were installed around a roost (maximum distance to the roost 777 m), recording bat activity for one night. 8 sampling sites were situated within a predicted corridor and 8 were away from corridors as control sites. Since artificial light is assumed to have a negative impact on bat activity, but prior attempts to include a light variable into the model failed, we manually measured illuminance (Lux-values) at every sampling site. For statistical analysis, we implemented a generalized linear mixed-effects model (GLMM) to determine the influence of variables of interest on bat activity, while simultaneously taking random effects into account.

We demonstrated highly significant negative effects of artificial light on commuting activity of both species examined. The Lux estimate value of the best performing model for *M. myotis* is -0.398, while the value for *R. hipposideros* is -15.829. Furthermore, comparison of the ratio of bat activity at dark and lit sites indicates that *R. hipposideros* is more sensitive to light than *M. myotis*.

Reliability of the predictive corridor models could not be proven satisfyingly. For *M. myotis* there was no significant effect of the commuting corridor model on bat activity. However, the *R. hipposideros* model including the numeric corridor model of “*current\_adv*” performed best and showed positive correlation with measured bat activity. Yet, in all analyses the other variables examined showed considerably higher effect on bat activity than the predictive corridor model, in particular the variable of light. Further adaption of the predictive commuting corridor model should therefore concentrate on the inclusion of the light variable.

**Keywords:** Chiroptera, habitat modelling, commuting corridors, *Myotis myotis*, *Rhinolophus hipposideros*, echolocation, light disturbance, generalized linear mixed modelling

---

## TABLE OF CONTENTS

LIST OF TABLES	
LIST OF FIGURES	
LIST OF ABBREVIATIONS	
INTRODUCTION.....	1
MATERIAL AND METHODS .....	3
Study species .....	3
Study sites .....	4
Study period .....	5
Predictive corridor models .....	6
Data collection – field work .....	11
Analysis of the recordings.....	12
Selection of explanatory variables.....	13
Statistical Analysis .....	15
RESULTS.....	18
Acoustic recordings & bat activity.....	18
Differences in bat activity at corridor and control sites.....	21
Light measurements .....	21
Deriving a best performing model for each species.....	22
DISCUSSION.....	28
Impact of artificial light on bat activity.....	28
Finding the best performing model.....	29
CONCLUSION .....	33
ACKNOWLEDGEMENT .....	34
REFERENCES.....	35
APPENDIX.....	39

---

## LIST OF TABLES

Table 1: Recording date of all sampled roost as well as its roost size according to the latest count. ....	6
Table 2: Available GIS data sets for every roost. All roosts were numbered whereby <i>M. myotis</i> roosts had number from 101 to 117 and <i>R. hipposideros</i> roosts 1001 to 1014. ....	7
Table 3: All explanatory variables tested statistically on their impact on bat activity. ....	14
Table 4: GIS model variable in fixed effects is Adv15, Subavg15 or Submax15. Insignificant effects were determined using a <i>glm</i> , and therefore dropped from the list of random effects. *There was no precipitation during any measurement of <i>R. hipposideros</i> site, thus <i>glm</i> generated no output for this variable. ....	16
Table 5: Start and end times of the ‘fly-out’ time slots defined for every study site individually. Total activity was measured throughout the whole night, but for analysing commuting activity towards foraging areas, only recorded activity within the ‘fly-out’ period was relevant. Percentage of activity within the time slot was generally higher for <i>M. myotis</i> than for <i>R. hipposideros</i> sites. ....	1
Table 6: The number of bat passes is significantly higher at corridor sites than at control sites for both species. ....	21
Table 7: There were considerably more dark than lit sampling sites and bat activity was significantly higher at dark sites for both species. The apparent difference in the dark/lit ratio between the two species indicates higher sensitivity to light of <i>R. hipposideros</i> than <i>M. myotis</i> . ....	22
Table 8: The three best performing models for <i>M. myotis</i> analysis with current density values of the GIS model Adv15 included. ....	22
Table 9: The three best performing models for <i>M. myotis</i> analysis with current density values of the GIS model Subavg15 included. ....	24
Table 10: The three best performing models for <i>M. myotis</i> analysis with current density values of the GIS model Submax15 included. ....	25
Table 11: The three best performing models for <i>R. hipposideros</i> data with current density values of the GIS model Adv15. ....	26
Table 12: The three best performing models for <i>R. hipposideros</i> data with current density values of the GIS model Sumavg15. ....	26
Table 13: The three best performing models for <i>R. hipposideros</i> data with current density values of the GIS model Submax15. ....	27
Table 14: Full data table .....	
Table 15: Filter queries applied to verify <i>M. myotis</i> calls .....	
Table 16: Full model ranking list for <i>M. myotis</i> data with Adv15 variable included. ....	
Table 17: Full model ranking list for <i>M. myotis</i> data with Subavg15 variable included. ....	
Table 18: Full model ranking list of <i>M. myotis</i> data with Submax15 variable included. ....	
Table 19: Full model ranking list of <i>R. hipposideros</i> data with Adv15 variable included. ....	
Table 20: Full model ranking list of <i>R. hipposideros</i> data with Subavg15 variable included. ....	
Table 21: Full model ranking list of <i>R. hipposideros</i> data with Submax15 variable included. ....	

---

## LIST OF FIGURES

Figure 1: Study sites of <i>M. myotis</i> concentrate on northern Switzerland, while sampled sites for <i>R. hipposideros</i> are located in pre alpine communities. Roosts of Surcasti and Uors are situated very close to each other (660 m) and therefore, appear as one icon on the map. ....	5
Figure 2: Every sampling category was recorded four times at every study site. ....	8
Figure 3: Model predicted commuting corridors for the roost of Beggingen. High current values (yellow to red) predict strong use of the area as corridor by <i>M. myotis</i> . ....	9
Figure 4: Sampling sites were chosen while the corridor data set of current_adv was overlaying the aerial photo. Sampling sites within corridors are marked as triangles and control sites as circles. Black icons mark dark places and yellow ones indicate artificially lit sampling sites. ....	10
Figure 5: Example of recording station during the test run at the WSL pond on 10.05.2019. The microphone is attached to a plastic post, the Batlogger is in the plastic box on the ground. ....	11
Figure 6: Total bat activity at 16 recording sites around the roost of Kallnach with peak of flying out activity between 22:10 and 22:30. The two red lines represent start and end time of the chosen 'fly-out' time slot. ....	18
Figure 7: Analysis of <i>M. myotis</i> data including current density values of the GIS model current_adv show negative impacts of all explanatory variables on bat activity. Estimate values: Dist_LCP = -0.417; Lux = -0.398; Dist_Roost = -0.209; Adv15 = -0.025. ....	23
Figure 8: Analysis of <i>M. myotis</i> data including current density values of the GIS model current_subavg show negative impacts of all explanatory variables on bat activity. Estimate values: Dist_LCP = -0.414; Lux = -0.397; Dist_Roost = -0.208; Subavg15 = -0.017. ....	24
Figure 9: Analysis of <i>M. myotis</i> data including current density values of the GIS model current_submax show negative impacts of all explanatory variables on bat activity. Estimate values: Dist_LCP = -0.415; Lux = -0.397; Dist_Roost = -0.206; Submax15 = -0.019. ....	25
Figure 10: Setting of the Batlogger M for bat activity recording. ....	
Figure 11: Correlation coefficient matrix of explanatory variables for <i>M. myotis</i> . ....	
Figure 12: Correlation coefficient matrix of explanatory variables for <i>R. hipposideros</i> . ....	
Figure 13: Distribution of total activity of <i>M. myotis</i> at all <i>M. myotis</i> study sites. ....	
Figure 14: Distribution of total activity of <i>R. hipposideros</i> at all <i>R. hipposideros</i> study sites. ....	
Figure 15: Distribution of total activity of <i>M. myotis</i> in Embrach during the first recording. Start and end time of 'fly-out' period in red. ....	
Figure 16: Distribution of total activity of <i>M. myotis</i> in Embrach. Start and end time of 'fly-out' period in red. ....	
Figure 17: Distribution of total activity of <i>M. myotis</i> in Lipperswil. Start and end time of 'fly-out' period in red. ....	
Figure 18: Distribution of total activity of <i>M. myotis</i> in Flawil during the first recording. Start and end time of 'fly-out' period in red. ....	
Figure 19: Distribution of total activity of <i>M. myotis</i> in Buochs. Start and end time of 'fly-out' period in red. ....	

---

Figure 20: Distribution of total activity of *M. myotis* in Buttisholz. Start and end time of 'fly-out' period in red. ....

Figure 21: Distribution of total activity of *M. myotis* in Kallnach. Start and end time of 'fly-out' period in red. ....

Figure 22: Distribution of total activity of *M. myotis* in Beggingen. Start and end time of 'fly-out' period in red. ....

Figure 23: Distribution of total activity of *M. myotis* in Wegenstetten. Start and end time of 'fly-out' period in red. ....

Figure 24: Distribution of total activity of *M. myotis* in Embrach during the second recording. Start and end time of 'fly-out' period in red. ....

Figure 25: Distribution of total activity of *M. myotis* in Flawil during the second recording. Start and end time of 'fly-out' period in red. ....

Figure 26: Distribution of total activity of *R. hipposideros* in Blumenstein. Start and end time of 'fly-out' period in red. ....

Figure 27: Distribution of total activity of *R. hipposideros* in Amsoldingen. Start and end time of 'fly-out' period in red. ....

Figure 28: Distribution of total activity of *R. hipposideros* in Därstetten. Start and end time of 'fly-out' period in red. ....

Figure 29: Distribution of total activity of *R. hipposideros* in Sachseln. Start and end time of 'fly-out' period in red. ....

Figure 30: Distribution of total activity of *R. hipposideros* in Giswil. Start and end time of 'fly-out' period in red. ....

Figure 31: Distribution of total activity of *R. hipposideros* in Castiel. Start and end time of 'fly-out' period in red. ....

Figure 32: Distribution of total activity of *R. hipposideros* in Waltensburg. Start and end time of 'fly-out' period in red. ....

Figure 33: Distribution of total activity of *R. hipposideros* in Uors. Start and end time of 'fly-out' period in red. ....

Figure 34: Distribution of total activity of *R. hipposideros* in Surcasti. Start and end time of 'fly-out' period in red. ....

---

## LIST OF ABBREVIATIONS

BAFU	= Bundesamt für Umwelt =Federal Office for the Environment (FOEN)
FOEN	= Federal Office for the Environment
GIS	= Geographic Information System
GLMM	= Generalized linear mixed-effects model
LCP	= Least Cost Path
<i>M. myotis</i>	= <i>Myotis myotis</i> = Greater mouse-eared bat
<i>MMY</i>	= <i>Myotis myotis</i>
<i>R. hipposideros</i>	= <i>Rhinolophus hipposideros</i> = Lesser horseshoe bat
SSF	= Stiftung zum Schutze unserer Fledermäuse in der Schweiz = Foundati- on for the Protection of Swiss bats
SWILD	= Name of local Urban Ecology & Wildlife Research Organisation
WSL	= Swiss Federal Institute for Forest, Snow and Landscape Research

## INTRODUCTION

Increasing human pressure on landscapes and natural environments in the last century led to a worldwide loss of habitat, which emerged to one of the most important issues within wildlife protection in recent decades. One factor for the reduction of habitat areas is direct conversion of natural habitats into settlements and industrially used areas. Besides this, altered landscape composition, as well as fragmentation of habitats, and consequently reduced connectivity of the remaining patches, worsened the situation of wildlife further (EFA, 2011; Grimm et al., 2008; Stoate et al., 2001). Switzerland's landscape is no exception in this development. Settlement expansion, intensification of agriculture and changed silvicultural practices led to a decline of many native species and made them appear on the Red List of Switzerland (Bundesamt für Umwelt, 2016).

Bats are among these endangered species (Bohnenstengel et al., 2014) and they are particularly sensitive to the above-mentioned land-use changes. Many bat species live in close vicinity of humans as they form maternity roosts under roofs of churches, barns or large houses (Güttinger, 1994; Drescher, 2004; Berkova et al., 2014). These roosting sites are in most cases protected by Swiss legislation (NHG – Natur- und Heimatschutzgesetz). For foraging some native species fly into forests and to forest edges daily. While those foraging areas are protected by the Federal Act on Forest (WaG - Waldgesetz), the flight paths in between these two habitats remain highly exposed to changes in urban and rural areas. Close to the roost within settlement areas bats face constraints due to artificial light. Several studies reported negative effects of the increasing level of artificially lighted areas on various bat species, such as different time of the fly-out and avoidance of light (Stone et al., 2012; Downs et al., 2003; Stone et al., 2009). Outside the settlement areas bats frequently have to pass agriculturally managed land, which has been altered as mentioned above, and therefore are not suitable for bats' echolocation orientation anymore. The actual flight paths of bats, commonly referred to as commuting corridors, are mostly unknown. This, although their existence has been discussed for a long time (Limpens & Kapteyn, 1991; Walsh & Harris, 1996). In fact, there is still a lack of knowledge about where these corridors effectively are, how to assess them, and how strongly bats depend on linear structures within their commuting corridors.

Protection of habitats is a major goal of conservation strategies, therefore these habitats must be known in the first place. For this purpose, Ravessoud (2017) established a numeric corridor model at WSL (Swiss Federal Institute for Forest, Snow and Landscape Research). Based on LIDAR data and the application of GIS-Software, commuting flyways of two native species (*Myotis myotis* and *Rhinolophus hipposideros*) can be predicted and made visible.

There is considerable demand for this predictive model by bat conservationists and landscape planners. The model contributes to a better understanding of commuting flyways of bats and it may help to evaluate areas in need of (further) species-specific conservation measures. In addition, it might also become an important tool in urban planning processes, e.g. street lighting regimes. Before going public and applying the model to all known roosts of *M. myotis* and *R. hipposideros* in Switzerland verification of the model's predictions needs to be done.

Therefore, the modelled outcomes were compared to empirically recorded bat activity on 18 locations (9 roosts *M. myotis* & 9 roosts *R. hipposideros*) throughout northern Switzerland. Furthermore, illuminance was measured at every recording site and incorporated in the generalized linear mixed model (GLMM) used for evaluation. Moreover, variables such as the weather, roost size, recording date or distance of the sampling site to its nearest Least Cost Path were taken into account. Lower bat activity was expected at sampling sites not lying within a predicted commuting corridor, e.g. with a low calculated corridor value, and at sites with high artificial light intensity. The overall aims of this master thesis were to A) test the output of the GIS-based corridor model developed by Ravessoud (2017) by comparing them to experimentally recorded bat activity; and B) assess the impact of artificial light on the flight activity of the two examined bat species.

## MATERIAL AND METHODS

### Study species

In the study of Ravessoud (2017) the selection of the two species, for which the model is developed, is justified by three criteria: A) species must be an evidential commuting species (spatially separated roost and foraging area); B) distribution and foraging areas should be well known, and C) local knowledge, such as current status of the roost should be available. These criteria qualify the two native species of Greater mouse-eared bat *Myotis myotis* and Lesser horseshoe bat *Rhinolophus hipposideros*.

*Myotis myotis* typically establishes nursery colonies under roofs of churches, barns or large houses within settlements (Güttinger, 1994; Drescher, 2004; Berkova et al., 2014), and hunts in and near deciduous forests, above freshly mown meadows, and in orchards (Güttinger, 1997; Zahn et al., 2005; Drescher, 2004). The main food sources for *M. myotis* are species of the order Coleoptera, with ground beetles (Carabidae) accounting for most of it (Graclik & Wasielewski, 2012; Steck & Güttinger, 2006). Greater mouse-eared bats are assumed to be dependent on structures, but also to be capable of passing open land for some distance. Arlettaz (1996) ascertained an average commuting distance of *M. myotis* of  $8.5 \pm 7$  km. The local commuting flyways are mostly unknown, although at some roosts attempts were made to follow out-flying individuals by foot to find out about their routes (Lea Morf, Bat Protection Responsible, pers. communication). *M. myotis* currently holds the status of a vulnerable bat species in the Swiss red list of bats (Bohnenstengel et al., 2004). At the same time, it is considered a species of highest priority (Bundesamt für Umwelt, 2011).

*Rhinolophus hipposideros* roosts are found in church attics of the nave and in undisturbed attics of old houses. For foraging they usually commute to light broadleaf forests in close vicinity. Bontadina et al. (2002) reported commuting distances of 600 meters as most common for foraging activity (max. 2.4 km), while Holzhaider et al. (2002) measured an average commuting distance of 2.4 km (max. 3.6 km). There is strong evidence that this species is highly dependent on vertical structural elements such as hedgerows to navigate from nursing place to feeding place (Motte & Libois, 2002). Furthermore, there is substantial proof that Lesser horseshoe bats react negatively on artificial light. A study by Stone, Jones & Harris (2012) showed that the activity of Lesser horseshoe bats was significantly lower along lit hedges than along unlit ones. Moreover, bats became active significantly later on nights when hedges were illuminated. Lesser horseshoe bats hunt for soft, slow and low-flying insects such as moths and flies (Diptera) (Beck et al, 1989). In the second half of 20<sup>th</sup> century there has been recorded an immense decline in number of *R. hipposideros* individuals and roosts (Bontadina et al., 2006), mainly due to the destruction of nursing sites by renovations

and the usage of toxic timber preservatives (Stebbing R.E. & Griffith F., 1986; Carravieri & Scheifler, 2013). *R. hipposideros* is on the Swiss red list of bats as an endangered species (Bohnenstengel et al. 2014), although their number has increased slowly but steadily in recent years (SSF - Stiftung zu Schutze unserer Fledermäuse in der Schweiz, Zürich, 2019). The Federal Office for Environment (FOEN) treats them as a species of national priority (Bundesamt für Umwelt BAFU, 2011).

### Study sites

For each of the two species 9 suitable study sites were chosen. We focused our study on the northern part of Switzerland according their distribution range: precisely, the Swiss Central Plain and Prealps for *M. myotis*, and Prealps and eastern central Alps for *R. hipposideros*. Southern and western Switzerland was excluded due to missing suitable roosts or logistic reasons.

The criteria for choosing a roost were as followed: A) foraging area is not directly connected to roost, so that bats have to commute at least 60 meters; B) latest counts showed at least 100 individuals living in the roosts (except two roosts of *R. hipposideros* only count 60 individuals, see table 1) and C) the area within 500 meter around the roost is safe and easy to access (neither steep nor loose debris). Most roosts were located within settlements which were situated in an intensively cultivated rural landscape. The studied roosts were selected in coordination with SSF (Foundation for the Protection of Swiss bats). The 18 study sites are shown in figure 1.

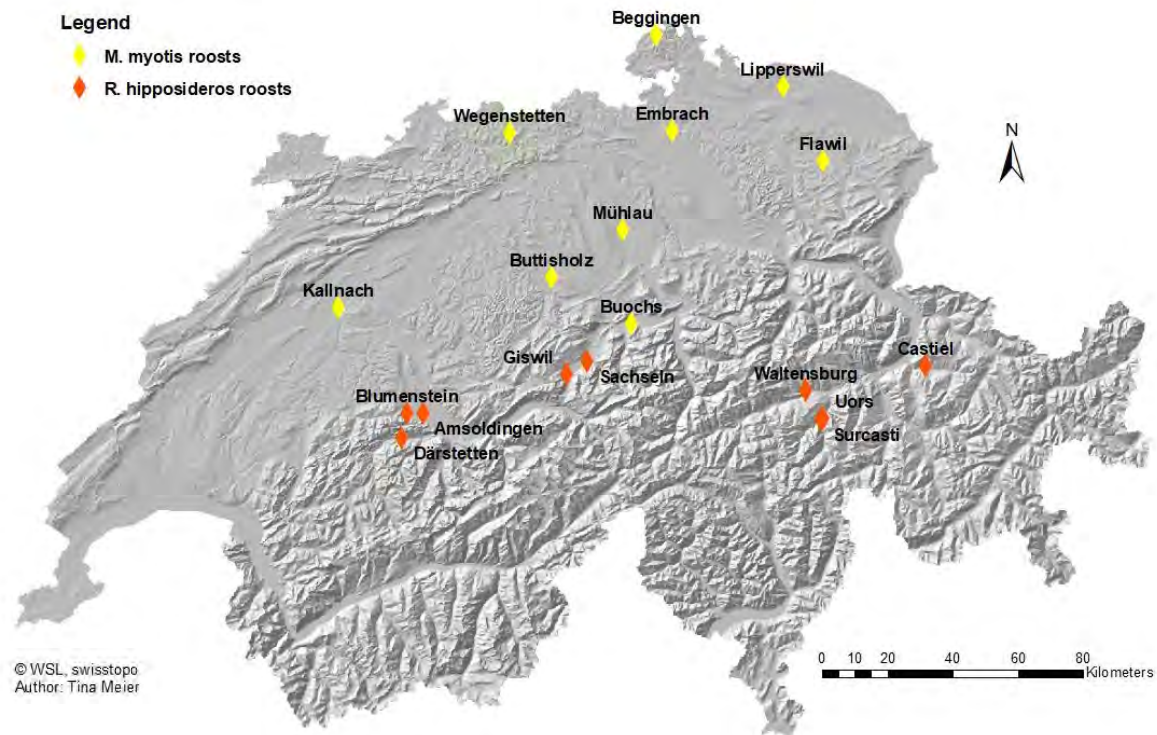


**Figure 1: Study sites of *M. myotis* concentrate on northern Switzerland, while sampled sites for *R. hipposideros* are located in pre alpine communities. Roosts of Surcasti and Uors are situated very close to each other (660 m) and therefore, appear as one icon on the map.**

### Study period

Bats move to their nursery roosts in spring. They give birth to one young, which they lactate for about 6 weeks before it flies out and goes hunting itself. It is assumed that juveniles explore the surrounding on their first fly-outs and gradually adapt to the established flight corridors of the adults. As this study is only interested in the established and frequently used flight corridors, we wanted to have our field survey finished before the juveniles fly out for hunting. Recordings of juveniles on exploration would falsify our detection of commuting corridors. Each roost was sampled one night only. We assumed that the studied species use the same flyways every night and thus, recordings during one night with favourable conditions yielding reliable data. Nights with unfavourable conditions like rain, temperatures below 7 ° C, strong wind and full moon (+/-1 night) were avoided.

May 2019 was unusually cold and wet. Local Bat Protection Responsible informed us, that the inhabitants of our chosen roosts have not yet appeared at the expected time of moving into their summer roosts. In fact, there was a general delay of about 3 weeks in moving into their roosts and gestation of Greater mouse-eared bats and Lesser horseshoe bats throughout Switzerland. A recent study of Linton & Macdonald (2018) found that spring weather con-

ditions indeed influence breeding phenology of bat populations. Hence, our sampling period had to be rescheduled. The first acoustic sampling took place on May 25<sup>th</sup> in Embrach ZH, the last on July 20<sup>th</sup> in Flawil SG. The recording dates of all roost sites are disclosed in table 1. Two measurements had to be retaken: 1) Embrach (25.05.2019), because the small number of recorded *M. myotis* on May 25<sup>th</sup> indicated that not all inhabitants of the roost had yet moved in; and 2) Flawil, where we were caught by an unexpected strong summer thunderstorm on June 19<sup>th</sup> 2019 (11.6 mm precipitation between 21.00h and 22.00h).

**Table 1: Recording date of all sampled roost as well as its roost size according to the latest count.**

Species	Roost	1 <sup>st</sup> Recording	2 <sup>nd</sup> Recording	Roost size	Last count
<i>M. myotis</i>	Embrach	25.05.2019	17.07.2019	298	2016
	Mühlau	06.06.2019		528	2019
	Lipperswil	18.06.2019		186	2016
	Flawil	19.06.2019	20.07.2019	275	2016
	Buochs	04.07.2019		230	2016
	Buttisholz	05.07.2019		569	2016
	Kallnach	09.07.2019		411	2012
	Beggingen	11.07.2019		630	2019
	Wegenstetten	16.07.2019		200	2019
	Blumenstein	30.05.2019		200	2019
<i>R. hipposideros</i>	Amsoldingen	31.05.2019		60	2009
	Därstetten	01.06.2019		110	2009
	Sachseln	12.06.2019		120	2016
	Giswil	13.06.2019		400	2017
	Castiel	24.06.2019		67	2017
	Waltensburg	25.06.2019		105	2017
	Uors	26.06.2019		234	2017
	Surcasti	27.06.2019		202	2017

### Predictive corridor models

In his study, Ravessoud (2017) performed an automatic model selection (LASSO – Least Absolute Shrinkage and Selection Operator) to obtain only the variables with the strongest impact on the response variable. Model selection involved cross-validation using training and testing sets. This way he was able to reduce the former number of 96 variables of the *M. myotis* model to 11 variables, and for the *R. hipposideros* model the variables were diminished from 90 to 7 relevant variables. These variables account for soft ground cover, trees, structures, terrain ruggedness, structure ruggedness and canopy ruggedness.

The appropriate set of variables was applied on our roosts of interest (*M. myotis* resp. *R. hipposideros*) within a frame of 5 x 5 km with a spatial resolution of 5 m<sup>2</sup>. This resulted in a

Habitat Suitability Map (HSM) which in the next step was transformed into a cost matrix (resistance map) using the inverse of the quality values of the Habitat Suitability. Within this resistance landscape Least-Cost Distance corridors were modelled connecting the roost with possible foraging areas. Further on, the circuit-theory approach was applied in different modes to gain multiple possible paths in the landscape (McRae et al., 2008). Over the last decade the circuit-theory has been widely applied in connectivity science and conservation for its strength to characterize relative frequency of routine movements along various possible paths through urban and other fragmented landscapes (Dickson et al., 2018; Braaker et al., 2014). Here, areas of high current density calculated with Circuitscape Version 4.0 (McRae, Shah & Mohapatra, 2013) represent high likelihood of commuting activity of bats. When modelling with Circuitscape, roosts were set as electric source and surrounding forest patches as grounds.

Within the Circuitscape process different settings of parameters led to various slightly differing current models of which three were selected to be tested in this project.

current\_subavg: current between every forest patch and the roost was modelled pairwise and the current values averaged over all possible maps were taken.

current\_submax: current between every forest patch and the roost was modelled pairwise and the maximum values considered over all possible maps were taken.

current\_adv: with the most recent version of Circuitscape ‘advanced’ mode was selected, that allowed to set the roost as source, activating all forest polygons as grounds simultaneously.

Table 2 lists the GIS data sets that were available for all test sites. They were used to select sampling sites and derive explanatory variables.

**Table 2: Available GIS data sets for every roost. All roosts were numbered whereby *M. myotis* roosts had number from 101 to 117 and *R. hipposideros* roosts 1001 to 1014.**

GIS layer	explanation	source
Roost 44x.shp	location of 44 roosts	© WSL
sNR_habitat.shp	Polygons used for computing least-cost corridors in Linkage Mapper and used as source (roost) and ground (forest) in Circuitscape per roost site (NR)	© WSL
sNR_roost_point.shp	1 single roost point	© WSL
sNR_subLCPsMerged.shp	Individual Least Cost Paths merged	© WSL
sNR_resistance.tif	Resistance used in Circuitscape	© WSL
sNR_current_adv.tif	Current version advanced	© WSL
sNR_current_submax.tif	Current version pairwise (maximum)	© WSL
sNR_current_subavg.tif	Current version pairwise (mean)	© WSL
Swissimage\swissimage_rgb_25cm_lv03_2017.lyr	Aerial photo of Switzerland (2017)	© Swisstopo

As light is considered to have a major impact on bat activity (see Introduction) there was an attempt to implement light data into the corridor model as well. Photos of the earth's surface taken at night by astronauts on the International Space Station (ISS) were tried to fit and geo-referenced on our roosts' surrounding to derive a brightness value for every sampling site. However, this approach was not incorporated into the model due to A) insufficient resolution of the ISS data in rural areas, where most of our roosts were located and B) low correlation of ISS photo values with Lux-values measured at the ground. Therefore, we decided to measure artificial light manually at every sampling site (see Data collection – field work).

### Spatial sampling design

We had 16 recording devices available to record bat activity at each study site. The actual place where such an acoustic measurement device was installed is defined as a *sampling site*, whereas, the term *study sites* stands for the roost and its surrounding of about 500 meters. Every sampling site was given a specific site-ID, ranging from site-ID 100 to site-ID 403 (see first column in table 14, Appendix I). One study site, Courtételle with site-IDs 100 to 115, was expelled later due to anomalies in the roost and organizational reasons. Hence, site-IDs in the full data table starts at 116.

To acquire balanced data, we decided to place eight devices within the predicted commuting corridors and eight Batloggers away from predicted corridors as control measurement. In addition, the impact of artificial light on commuting bats was examined. For this purpose, we located eight loggers each, in artificially illuminated sites and unlit places, respectively. This results in four sampling categories, as shown in figure 2.

	Bright	Dark
Corridor	4 batloggers	4 batloggers
Control	4 batloggers	4 batloggers

**Figure 2: Every sampling category was recorded four times at every study site.**

Pre-examination of the location of the roosts and its surrounding and selection of the 16 sampling sites around each roost were done in the office using the software of ArcMap GIS Desktop 10.7 (ERSI Schweiz, Zürich, Switzerland). The software was provided by WSL (Swiss Federal Institute for Forest, Snow and Landscape Research), geographic data and aerial photographs by swisstopo (Federal Office of Topography).

To get a stratified sampling over all study sites in terms of distances of sampling sites to the roost, we first drew three imaginary circles around each roost with radii of 60, 200 and 400 meters. As a guideline we placed four Batloggers on the inner (60 meter radius), eight on the middle (200 meter radius) and four on the outer circle (400 meter radius). This approach should get us a more or less comparable distribution of sampling sites around all examined roosts. However, it was not possible to follow this setting strictly at every study site.

Corridor vs. non-corridor sites were chosen with the layer of current\_adv model overlaid on the aerial picture (figure 3 and 4). The chosen sites were also checked against the other two models. They accorded rather well, only very few positional adjustments of sampling sites had to be taken to make all model types equally testable. To distinguish lit and dark places, and to locate street lights and other possible artificial light sources we looked for signs of them in aerial photos and Google street view (Google LLC, Mountain View, California, USA).

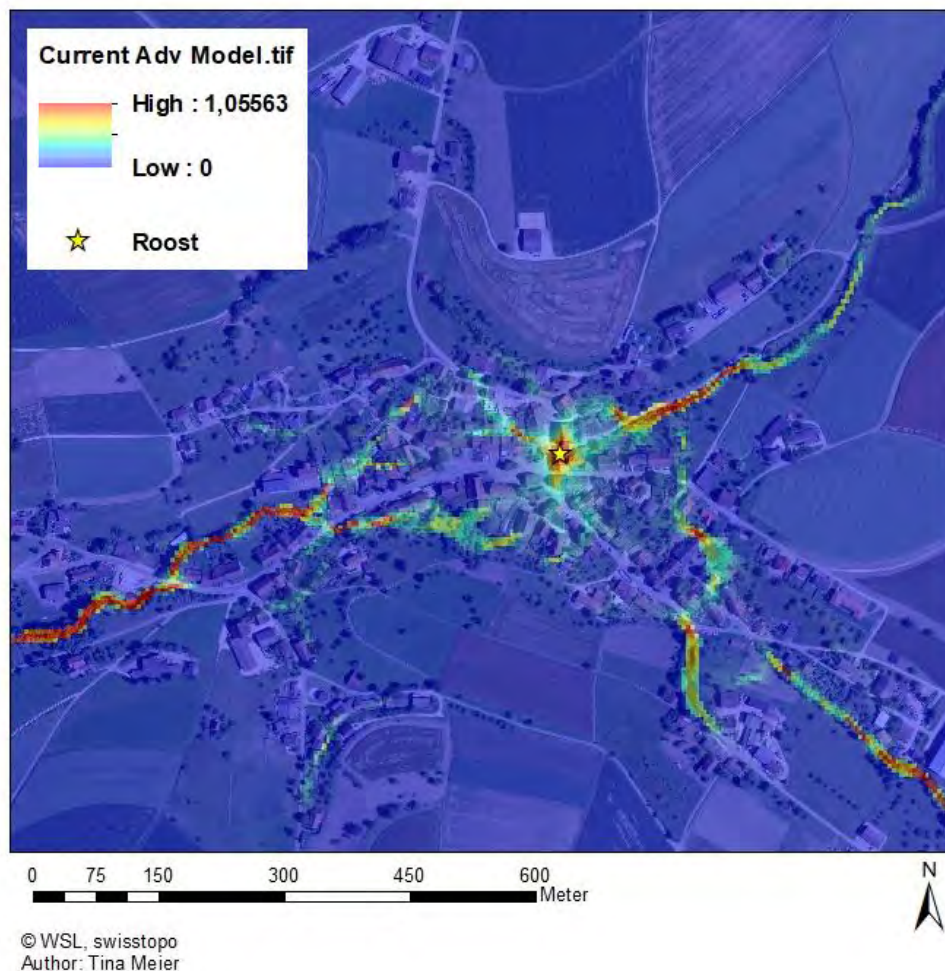


**Figure 3: Model predicted commuting corridors for the roost of Beggingen. High current values (yellow to red) predict strong use of the area as corridor by *M. myotis*.**

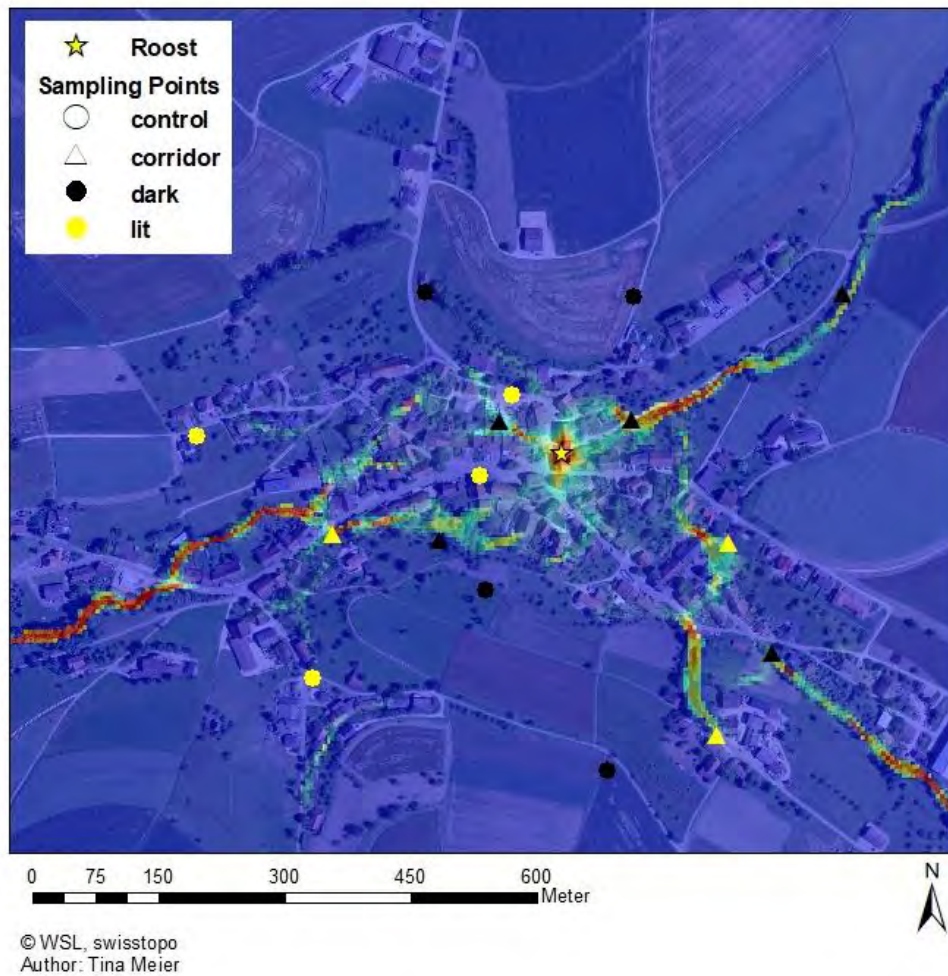


**Figure 4: Sampling sites were chosen while the corridor data set of current\_adv was overlaying the aerial photo. Sampling sites within corridors are marked as triangles and control sites as circles. Black icons mark dark places and yellow ones indicate artificially lit sampling sites.**

The recording devices used were provided by WSL, SSF, and SWILD (Urban Ecology & Wildlife Research organisation, Zürich, Switzerland). A Batlogger M (BATLOGGER M, Elekon AG, Lucerne, Switzerland) is an automatic ultrasound recorder with a sensitivity range of 10 kHz to 150 kHz. Prior to field work the recording settings were set as followed. Recordings were carried out for one day, starting 15 minutes before sunset and stopping 15 minutes after sunrise. The recording mode was set to “Period”, so that recording was triggered automatically by tonal ultrasound signals. While recording GPS was enabled, Time Mode was set to “Manual” instead of “Auto Update via GSM”. That is because in earlier field works there occurred leaps in time due to temporal missing GPS signals and consequently resulting in wrong time stamping of recordings. For further settings please see figure 10 in Appendix II.

All recordings were stored as a wav-file which later on we defined as a “sequence” of echolocation calls. For each wav-file, a meta data xml-file recorded date, time, trigger parameters, location as well as temperature. One sequence equates one count of bat activity. Bat activity is defined as a passing of a bat, but not the number of passing bats. One bat could actually pass a recorder several times when flying back and forth. However, we assumed that on their commuting way bats would mainly fly in one direction, namely towards their foraging area, but possibly still pass by multiple recorders.

### Data collection – field work

Maps as shown in figure 4 were used to locate sampling sites around a roost in the field. If we encountered unfavourable conditions at an intended sampling site, we had to move it for some meters, looking for a place still fulfilling the same criteria (corridor or non-corridor, dark or lit). Highly frequented roads or noisy watercourses for example are disadvantageous for ultrasound recordings. It also occurred that landowners did not want to have any sort of recording devices on their land, forcing us to look for acceptable replacement.

Batloggers were equipped with an ultrasound microphone, which was attached to a plastic fence post around 1.5 meters above ground (figure 5). The recording device itself was put in a plastic box on the ground to protect it from rain. An information sign with contact details and a “Please, do not touch” remark was affixed to the box. Microphones were fastened pointing in the direction of the roost and slightly towards the ground to protect them from direct rain.

Sampling sites at a predicted corridor were usually close to a vertical structure, such as hedges or wooded banks. Microphones were then installed in distances of about 3 to 7 meters from the structure, depending on the topographic circumstances. Judging from the characteristics of echolocation calls of the species, we assumed the maximum detection distance of *R. hipposideros* to be 5 meters, which forces them to fly rather close to structures. For *M. myotis* we estimated larger detection range as this species calls at lower fre-



**Figure 5: Example of recording station during the test run at the WSL pond on 10.05.2019. The microphone is attached to a plastic post, the Batlogger is in the plastic box on the ground.**

quencies and should therefore be able to capture structures further away. Nevertheless, we went for the same distances of microphones to structures as with *R. hipposideros* sites. Sampling sites lying in the open field (controls, i.e. far from corridors) we tried to place as far away from any structures as possible.

The recording devices were installed in the afternoon usually between 16:00 h and 19:00 h. Site-ID, device number, coordinates, and if necessary particular local conditions were noted. Although Batloggers register GPS coordinates automatically, we captured coordinates manually using a GPS device (GARMIN GPSMAP 62st) as control. Additionally, a photograph of the recording site was taken for documentation.

Around 22:00 h we observed the fly-out of bats and around 22:45 h, when it was dark enough, we started to measure brightness at the sampling sites using a TESTO 540 digital Luxmeter (measuring range: 1 – 99'999 lx; resolution: 1 lx). Light measurements were taken at about 1.5 meter height, once right above the microphone and four times at a distance of 2 meters from the microphone in all directions. For later statistical analysis, the mean of these five measured Lux-values was calculated. Sampling sites that were dangerous to access by night and/or were obviously dark were not actually measured but assumed to be 0 lx.

The next morning all devices were collected, recharged and the recordings saved on a laptop computer as well as an external storage disk. Data were checked for errors and inconsistencies, such as missing spatial references, and were corrected manually. For sampling sites which had to be moved, coordinates were adjusted in ArcGIS.

### Analysis of the recordings

All recordings were processed with the software BatScope 4.0 (Obrist & Boesch, 2018). As of now, a single recording shall be referred to as a sequence, in accordance to the term used in BatScope. In a first step, sequences were checked for animal calls and, if successful, cut into individual calls. The method used here is "Period Cutter", an algorithm that detects sinusoidal signal parts identical to the trigger algorithm in the Batloggers, and then cuts sequences in calls of 25 ms length. The calls were then inspected, and the identifying parameters numerically recorded. In a third step, the calls of a sequence were classified automatically. A reference data base containing 27 European bat species is incorporated. In this approach, all six available machine learning algorithms available in BatScope4 were applied to determine the most frequent species in a sequence. The identified species must then be verified manually. Filtering queries can be built referring to automatic classification and characteristics of a species' call to validate or eliminate automatic classification of sequences.

The echolocation of *Rhinolophus hipposideros* is unique for Switzerland. Their calls are at a very high and constant frequency (Peak frequency  $\approx$  110 kHz). Therefore, automatic classification for this species was considered to be trustworthy and was verified without any further checking. The calls of *Myotis myotis* are less clear, as on the one hand they emit distinct modulated calls and on the other, they call at lower frequencies like several other species. Confusion with calls of *Myotis daubentonii*, *Myotis bechsteinii*, *Nyctalus leisleri*, *Eptesicus nilssoni* and *Eptesicus serotinus* is possible. To test sequences with *Myotis myotis* calls, 17 filter queries were applied (Appendix III) and the resulting sequences checked visually. Only verified sequences were exported to an Excel table for further processing.

Recordings were taken for the whole night. Yet, we were only interested in bat activity reflecting commuting activity. Thus, we had to identify a time slot for the 'fly-out' period. The Excel tools PivotTable and bar chart were used to visualise bat activity over time. Bats of differing roosts flew out at different times depending on local conditions. Therefore, we could not set a fixed time slot for all roost, but had to specify a slot for each roost individually. However, the same duration was specified for all time slots off roosts of the same species.

#### Selection of explanatory variables

Bat activity during the commuting period is the response variable which is tested against various explanatory variables, as listed in table 3. Characteristics of the field setting, such as the Batlogger device used or the date of the recording night, might have an influence on the survey (e.g. faulty device). Also, the roost size (number of inhabiting bats) has to be considered for statistical analysis. The chapter "Data collection – field work" describes the field measurement of light intensity as a disturbing factor in commuting corridors.

We decided to test each of the three models within two buffer distances at each sampling site. In accordance with the detection distance of *R. hipposideros*, we derived mean current density values (also corridor value) of each model within a five meter radius, using the ArcGIS tool *Focal Statistics* and *Extract Multi Values to Points*. Thereby, higher current density indicates higher likelihood for the existence of a commuting corridor. The second radius of fifteen meters was chosen to consider the longer detection distance of *M. myotis* on the one side and to overcome the rather poor resolution of the models on the other side. The pixel size of all models is 5 x 5 meters. Hence, with a five meter radius, the corridor value only bases on the current density value of one pixel, whereas the fifteen meter radius captures at least nine pixels.

It was not always possible to place a recording device right in the centre of the predicted corridors, but some meters away. We hypothesised that the closer a device to the centre of a

corridor was, the higher the chance of recording all bats passing by would be. Therefore, we referred to the GIS data set of Least Cost Path computed during the development of the models. Our variable consists of the distance between the sampling site and the closest Least Cost Path and was determined using the ArcGIS tool *Near*. In addition, we expected that the distance of a sampling site to the roost would have an impact on the number of recordings at that site.

Bats are known to avoid unfavourable weather conditions (Burles et al., 2009; Rydell, 1989). Thus, we also included the actual weather conditions of the recording night in our statistical analysis. Values from the weather station closest to the sampled roost were extracted. We determined the following four weather variables: temperature, humidity, precipitation and wind speed. Means were calculated by averaging the hourly values from 21:00 h to 24:00 h. All weather data was extracted from the Climap Application by MeteoSchweiz.

**Table 3: All explanatory variables tested statistically on their impact on bat activity.**

Variable	Code	Source	Value range
Community (location of roost)	Comm	-	-
Batlogger device	BL	-	-
Day of the Year	DOY	-	145 - 201
Roost size	R_size	SSF	60 – 630
Mean of 5 measured Lux-values [lx]	Lux	Field data	0 – 42.8
Distance of sampling site to roost [m]	Dist_Roost	Field data	21 – 777
Mean of corridor value of model current_adv within a 5 meter radius	Adv5	Numeric corridor model	4.64E-8 – 0.352
Mean of corridor value of model current_adv within a 15 meter radius	Adv15	Numeric corridor model	6.34E-8 – 0.466
Mean of corridor value of model current_subavg within a 5 meter radius	Subavg5	Numeric corridor model	5.49E-8 – 0.137
Mean of corridor value of model current_subavg within a 15 meter radius	Subavg15	Numeric corridor model	5.54E-8 – 0.106
Mean of corridor value of model current_submax within a 5 meter radius	Submax5	Numeric corridor model	8.32E-8 – 0.138
Mean of corridor value of model current_submax within a 15 meter radius	Submax15	Numeric corridor model	8.39E-8 – 0.134
Distance of sampling site to closest Least Cost Path [m]	Dist_LCP	Numeric corridor model	0 – 625.6
Mean temperature at recording night between 21.00 – 24.00 [°C]	Temp	MeteoSchweiz	8.9 – 21.5
Mean relative humidity at recording night between 21.00 – 24.00 [%]	Humi	MeteoSchweiz	51.1 – 95.5
Mean precipitation at recording night between 21.00 – 24.00 [mm]	Prec	MeteoSchweiz	0 – 3.9
Mean wind speed at recording night between 21.00 – 24.00 [m/s]	Wind	MeteoSchweiz	0.3 – 2.6

### Statistical Analysis

Data were prepared in Microsoft Excel and statistical analyses were performed with the software R Version 3.5.0 (2018-04-23) (R Core Team, 2018). In a first step, numeric explanatory variables were standardized (mean = 0, standard deviation = 1, R-tool: *scale*). Secondly, all explanatory variables were checked for correlation (Spearman Correlation Test, R-tool: *pairs*). Variables with correlation coefficients higher than 0.7 should not be implemented into the same generalized linear mixed-effects model (GLMM) as an explanatory variables' impact on the response variable tends to be less precise if it correlates with another variable. For both species very high correlation emerged among the same GIS-models with different radius sampling of current density values (5 & 15 meters) and also among the three GIS-models themselves (see correlation coefficient matrices in Appendix IV). We decided to only use the fifteen meter current density value models for any further analysis, because the five meter radius current density is based only on one pixel of the Circuitscape data set. In addition, for both species three separate analyses were carried out, each incorporating one of the GIS-model versions. Performance quality of the three GIS-models among each other is compared afterwards. For *R. hipposideros* analysis, correlation emerged also among the variables of 'community' and 'day of the year' as was to be expected. Consequently, the variable of 'community' was dropped. Additionally the correlation coefficient for 'distance to roost' and 'distance to LCP' was 0.71. Nevertheless, we kept both variables for further analysis as we considered both of them relevant and could not comprehend what caused the correlation. Visual check of the response variable (bat activity) revealed a clear 'Poisson' distribution for both species (R-tool: *hist*).

We intended to use an automatic model selection to find the best performing model containing only the most relevant variables. Generalized linear mixed models (GLMM) are appropriate for this purpose and specifically suitable for our data, as they can handle non-normal data (bat activity is count data), and random effects can be taken into account (Bolker et al., 2009). We used the *glmer* tool of the lme4-package (Bates et al., 2015). The *glmer* fits a generalized linear mixed model and incorporates fixed effects parameters as well as random effects via maximum likelihood (Bates et al., 2019). We defined as fixed effects those variables that we assume to have a direct influence on the response variable which we wanted to determine. We set the following variables as fixed effects: current density of one of the GIS-models (Adv15, Subavg15 or Submax15), distance of the sampling point to the roost (Dist\_Roost), mean Lux-value (Lux) and distance of the sampling point to its closest Least Cost Path (Dist\_LCP). Random effects, on the other hand, are factors whose interest lies in the variation among them rather than their specific effects on the response variable (Bolker

et al., 2009). In this study, we identified eight random effects: the roost itself (Comm), the Batlogger used (BL), what day of the year measurement was taken (DOY), number of inhabiting bats of a roost (R\_size) and weather conditions of the specific place and date (temperature, relative humidity, precipitation and wind speed).

With each additional variable, linear models tend to get more and more complex which often results in unsolvable models. To prevent failure (warnings or errors), model complexity can be reduced by manually removing random effects (Bolker et al., 2009). Hence, prior to *glmer*, we implemented a generalized linear model (*glm* of R-package ‘stats’ (R Core Team, 2018)) with all available variables included and manually removed one after the other variable with insignificant effect (p-value > 0.05) on the response variable. After every removal *glm* model was run again and p-values were checked for changes. This resulted in a model of total nine variables for *M. myotis* and seven variables for *R. hipposideros* (table 4) that was further processed with *glmer*.

**Table 4: GIS model variable in fixed effects is Adv15, Subavg15 or Submax15. Insignificant effects were determined using a *glm*, and therefore dropped from the list of random effects. \*There was no precipitation during any measurement of *R. hipposideros* site, thus *glm* generated no output for this variable.**

effect level	<i>M. myotis</i> models	<i>R. hipposideros</i> models
fixed effects	GIS-model Lux Dist_Roost Dist_LCP	GIS-model Lux Dist_Roost Dist_LCP
random effects	BL R_size Humi Wind Prec	R_size Humi Wind
insignificant effects	Comm DOY Temp	BL Comm DOY Temp Prec*

An automated model selection (*dredge*, package: MuMIn (Barton, 2019)) was performed on the outputs of *glmer*, ranking models with all possible variable combinations according their AICc value. Akaike information criterion AIC (Akaike, 1998) is an estimate of the quality of each model of a set of statistical models relative to each other model of the set. Thereby, the AIC optimises the trade-off between ‘loss of information’ and model complexity (Burnham & Anderson, 2004; Harrison et al., 2018). We utilized AICc, which is the corrected value for small sample size analysis. While the individual AICc values are not interpretable, their delta-values ( $\Delta\text{AIC}$ ) can be used to select the best model among the set of candidate models. Models with  $\Delta\text{AIC} \leq 2$  have the same explanatory power and can therefore be regarded as equivalent.

With the command *get.models* (package: MuMIn) and a  $\Delta\text{AIC} \leq 2$ , we selected a set of ‘best performing models’ of which we computed a final single ‘best model’ by averaging them using *model.avg* (package: MuMIn). Model averaging was performed for *M. myotis* data, but not necessary for *R. hipposideros* data. The automated model selection rendered one best model for *R. hipposideros* analyses with the second best model having a  $\Delta\text{AIC} > 9$ , and therefore indicating a weaker performance.

## RESULTS

### Acoustic recordings & bat activity

Recordings were taken during 20 nights at 318 sampling sites in total, comprising 20 bat roosts. At three sites we did not yield any recordings, either because of incorrect handling of the bat recorder or due to manipulation by strangers. As a result we got a total of 48'358 sequences at *M. myotis* sites and 45'644 sequences at *R. hipposideros* sites, giving a total of 94'002 bat passes recorded.

After automatic classification and manual verification, 1'858 sequences were attributed to *M. myotis* at *M. myotis* sites and 1'357 sequences to *R. hipposideros* at *R. hipposideros* sites. Bat activity plotted over the duration of recording night, as shown in figure 6, exemplary for the roost of Kallnach, helped us to define the 'fly-out' period for each roost. The chosen 'fly-out' slot for *M. myotis* is 1 hour 25 minutes and the one for *R. hipposideros* 1 hour 15 minutes. The exact start and end times of the time slot for all roosts can be found in table 5. At *M. myotis* sites, 1'082 sequences were recorded during the 'fly-out' time slot which accounts for 58 % of total *M. myotis* activity. *R. hipposideros* activities also show peaks shortly after the sunset. In contrast to *M. myotis*, the recording sequences of *R. hipposideros* are more distributed over the whole night and less concentrated at the commuting fly-out period. Hence, only 37% (496 out of 1'357) of *R. hipposideros* activity was recorded within the defined time slot (cf. figure 13 and 14 in Appendix V). The exact numbers of total activity and activity within 'fly-out' period for each study site are listed in table 5.

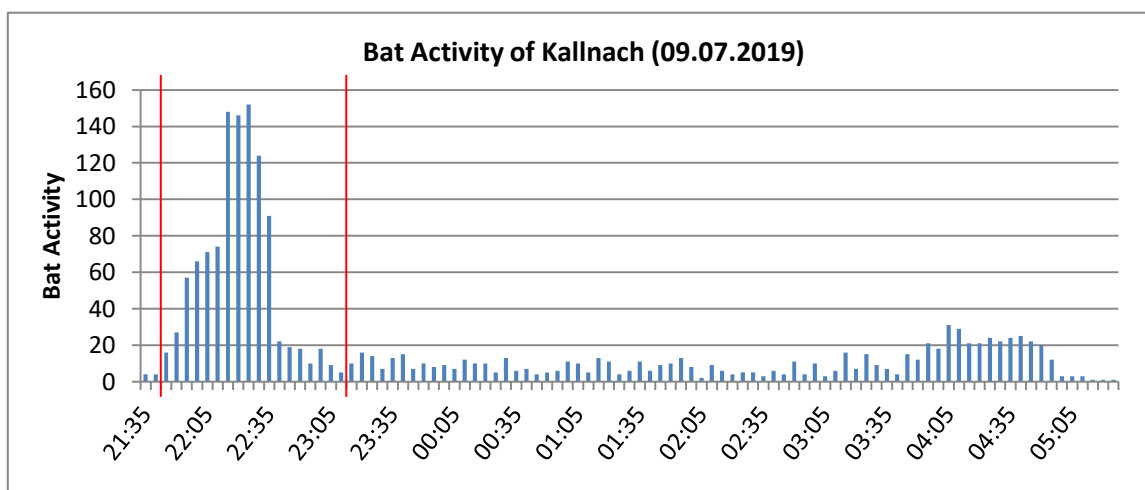


**Figure 6: Total bat activity at 16 recording sites around the roost of Kallnach with peak of fly-out activity between 22:10 h and 23:00 h. The two red lines represent start and end time of the chosen 'fly-out' time slot.**

On both study sites (Embrach, Flawil) where measurements were repeated (see chapter “Study period”), total bat activity was remarkably higher the second time of measurement. The first night in Embrach we recorded 65 sequences of Greater mouse-eared bats, 57 of them within the time slot, whereas in the second measurement we obtained 211 sequences of which 83 were assigned to the ‘fly-out’ period. Similarly, bat activity in Flawil was higher the second time of recording: 192 sequences of total activity in the second recording night, compared to 84 in the first one; and 76 versus 12 sequences within the ‘fly-out’ period. The time slots of these two measurements were identical for both nights.

**Table 5: Start and end times of the ‘fly-out’ time slots defined for every study site individually. Total activity was measured throughout the whole night, but for analysing commuting activity towards foraging areas, only recorded activity within the ‘fly-out’ period was relevant. Percentage of activity within the time slot was generally higher for *M. myotis* than for *R. hipposideros* sites.**

Species	Roost	Rec. Date	Duration	Start	End	Total Activity all night	Total Activity in time slot	% of all Activity
<i>M. myotis</i>	Embrach (1 <sup>st</sup> )	27.05.2019	1 h 25 min	21.45	23.10	65	57	88
	Mühlau	06.06.2019		22.05	23.30	87	76	87
	Lipperswil	18.06.2019		21.35	23.00	95	70	74
	Flawil (1 <sup>st</sup> )	19.06.2019		21.45	23.10	84	12	14
	Buochs	04.07.2019		22.15	23.40	55	26	47
	Buttisholz	05.07.2019		22.10	23.35	360	255	71
	Kallnach	09.07.2019		21.45	23.10	346	187	54
	Beggingen	11.07.2019		21.45	23.10	182	105	58
	Wegenstetten	16.07.2019		21.45	23.10	181	135	75
	Embrach (2 <sup>nd</sup> )	17.07.2019		21.45	23.10	211	83	39
	Flawil (2 <sup>nd</sup> )	20.07.2019		21.45	23.10	192	76	40
<b>Total <i>M. myotis</i></b>						<b>1'858</b>	<b>1'082</b>	<b>58</b>
<i>R. hipposideros</i>	Blumenstein	30.05.2019	1 h 15 min	21.25	22.40	231	72	31
	Amsoldingen	31.05.2019		21.25	22.40	119	39	33
	Därstetten	01.06.2019		21.40	22.55	148	28	19
	Sachsels	12.06.2019		21.25	22.40	47	12	26
	Giswil	13.06.2019		21.55	23.10	167	65	39
	Castiel	24.06.2019		21.25	22.40	21	3	14
	Waltensburg	25.06.2019		21.55	23.10	74	19	26
	Uors	26.06.2019		22.25	23.40	421	196	47
	Surcasti	27.06.2019		21.55	23.10	129	62	48
<b>Total <i>R. hipposideros</i></b>						<b>1'357</b>	<b>496</b>	<b>37</b>

Differences in bat activity at corridor and control sites

Each study site was sampled the same way concerning corridor and control sites. At *M. myotis* sites we had 88 sites being situated in a corridor and the same number for control sites. For *R. hipposideros* 71 sampling sites were situated in a corridor and 71 outside (control). Table 6 discloses that *M. myotis* bat passes were 2.8-fold higher at corridor sites (798 passes) compared to control sites (284 passes). Hence, there is a significantly higher activity of *M. myotis* at sampling places of modelled corridors (p-value <2e-16). *R. hipposideros* was recorded 311 times at corridor sites in comparison to 185 records at control sites. This difference is also statistically significant (p-value <2e-16).

**Table 6: The number of bat passes is significantly higher at corridor sites than at control sites for both species.**

Species	Location of sampling sites	Number of sampling sites	Bat passes
<i>M. myotis</i>	corridor	88	798
	control	88	284
<i>R. hipposideros</i>	corridor	71	311
	control	71	185

Light measurements

The mean Lux-values of all measurements range from 0 lx to 42.8 lx. While light measurement resulted in a gradual scale of values, choosing sampling points in daytime was based on the assumption of whether a place would be dark at night with no light source in close vicinity or artificially lit by any kind of light source. For further analyses a reasonable threshold of  $\leq 0.5$  lx was determined to differentiate between dark and artificially lit sites. According this delimiter, it turned out we had sampled a total of 221 dark and 94 lit sites.

Low Lux-values ( $lx \leq 0.5$ ) evidently occurred more often than high values (table 7). At 108 *M. myotis* sites, the mean Lux-value was lower or equal to 0.5 lx, at 66 sites we measured higher values. 31 of the sites with 0 lx were considered dangerous to access by night (situated on a steep slope and/or pitch darkness), so that a Lux-value of 0 was assumed. However, at 77 other *M. myotis* sampling sites we actually measured mean Lux  $\leq 0.5$ . At these 108 dark sites we recorded 869 *M. myotis* passes which accounts for eight bat passes per dark sampling site, whereas 213 passes at 66 sites yield 3.2 bat passes per lit site. Consequently, the ratio of bat passes per dark sites compared to the ones in lit sites is 2.5.

For *R. hipposideros* 113 sampling sites were measured with mean Lux-values lower than 0.5 lx, while 28 sites were affected by artificial light with Lux-values higher than 0.5. Here, 36

sampling sites were not visited and assumed to yield 0 lx, at 77 sites measured mean Lux-values were  $\leq 0.5$  lx. 485 *R. hipposideros* passes were recorded at these 113 dark sites, yielding in 4.3 bat passes per dark site. At 28 lit places we recorded 11 *R. hipposideros* passes which is 0.4 passes per lit site. The ratio of dark to lit sites concerning Lesser horse-shoe bats is 10.9.

For both species a generalized linear model analysis (*glm*) revealed highly significant effects of Lux-values on bat activity (*M. myotis*: estimate: -0.2893; p-value  $<2e-16$ ; *R. hipposideros*: estimate: -2.3514; p-value  $8.84e-14$ )

**Table 7: There were considerably more dark than lit sampling sites and bat activity was significantly higher at dark sites for both species. The apparent difference in the dark/lit ratio between the two species indicates higher sensitivity to light of *R. hipposideros* than *M. myotis*.**

Species	Lux category	No. of sites	No. bat passes	No. passes per site	Ratio dark/lit
<i>M. myotis</i>	0 – 0.5 lx	108	869	8.0	2.5
	$\geq 0.5$ lx	66	213	3.2	
<i>R. hipposideros</i>	0 – 0.5 lx	113	485	4.3	10.9
	$\geq 0.5$ lx	28	11	0.4	

#### Deriving a best performing model for each species

Generalized linear mixed-effect models (GLMM) were run for both species three times, incorporating one of the GIS-models' current density values each (GLMM 1 to 6). The following tables 8 to 13 show and explain the three best performing models for each *glmer* and *dredge* analysis. The models are ranked according to their AICc values. Models with  $\Delta AIC \leq 2$  have the same explanatory power and can therefore be regarded as equivalent. The full tables of all analyses are given in Appendix VI.

#### ➤ **GLMM 1: *M. myotis* data including the current\_adv GIS model**

**Table 8: The three best performing models for *M. myotis* analysis with current density values of the GIS model Adv15 included.**

rank	Adv15	Dist_LCP	Dist_Roost	Lux	df	logLik	AICc	delta	weight
1	-	-0.406	-0.205	-0.397	9	-849.938	1718.973	0.000	0.530
2	-0.052	-0.428	-0.216	-0.399	10	-848.930	1719.209	0.237	0.470
3	-	-0.478	-	-0.383	8	-867.068	1751.009	32.036	5.85e-8

Table 8 classifies the three best performing models for *M. myotis* data including the current density values of GIS Adv15 model. The best ranked model includes explanatory variables of

distance to LCP and roost, as well as the light variable. However, the second-best model, which includes the Adv15 variable, does only have a slightly higher AIC value ( $\Delta AIC = 0.237$ ), wherefore this model the same explanatory power is assigned as the first one. Model three is clearly less powerful ( $\Delta AIC = 32.036$ ) than the first two models. When averaging the first two models, they get weighted similarly strong, as indicated in the last column. All four explanatory variables have a negative impact on our response variable, as figure 7 graphically illustrates. The distance to LCP and the Lux-value have almost the same strongest negative impact on bat activity, while the estimate for Adv15 is close to zero and its confidence intervals cross the zero line.

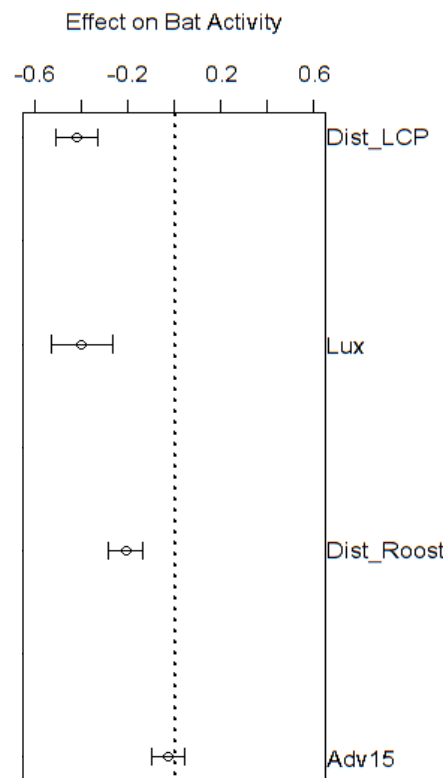


**Figure 7: Analysis of *M. myotis* data including current density values of the GIS model `current_adv` show negative impacts of all explanatory variables on bat activity. Estimate values: Dist\_LCP = -0.417; Lux = -0.398; Dist\_Roost = -0.209; Adv15 = -0.025.**

➤ **GLMM 2: *M. myotis* data including the current\_subavg GIS model**

**Table 9: The three best performing models for *M. myotis* analysis with current density values of the GIS model Subavg15 included.**

rank	Subavg15	Dist_LCP	Dist_Roost	Lux	df	logLik	AICc	delta	weight
1	-	-0.406	-0.205	-0.397	9	-849.938	1718.973	0.000	0.609
2	-0.043	-0.426	-0.214	-0.397	10	-849.255	1719.860	0.888	0.391
3	-	-0.478	-	-0.383	8	-867.068	1751.009	32.036	6.73e-8

Again, the best performing model to explain bat activity does not include the current density values of the GIS model, here current\_subavg15, but is included in the secondly ranked model (table 9). In fact, this has the same significance as the first model, since the difference in the AICc value is only 0.888. Model three has significantly less explanatory power (deltaAIC = 32.036). Model one is weighted significantly higher than model two in the model averaging process (cf. column 'weight'). Figure 8 displays effects of all averaged estimates. Like before, distance to LCP and Lux-value have stronger negative effects on bat activity than distance to roost. Current density of the GIS model has an estimate of -0.043 and confidence intervals cross the zero line, indicating little to no impact of the Subavg15 model on the response variable.

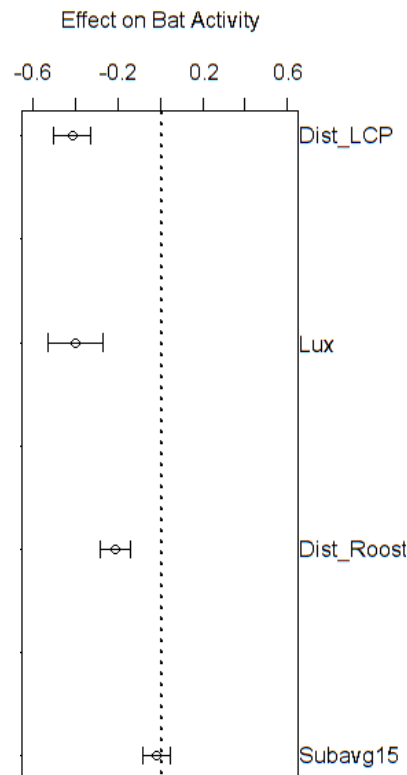


**Figure 8: Analysis of *M. myotis* data including current density values of the GIS model current\_subavg show negative impacts of all explanatory variables on bat activity. Estimate values: Dist\_LCP = -0.414; Lux = -0.397; Dist\_Roost = -0.208; Subavg15 = -0.017.**

➤ **GLMM 3: *M. myotis* data including the current\_submax GIS model**

In the 3<sup>rd</sup> GLMM analysis, current values of the Submax15 GIS model are included (table 10). As before, the best performing model of this set only combines the variables of ‘distance to LCP’, ‘distance to roost’ and ‘Lux’. Submax15 is incorporated into the secondly ranked model, which has the same strong explanation power as the first one (deltaAIC = 0.695). Once more, the third model is significantly less powerful than the first two (deltaAIC = 32.036).

**Table 10: The three best performing models for *M. myotis* analysis with current density values of the GIS model Submax15 included.**

rank	Submax15	Dist_LCP	Dist_Roost	Lux	df	logLik	AICc	delta	weight
1	-	-0.406	-0.205	-0.397	9	-849.938	1718.973	0.000	0.586
2	-0.047	-0.428	-0.208	-0.397	10	-849.159	1719.668	0.695	0.414
3	-	-0.478	-	-0.383	8	-867.068	1751.009	32.036	6.48e-8

The first two models were averaged and the estimate values of each explanatory variable were plotted in figure 9. As in the previous analyses, effects of all variables on bat activity are negative. Distance to LCP and Lux-values are similarly stronger than distance to roost, and the estimate of the GIS model Submax15 is again very close to the zero line.

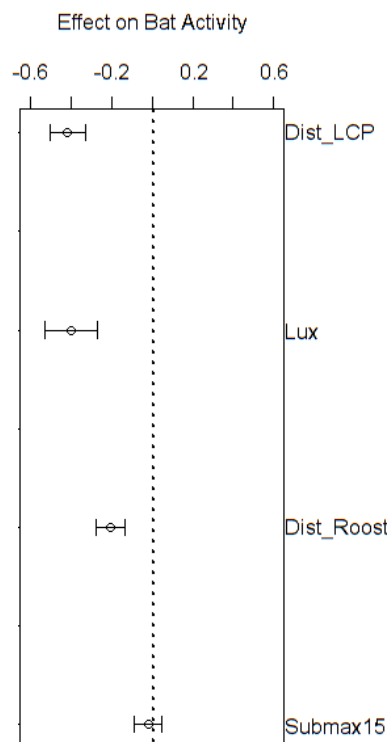


**Figure 9: Analysis of *M. myotis* data including current density values of the GIS model current\_submax show negative impacts of all explanatory variables on bat activity. Estimate values: Dist\_LCP = -0.415; Lux = -0.397; Dist\_Roost = -0.206; Submax15 = -0.019.**

➤ **GLMM 4: *R. hipposideros* data including the current\_adv GIS model**

**Table 11: The three best performing models for *R. hipposideros* data with current density values of the GIS model Adv15.**

rank	Adv15	Dist_ LCP	Dist_ Roost	Lux	df	logLik	AICc	delta	weight
1	0.345	-0.737	0.407	-15.829	8	-586.655	1190.552	0.000	1.000
2	0.219	-0.629	-	-19.435	7	-603.242	1221.442	30.890	1.96e-7
3	-	-0.937	0.205	-20.264	7	-608.490	1231.938	41.386	1.03e-9

In contrast to the analyses of *M. myotis* data, here the best performing model contains all four explanatory variables (table 11). Additionally, this firstly ranked model possesses significantly higher explanatory power than the next-best model (deltaAIC = 30.890). Model averaging was therefore not necessary, since we have already obtained our best performing model with *R. hipposideros* data and the Adv15 GIS model. The current density values of the Adv15 GIS model do have a positive effect on bat activity. On the other side, distance to LCP seems to have a moderately negative impact on bat activity, while an estimate of the Lux-value of -15.829 suggests an extremely negative effect.

➤ **GLMM 5: *R. hipposideros* data including the current\_subavg GIS model**

**Table 12: The three best performing models for *R. hipposideros* data with current density values of the GIS model Sumavg15.**

rank	Subavg15	Dist_ LCP	Dist_ Roost	Lux	df	logLik	AICc	delta	weight
1	0.322	-0.761	0.418	-15.826	8	-589.689	1196.620	0.000	1.000
2	0.181	-0.662	-	-19.694	7	-606.139	1227.235	30.615	2.25e-7
3	-	-0.937	0.205	-20.264	7	-608.490	1231.938	35.318	2.14e-8

Generalized linear mixed model analysis yielded a best performing model containing all variables of interest (table 12). With an estimate value of 0.322, the Subavg15 variable has a slightly positive influence on bat activity, while distance to LCP and the Lux-value have a strong negative influence on bat activity. The second best model has significant less explanatory power (deltaAIC = 30.615).

➤ **GLMM 6: *R. hipposideros* data including the current\_submax GIS model**

**Table 13: The three best performing models for *R. hipposideros* data with current density values of the GIS model Submax15.**

rank	Submax15	Dist_ LCP	Dist_ Roost	Lux	df	logLik	AICc	delta	weight
1	0.163	-0.854	0.301	-17.816	8	-602.754	1222.749	0.000	0.990
2	-	-0.937	0.205	-20.264	7	-608.490	1231.938	9.189	0.010
3	0.081	-0.765	-	-20.670	7	-612.043	1239.043	16.294	2.86e-4

Table 13 lists the three best performing models for *R. hipposideros* data with the GIS model of Submax15 included in the analysis. The model ranking first keeps all four implemented variables in the model. The second best model has a deltaAIC of 9.189 and is therefore considerably less powerful than the first model. The Submax15 variable appears to have a slight positive effect on bat activity, whereas the Lux-value in this analysis has even a greater negative impact on bat activity than in the two previous analyses (-17.816).

Overall, if we compare the AICc-values of the three *M. myotis* analyses they show a very similar performance. In fact, the averaged AICc of all three approaches are within a deltaAIC  $\leq 2$  (AICc<sub>Adv15</sub> = 1719.084; AICc<sub>Subavg15</sub> = 1719.319; AICc<sub>Submax15</sub> = 1719.260). Hence, all three approaches have the same explanatory power. In contrast, AICc-values of *R. hipposideros* analyses are significantly different. Certainly, the model which includes the Adv15 GIS model (GLMM 4) performs better than the other two GIS models (AICc<sub>Adv15</sub> = 1190.552; AICc<sub>Subavg15</sub> = 1196.620; AICc<sub>Submax15</sub> = 1222.749). Consequently, the GIS model of “current\_adv” is the most accurate for predicting *R. hipposideros* commuting corridors.

## DISCUSSION

### Impact of artificial light on bat activity

Although we intended to sample equal dark and artificial lit sites, it was not possible to find the same amount of bright and dark places. Light conditions at some sampling sites were not as expected. Surprisingly, it occurred more often that a place expected to be illuminated was in fact dark, but rarely the other way around. It turned out, that five study sites only had very few light sources in the vicinity of the roost (Giswil, Buttisholz, Amsoldingen, Blumenstein, Surcasti), while at the site of Lipperswil the only road with street lights close by was under construction and all street lamps were powered off during recording. Hence, we sampled considerably more places with low Lux-values than higher ones. To distinguish between dark and lit places, a sensible threshold for a Lux-value had to be chosen, which we based on personal perception during light measurement on the one hand, and derived from prior studies on the other hand. Stone et al. (2012) demonstrated significantly reduced activities of *R. hipposideros* and *Myotis ssp.* during low light level of 3.6 lx, and Azam et al. (2018) ascertained that illuminance has a negative effect on *Myotis sp.*, even below 1 lx. We lowered this limit once more and opted for a threshold of 0.5 lx. Despite this low chosen lux level, we resulted more dark than lit sites, which led to the fact that we could not simply compare bat passes of dark sites to sites where we measured higher Lux-values. Therefore, a generalized linear model analysis (*glm*) with 'Poisson' data distribution was conducted, based on the original unscaled data. This allows the detection of statistical significance of the tested variable, as well as to quantify the impact of the Lux variable on bat activity. The analysis revealed highly significant effects of artificial light on bat activity for both species. The estimate of the Lux variable of *M. myotis* indicates a decrease in bat activity of -0.2893. Thus, if the Lux-value increases by one unit (1 lx), bat activity decreases by almost one third. For *R. hipposideros* the estimate is -2.3514, which implies a reduction of bat activity of 235 % when illuminance increases by 1 lx. This is incredible when considering that a Luxmeter is very sensitive and 1 lx difference is reached easily by just standing approximately one meter closer to a light source or even turning the lux-meter slightly towards the light, allowing direct light beam onto the optical sensor. Yet, our results are consistent with the findings of several previous studies concerning negative impacts of artificial light on the commuting behaviour of bats (cf. Stone et al., 2009; Stone et al., 2012; Azam et al., 2018; Pauwels et al., 2019). Moreover, the calculated ratios of dark to lit places also indicate that *R. hipposideros* are probably more sensitive to light than *M. myotis*.

As a possible solution to this problem scientists have suggested installing street lights with dimming capacities (Stone et al., 2015; Azam et al. 2018). This approach was not examined

in this study. However, during measurement of Lux-values at sampling points we encountered dimmable street lamps at two sites and both were located within predicted commuting corridors. At sampling site 184 in Embrach we measured mean illuminance of 15.4 lx with full luminosity and approximately 10 lx when the light was dimmed. During commuting time, the road beneath this lamp was highly frequented. Thus, we incorporated the higher value in our analyses. We sampled 12 bat passes at this site. In Kallnach at site 117, the Lux-value was approximately 5 lx with full luminosity and 2.6 lx when dimmed. This road was rarely frequented, therefore we calculated with the lower measurement. Here, we recorded 3 bats passing. Surprisingly, we recorded higher bat activity at the brighter site in Embrach than at the more dimmed site in Kallnach. We explain this by the fact, that there were a lot of bushes around the street light in Embrach. Hence, the bats could probably move unaffected by the light in the shade of these bushes. Notwithstanding the above, we were amazed by the amount of reduced Lux-value when light is dimmed. Further research on artificial light with dimming capacity and its impact on bat activity is therefore suggested.

#### Finding the best performing model

Our statistical analysis method of choice was a generalized linear mixed model (GLMM), as it provides a flexible approach for analysing non-normal data when random effects have to be taken into account (Bolker et al. 2009). Our data was 'count' with 'Poisson' distribution, and we had four fixed effects of interest and three and five random effects, respectively. Consequently, we built one model with seven effects in total and another model with nine effects. Generally, the R-tool '*glmer*' can handle approximately ten to twelve variables without difficulties. By ranking and averaging the outputs, we gained one best performing model for each numeric GIS model and species. In all six analyses, the final best performing model contained all four examined explanatory variables.

The distance of a sampling point to its nearest Least Cost Path (Dist\_LCP) correlated significantly negative with bat activity. Hence, the further away from a Least Cost Path we sample, the less likely it is to encounter commuting bats. GLMM 1 to 3 show that this variable has the biggest impact on *M. myotis* activity in our study. The average estimate values for all three analyses were almost equal (GLMM 1 = -0.417; GLMM 2 = -0.414; GLMM 3 = -0.415). Bat activity of *R. hipposideros* even stronger negatively correlates with the distance to a Least Cost Path (GLMM 4 = -0.737; GLMM 5 = -0.761; GLMM 6 = -0.854). Least Cost Paths usually run along ecological structures on which bats are expected to depend for echolocation. The negative effect of the distance to a Least Cost Path for both species supports this assumption. Moreover, the stronger negative effect in *R. hipposideros* analyses confirms our presumption of the higher dependency of *R. hipposideros* on structures compared to *M. myotis*.

The separate analysis of the Lux variable, as discussed above, already revealed a significant negative effect of light on bat activity. Our results of the GLMM analyses confirm this. Estimate values for the Lux variable in *M. myotis* models are similarly high to the ones for Dist\_LCP (cf. figure 7, 8 and 9). However, the negative estimates of the Lux variable in *R. hipposideros* analyses are much larger (GLMM 4 = -15.829; GLMM 5 = -15.826; GLMM 6 = -17.816). To test the credibility of these values, we reran the same analyses (GLMM 4 to 6) but dropped the Lux variable. The number one models in these analyses were identical with each 7<sup>th</sup> ranked model in the original analyses (see green rows in table 19, 20 and 21 in Appendix VI). Comparing the AICcs of these two models in each analysis, all models containing the Lux variable are significantly more powerful. It was decided to keep the Lux variable in all analyses and approve these high estimates.

The distance of a sampling point to the roost (Dist\_Roost) seems to correlate negatively with *M. myotis* but has a positive effect on *R. hipposideros* activity. When consulting the tables 16 to 10 in Appendix VI, we see that the estimates of Dist\_Roost in *M. myotis* analyses are always negative, whereas the ones for *R. hipposideros* analyses change randomly from negative to positive with decreasing power of the model (tables 19 to 21). We could neither think of a reasonable explanation for the opposite effect of this variable on the two species, nor the changing impact within *R. hipposideros* models. Consequently, we determined this variable as little informative for the *latter*. In any potential further analysis, the variable of distance to roost could be implemented as a random effect instead of as fixed.

Since the numeric corridor models for the two examined species were slightly different we evaluated them separately. Thereby, it is striking that within each averaged model for *M. myotis*, all three GIS model variables appear to have a slight negative effect on the response variable (table 8, 9, 10), while the estimates of the same variables are positive in each best ranked model for *R. hipposideros* (table 11, 12, 13). In fact, estimates of the GIS-model variables for *R. hipposideros* data are positive in all possible model combinations (see orange column in table 19, 20 and 21 in Appendix XI). Furthermore, the estimate values are sufficiently large so that possible variances should not cross the zero line. Hence, we approve the validity of these estimate values and suggest a positive correlation between the numeric GIS models and bat activity of *R. hipposideros*.

However, estimates of all three GIS-model variables for *M. myotis* data are less consistent. In analyses of Adv15 and Submax15, estimates of these variables in the upper eight models are negative, whereas in the lower eight models they become positive (table 16 and 18). Also, in the analysis where Subavg15 is incorporated, algebraic sign of its estimate changes randomly with decreasing power of the model (table 17). Therefore, this study can neither

state a positive nor a negative significant effect of the numeric corridor model on bat activity of *M. myotis*.

This contradicts the outcome of the simple comparison of bat activity in corridor vs. control sites. Selecting sampling points in ArcGIS with the corridor model overlaying an aerial photo was challenging and error-prone. On the map corridor sampling points seemed to lie within a corridor, but when extracting the current density value at the exact location where the Batlogger was recording, some sampling points generated only very small values. That is because high current density values occur only in the centre of a corridor and decrease with increasing distance to the centre. However, we installed the Batloggers approximately five meters beside a structure as explained in the chapter “Data collection – field work”. Therefore, some designated corridor sampling point actually had very small current density values. Since measured bat activity was higher at designated corridor sites, adaption of the corridor model concerning this shortage is recommended. Possibly the sharp decrease of current density values with increasing distance to the corridor centre could be reduced. In this way, predicted corridors were wider. This would take the longer detection range of *M. myotis* into account, which presumably fly along structures in some distance.

For the *M. myotis* analyses (GLMM 1 - 3), all three models result in the same AICc of 1719. Therefore, we conclude that all three GIS-model versions for *M. myotis* corridor prediction perform equally well. This was to be expected, as the correlation coefficient matrix already showed very high correlation (0.95 and 0.94) among the three different model versions (figure 11, Appendix IX). In *R. hipposideros* analyses (GLMM 4 - 6) occurred significant differences in the AICcs, which suggests the GIS-model version of “current\_adv” to be the most accurate for predicting *R. hipposideros* commuting corridors.

Since both numeric corridor models greatly rest on structure ruggedness, terrain ruggedness and structures themselves, predicted corridors coincide largely with ecological structures such as trees, hedgerows, courses of streams and riparian vegetation. *R. hipposideros* have been reported to rely on such structures (Schofield, 1996; Motte & Libois, 2002), while *M. myotis* are assumed to be less dependent on them. This species' specific ecological characteristic might explain why the numeric corridor model performs better for *R. hipposideros* than for *M. myotis*. This finding corresponds to our first impression we received when visually checking the recorded bat activity with the properties of its recording location. We observed a considerable number of *M. myotis* passes at control sites, e.g. far from predicted corridors, if they were unaffected by artificial light. On the opposite, we had sampling points located within corridors but lit, where we measured no activity at all. For *M. myotis*, we therefore assumed higher effect of light on bat activity than the presence of structures.

In all analyses, effects of the other three examined variables were higher than the impact of any predictive corridor model. To enhance the accuracy of the predictive corridor models further attempts to include light data into the numeric corridor models should be made. Incorporating ISS aerial photos was not successful due to insufficient resolution of data in rural areas and low correlation of the light values of the photos with Lux-values measured at the ground. A promising approach that emerged lately is to gather environmental measurement data and take aerial pictures by drones. Images of the surrounding of a roost taken at night could be calibrated like the ISS photos and be incorporated in the numeric corridor models. The insufficiencies of the ISS images should be overcome by this approach.

## CONCLUSION

In this study we demonstrated highly significant negative effects of artificial light on commuting bat activity for both species examined, Greater mouse-eared bat and Lesser horseshoe bat. The comparison of the ratio of bat activity at dark and lit sites suggests that *R. hipposideros* is more sensitive to light than *M. myotis*. In addition, the distance of a sampling point to its nearest Least Cost Path correlated significantly with bat activity. However, reliability of the predictive corridor models could not be proven satisfyingly. For *M. myotis*, there was no significant effect of the commuting corridor model on bat activity. The *R. hipposideros* model including the numeric corridor model of “current\_adv” performed best and showed positive correlation with measured bat activity. For any further efforts to enhance the predictive corridor model, we suggest to focus on the most recent version of Circuitscape ‘advanced’. In all analyses, the other three variables examined (‘distance to LCP’, ‘distance to roost’, ‘Lux-value’) showed higher effect on bat activity than the predictive corridor models, in particular the variable of light. Further adaption of the predictive corridor models should therefore concentrate on the inclusion of the light variable. This can be accomplished for example, by gathering comprehensive light data by taking pictures at night with drones. This is a promising approach and should be pursued.

## ACKNOWLEDGEMENT

I would like to thank my supervisor Dr. Martin Obrist for his professional assistance and guidance throughout this project. His practical tips and feedback on the sampling design, field work, analysis of recordings and statistical analysis I appreciated very much.

My gratitude also goes to Lucretia Deplazes for introducing me to the process of field work with bats and assisting during my early sampling.

Dr. Klaus Ecker I would like to thank for all his help concerning GIS data preparation, editing and support.

All equipment necessary for recording bats in the field was provided by KOF (Koordinationsstelle Ost für Fledermausschutz), SWILD (research and consulting association, Zurich) and WSL (Swiss Federal Institute for Forest, Snow and Landscape Research). I very much appreciated the uncomplicated handling of the lending.

Many thanks also to all involved cantonal bat protection responsables as well as concerned roost care-takers for their collaboration and sharing of information. A special thank you goes to Rob van der Es for letting me visit the Blumenstein roost.

Throughout my later field recordings I was lucky to be accompanied by several field assistants. Therefore, many thanks to Annabarbara Beilstein, Heidi Budmiger, Julia Fürst, Martina Hongler, Céline Meier, Peter Meier, Heidi Meier and Sarah Wirth.

As a special occasion, this project was portrayed in a TV production "Graubünden – wo der Himmel die Erde berührt", produced by the film production company 'Filmquadrat.dok GmbH'. Hence, during the sampling of the roost of Surcasti I was accompanied by a film team. I would like to thank Verena Schönauer (film director) and her team for the experience and insight to a film production and giving us the opportunity to call attention to the critical situation of Lesser horseshoe bats in Switzerland.

I further acknowledge Niels Hagenbuch (Statistical consulting service of ETH) and Dr. Simone Fontana (PostDoc, WLS) for utmost helpful advices on statistical evaluation.

Last but not least I would like to show gratitude to Céline Meier for English language revision and critical reading examination of this thesis.

## REFERENCES

- Akaike H. (1998). Information theory and an extension of the maximum likelihood principle. In: Parzen E., Tanabe K., Kitagawa G. (eds). Selected Papers of Hirotugu Akaike. Springer Series in Statistics (Perspectives in Statistics). Springer, New York, NY, [https://doi.org/10.1007/978-1-4612-1694-0\\_15](https://doi.org/10.1007/978-1-4612-1694-0_15).
- Arlettaz R. (1996). Feeding behaviour and foraging strategy of free-living mouse-eared bats, *Myotis myotis* and *Myotis blythii*. *Animal Behaviour*, 51 (1): 1-11. <https://doi.org/10.1006/anbe.1996.0001>
- Barton K. (2019). MuMIn: Multi-Model Inference. R package version 1.43.6. <https://CRAN.R-project.org/package=MuMIn>
- Bates D., Maechler M., Bolker B. and Walker S. (2015). Fitting Linear Mixed-Effects Models using lme4. *Journal of Statistical Software* 67 (1): 1-48. <https://doi.org/10.18637/jss.v067.i01>.
- Bates D., Maechler M., Bolker B., Walker S., Christensen R.H.B., Singmann H., Dai B., Scheipl F., Grothendieck G., Green P., Fox J. (2019). Package ‘lme4’ - Linear Mixed-Effects Models using ‘Eigen’ and S4. Version 1.1-21 (March 5, 2019). Available on <https://cran.r-project.org/web/packages/lme4/lme4.pdf> (14.10.2019).
- Beck A., Stutz H-P. B. and Ziswiler V. (1989). Das Beutespektrum der Kleinen Hufeisennase *Rhinolophus hipposideros* (Bechstein, 1800) (Mammalia, Chiroptera). *Revue suisse Zoologie*, 96 (3): 643-650. <https://www.biodiversitylibrary.org/page/41306082#page/168/mode/2up>
- Berkova H., Pokorny M. & Zupal J. (2014). Selection of buildings as maternity roosts by greater mouse-eared bats (*Myotis myotis*). *Journal of Mammalogy*, 95 (5): 1011-1017. <https://doi.org/10.1644/13-MAMM-A-102>.
- Bohnenstengel T., Krättli H., Obrist M.K., Bontadina F., Jaberg C., Ruedi M., Moeschler P. (2014). Rote Liste Fledermäuse. Gefährdete Arten der Schweiz, Stand 2011. Bundesamt für Umwelt, Bern; Centre de Coordination Ouest pour l'étude et la protection des chauvessouris, Genève; Koordinationsstelle Ost für Fledermausschutz, Zürich; Schweizer Zentrum für die Kartografie der Fauna, Neuenburg; Eidgenössische Forschungsanstalt für Wald, Schnee und Landschaft, Birmensdorf. Umwelt-Vollzug Nr. 1412: 95 S.
- Bolker B.M., Brooks M.E., Clark C.J., Geange S.W., Poulsen J.R., Stevens M.H.H. and White J-S.S. (2009). Generalized linear mixed models: a practical guide for ecology and evolution. *Trends in Ecology & Evolution*, 24 (3): 127-135. <https://doi.org/10.1016/j.tree.2008.10.008>.

- Bontadina F., Schofield H. & Naef-Daenzer B. (2002). Radio-tracking reveals that lesser horseshoe bats (*Rhinolophus hipposideros*) forage in woodland. *Journal of Zoology* 258 (3): 281-290. <https://doi.org/10.1017/S0952836902001401>.
- Bontadina F., Hotz T., Märki K. (2006). Die Kleine Hufeisennase im Aufwind. Ursachen der Bedrohung, Lebensraumsprüche und Förderung einer Fledermausart. Haupt Verlag: 79 S.
- Braaker S., Moretti M., Boesch R., Ghazoul J., Obrist M.K. and Bontadina F. (2014). Assessing habitat connectivity for ground-dwelling animals in an urban environment. *Ecological Applications*, 24 (7): 1583-1595. <https://doi.org/10.1890/13-1088.1>.
- Bundesamt für Umwelt – BAFU. (2011). Liste der Nationalen Prioritären Arten. Arten mit nationaler Priorität für die Erhaltung und Förderung, Stand 2010. Bundesamt für Umwelt, Bern. Umwelt-Vollzug Nr. 1103: 132 S.
- Bundesamt für Umwelt – BAFU. (2016). Rote Listen: Gefährdete Arten der Schweiz. *Umwelt-Vollzug*.  
<https://www.bafu.admin.ch/bafu/de/home/themen/biodiversitaet/publikationen-studien/publikationen/rote-listen-gefaehrdete-arten.html>.
- Burles D.W., Brigham R.M., Ring R.A., Reimchen T.E. (2009). Influence of weather on two insectivorous bats in a temperate Pacific Northwest rainforest. *Canadian Journal of Zoology*, 87: 132-138. <https://doi.org/10.1139/Z08-146>.
- Burnham K.P. & Anderson D.R. (2004). Multimodel Inference: Understanding AIC and BIC in Model Selection. *Sociological Methods & Research* 33 (2): 261-304.  
<https://doi.org/10.1177/0049124104268644>.
- Carravieri A. & Scheifler R. (2013). Effets des substances chimiques sur les chiroptères: Synthèse bibliographique. *Le Rhinolophe* 19: 1–46.
- Dickson B.G., Albano C.M., Anantharaman R., Beier P., Fargione J., Graves T.A., Gray M.E., Hall K.R., Lawler J.L., Leonard P.B., Littlefield C.E., McClure M.L., Novembre J., Schloss C.A., Schumaker N.H., Shah V.B. and Theobald D.M. (2018). Circuit-theory applications to connectivity science and conservation. *Conservation Biology*, 33 (2): 239-249. <https://doi.org/10.1111/cobi.13230>.
- Drescher C. (2004). Radiotracking of *Myotis myotis* (Chiroptera, Vespertilionidae) in South Tyrol and implications for its conservation. *Mammalia*, 68 (4), pp. 387-395.  
<https://doi.org/10.1515/mamm.2004.038>
- Downs N.C., Beaton V., Guest J., Polanski J., Pobinson S.L., Racey P.A. (2003). The effects of illuminating the roost entrance on the emergence behaviour of *Pipistrellus pygmaeus*. *Biological Conservation*, 111, 247-252. [https://doi.org/10.1016/S0006-3207\(02\)00298-7](https://doi.org/10.1016/S0006-3207(02)00298-7)

- EFA – European Environment Agency (2011). Landscape fragmentation in Europe. Joint EFA-FOEN report. *EFA Report* No 2/2011.  
<https://www.eea.europa.eu/publications/landscape-fragmentation-in-europe>.
- Graclik A. & Wasielewski O. (2012). Diet composition of *Myotis myotis* (Chiroptera, Vespertilionidae) in western Poland: results of fecal analyses. *Turkish Journal of Zoology*, 36 (2), 209-213. <https://doi.org/10.3906/zoo-1007-35>.
- Grimm N.B., Faeth S.H., Golubiewski N.E., Redman C.L., Wu J., Bai X. and Briggs J.M. (2008). Global Change and the Ecology of Cities. *Science* 319 (5864): 756-760.  
<https://doi.org/10.1126/science.1150195>.
- Güttinger R. (1994). Ist in Mitteleuropa das Klima der primär begrenzende Faktor für das Vorkommen von Fortpflanzungskolonien des Grossen Mausohrs (*Myotis myotis*)?. *Berichte der St. Gallischen Naturwissenschaftlichen Gesellschaft*. 87. Band, pp. 87-92.
- Güttinger R. (1997). Jagdhabitats des Grossen Mausohrs (*Myotis myotis*) in der modernen Kulturlandschaft. BUWAL-Reihe Umwelt, Nr. 288. Bundesamt für Umwelt, Wald und Landschaft. 140 Seiten.
- Harrison X.A., Donaldson L., Correa-Cano M.E., Evans J., Fisher D.N., Goodwin C.E.D., Robinson B.S., Hodgson D.J. and Inger R. (2018). A brief introduction to mixed effects modelling and multi-model inference in ecology. *PeerJ* 6:e4794.  
<https://doi.org/10.7717/peerj.4794>
- Holzhaider J., Kriner E., Rudolph B-U., Zahn A. (2002). Radio-tracking a Lesser horseshoe bat (*Rhinolophus hipposideros*) in Bavaria: an experiment to locate roosts and foraging sites. *Myotis*, 40, 47-54.
- Limpens H.J.G.A. & Kapteyn K. (1991). Bats, their behaviour and linear landscape elements. *Myotis*, 29: 39-48. Bonn, Okt. 1991.
- Linton D.M. & Macdonald D.W. (2018). Spring weather conditions influence breeding phenology and reproductive success in sympatric bat populations. *Journal of Animal Ecology*, 87 (4): 1080-1090. <https://doi.org/10.1111/1365-2656.12832>.
- McRae B.H., Dickson B.G., Keitt T.H. and Shah V.B. (2008). Using circuit theory to model connectivity in ecology, evolution and conservation. *Ecology*, 89 (19): 2712-2724.  
<https://doi.org/10.1890/07-1861.1>.
- McRae B.H., Shah V.B. & Mohapatra T.K. (2013). Circuitscape 4 User Guide. The Natural Conservancy. <https://circuitscape.org>.
- Motte G. & Libois R. (2002). Conservation of the lesser horseshoe bat (*Rhinolophus hipposideros* Bechstein, 1800) (Mammalia: Chiroptera) in Belgium. A case study of feeding habitat requirements. *Belgian Journal of Zoology*, 132 (1), 47-52.

- Obrist M.K. & Boesch R. (2018). BatScope manages acoustic recordings, analyses calls and classifies bat species automatically. *Canadian Journal of Zoology*, 96, pp. 939-954. <https://doi.org/10.1139/cjz-2017-0103>. <http://www.batscope.ch>.
- Pauwels J., Le Viol I., Azam C., Valet N., Julien J.-F., Bas Y., Lemarchand C., Sanchez de Miguel A. and Keribirou C. (2019). Accounting for artificial light impact on bat activity for a biodiversity-friendly urban planning. *Landscape and Urban Planning* 183: 12-25. <https://doi.org/10.1016/j.landurbplan.2018.08.030>.
- R Core Team (2018). R: a language and environment for statistical computing. F Foundation for Statistical Computing, Vienna, Austria. URL: <https://www.R-project.org/>.
- Ravessoud T. (2017). Finding a method to predict the commuting activity of bats (unpublished). Master Thesis, Université de Lausanne.
- Rydell J. (1989). Feeding activity of the northern bat *Eptesicus nilssonii* during pregnancy and lactation. *Oecologica*, 80 (4): 562-565
- Schofield H.W. (1996). The ecology and conservation biology of *Rhinolophus hipposideros*, the lesser horseshoe bat. PhD thesis, University of Aberdeen, UK.
- Stebbing R.E. & Griffith F. (1986). *Distribution and status of Bats in Europe*. Abbots Ripton, Hutingdon UK, Institute of Terrestrial Ecology, 142pp.
- Steck C. & Güttinger R. (2006). Heute wie vor hundert Jahren: Laufkäfer sind die Hauptbeute des Grossen Mausohrs (*Myotis myotis*). *Schweizerische Zeitschrift für Forstwesen* 157, 8: 339-347.
- Stoate C., Boatman N.D., Borralho R.J., Rio Carvalho C., de Snoo G.R., Eden P. (2001). Ecological impacts of arable intensification in Europe. *Journal of Environmental Management*, 63, 337-365. <https://doi.org/10.1006/jema.2001.0473>
- Stone E.L., Jones G. & Harris S. (2009). Street Lighting Disturbs Commuting Bats. *Current Biology*, 19, 1123-1127. <https://doi.org/10.1016/j.cub.2009.05.058>
- Stone E.L., Jones G. & Harris S. (2012). Conserving energy at a cost to biodiversity? Impacts of LED lighting on bats. *Global Change Biology*, 18, 2458-2465. <https://doi.org/10.1111/j.1365-2486.2012.02705.x>
- Stone E.L., Harris S. & Jones G. (2015). Impacts of artificial lighting on bats: a review of challenges and solutions. *Mammalian Biology* 80 (3): 213-219. <https://doi.org/10.1016/j.mambio.2015.02.004>.
- Walsh A.L. & Harris S. (1996). Foraging habitat preferences of vespertilionid bats in Britain. *Journal of Applied Ecology*, 33, 508-518. <https://doi.org/10.2307/2404980>
- Zahn A., Haselbach H., Güttinger R. (2005). Foraging activity of central European *Myotis myotis* in a landscape dominated by spruce monocultures. *Mammalian Biology*. 70:1: 265-270.

## APPENDIX

Full data table	Appendix I
Setting of Batlogger M for recording	Appendix II
Filter queries applied to verify <i>M. myotis</i> calls	Appendix III
Correlation Coefficient matrices	Appendix IV
Distribution of total bat activity for each study site	Appendix V
Full model ranking tables	Appendix VI
Eigenständigkeitserklärung	

## Appendix I

Table 14: Full data table

site-ID	Community	x-Koord	y-Koord	Bat-logger	Recording Date	Bat Species	Bat Activity	Distance site to roost [m]	Roost size [individuals]	Lux1	Lux2	Lux3	Lux4	Lux5	Lux_mean	light	Corridor	Corridor value current_adv 5	Corridor value current_adv 15	Corridor value current_subavg 5	Corridor value current_subavg 15	Corridor value current_submax 5	Corridor value current_submax 15	Distance Site to LCP [m]	Weather Station	Distance Stat. to Roost [km]	Temperature [°C]	Humidity [%]	Precipitation [mm]	Wind speed [m/s]	Comment	
site-ID	Comm			BL	Rec_Date		Activity	Dist_Roost	R_size								Corridor	Adv5	Adv15	Subavg5	Subavg15	Submax5	Submax15	Dist_LCP			Temp	Humi	Prec	Wind	Variable name for GLMM	
116	Kallnach	584652	207463	1061	09.07.2019	M.m.	20	61	411	0	0	0	0	0	0	0	no	yes	0.130979	0.125369	0.037107	0.027962	0.038701	0.029265	31.8	Mühleberg	5.9	16.1	70.6	0	1.1	
117	Kallnach	584783	207563	1053	09.07.2019	M.m.	3	211	411	2	2	2	2	5	2.6	yes	yes	0.027690699	0.027690699	0.00666552	0.00666552	0.00742969	0.00742969	26.5	Mühleberg	5.9	16.1	70.6	0	1.1	Dimable street lamp (5 lx when traffic; 2 lx without traffic)	
118	Kallnach	584904	207860	1048	09.07.2019	M.m.	4	497	411	0	0	0	0	0	0	no	yes	0.0142223	0.0142223	0.00382911	0.00382911	0.00464098	0.00464098	121.1	Mühleberg	5.9	16.1	70.6	0	1.1		
119	Kallnach	584703	207524	1029	09.07.2019	M.m.	4	122	411	0	0	0	0	0	0	yes	yes	0.045030199	0.045030199	0.0118896	0.0118896	0.0127709	0.0127709	20.5	Mühleberg	5.9	16.1	70.6	0	1.1		
120	Kallnach	584559	207378	1057	09.07.2019	M.m.	NA	101	411	0.5	0.5	1	0.5	0.5	0.6	yes	no	0.024319001	0.024319001	0.00507028	0.00507028	0.00682226	0.00682226	28.9	Mühleberg	5.9	16.1	70.6	0	1.1	NoData-> microphone possibly damaged (open)	
121	Kallnach	584474	207454	1037	09.07.2019	M.m.	0	120	411	7	8	7	5	6	6.6	yes	no	0.0176121	0.0176121	0.00441713	0.00441713	0.0059535	0.0059535	71.4	Mühleberg	5.9	16.1	70.6	0	1.1		
122	Kallnach	584579	207522	1032	09.07.2019	M.m.	0	51	411	1	1	1	0.5	1	0.9	yes	yes	0.0607704	0.0607704	0.0153597	0.0153597	0.016778201	0.016778201	48.1	Mühleberg	5.9	16.1	70.6	0	1.1		
123	Kallnach	584526	207284	1075	09.07.2019	M.m.	12	200	411	0	0	0	0	0	0	yes	no	0.0110964	0.0110964	0.00262088	0.00262088	0.00341375	0.00341375	68.5	Mühleberg	5.9	16.1	70.6	0	1.1		
124	Kallnach	584529	207078	1073	09.07.2019	M.m.	65	400	411	0	0	0	0	0	0	no	yes	0.0159657	0.0159657	0.00398686	0.00398686	0.00559038	0.00559038	20.5	Mühleberg	5.9	16.1	70.6	0	1.1		
125	Kallnach	584565	207152	1031	09.07.2019	M.m.	31	322	411	0.5	0	0	0	0.5	0.2	yes	yes	0.021523301	0.021523301	0.00506903	0.00506903	0.00718839	0.00718839	0.5	Mühleberg	5.9	16.1	70.6	0	1.1		
126	Kallnach	584765	207406	1063	09.07.2019	M.m.	22	186	411	0	0	0	0	0	0	no	yes	0.0241218	0.0241218	0.00598213	0.00598213	0.00638468	0.00638468	149.2	Mühleberg	5.9	16.1	70.6	0	1.1		
127	Kallnach	585044	207418	1074	09.07.2019	M.m.	3	455	411	0	0	0	0	0	0	no	no	0.00489142	0.00489142	0.0014938	0.0014938	0.00171673	0.00171673	302.1	Mühleberg	5.9	16.1	70.6	0	1.1		
128	Kallnach	584731	207321	1056	09.07.2019	M.m.	1	206	411	0.5	0	0	0	0	0.1	no	no	0.0112099	0.0112099	0.00262128	0.00262128	0.003511	0.003511	136.7	Mühleberg	5.9	16.1	70.6	0	1.1		
129	Kallnach	584383	207446	1034	09.07.2019	M.m.	2	211	411	0	0	0	0	0	0	no	no	0.0100002	0.0100002	0.00230017	0.00230017	0.00341776	0.00341776	111.9	Mühleberg	5.9	16.1	70.6	0	1.1		
130	Kallnach	584493	207643	1049	09.07.2019	M.m.	18	197	411	1	0	0.5	0.5	1	0.6	yes	no	0.0149779	0.0149779	0.00393202	0.00393202	0.00521801	0.00521801	103.5	Mühleberg	5.9	16.1	70.6	0	1.1		
131	Kallnach	584300	207759	1236	09.07.2019	M.m.	2	409	411	0	0	0	0	0	0	no	no	0.00472915	0.00472915	0.00130418	0.00130418	0.00324199	0.00324199	112.4	Mühleberg	5.9	16.1	70.6	0	1.1		
132	Därstetten	604201	167465	1037	01.06.2019	R.h.	2	65	110	0	0	0	0	0	0	yes	yes	0.0610594	0.061362401	0.0152393	0.0153139	0.0155674	0.015645299	7.8	Boltigen	9.3	11.6	90.6	0	0.9		
133	Därstetten	604116	167606	1249	01.06.2019	R.h.	0	113	110	0	0.5	0	0	0	0	1	yes	yes	0.058584198	0.052783899	0.0145866	0.013151	0.0151203	0.0136328	113.2	Boltigen	9.3	11.6	90.6	0	0.9	
134	Därstetten	604373	167465	1036	01.06.2019	R.h.	0	185	110	2	3	2	1	30	7.6	yes	no	0.0136542	0.0122777	0.00341461	0.00306948	0.00357669	0.00319935	127.5	Boltigen	9.3	11.6	90.6	0	0.9		
135	Därstetten	604119	167537	1074	01.06.2019	R.h.	0	81	110	0	1	1	0	0	0.4	no	no	0.0461585	0.0475673	0.0116346	0.0120337	0.0120736	0.0126002	79.1	Boltigen	9.3	11.6	90.6	0	0.9		
136	Därstetten	604213	167403	1031	01.06.2019	R.h.	3	128	110	0	0	0	0	0	0	no	yes	0.103514999	0.100339003	0.026148099	0.025335699	0.0280184	0.0271322	5.5	Boltigen	9.3	11.6	90.6	0	0.9		
137	Därstetten	604330	167803	1057	01.06.2019	R.h.	2	302	110	0	0	0	0	0	0	no	yes	0.00569192	0.00737677	0.00150186	0.0019476	0.001526	0.00197788	305.7	Boltigen	9.3	11.6	90.6	0	0.9		
138	Därstetten	604075	167651	1063	01.06.2019	R.h.	2	174	110	0	0	0	0	0	0	no	no	0.031519599	0.032044601	0.00782876	0.00795922	0.00857955	0.00871799	173.9	Boltigen	9.3	11.6	90.6	0	0.9		
139	Därstetten	604388	167626	1073	01.06.2019	R.h.	0	211	110	0	0.5	0	0	0.5	0.2	no	no	0.00921198	0.00953682	0.00228078	0.00236432	0.00254994	0.00263549	214.5	Boltigen	9.3	11.6	90.6	0	0.9		
140	Därstetten	604566	167278	1048	01.06.2019	R.h.	10	444	110	0	0	0	0	0	0	yes	yes	0.0262377	0.0358398	0.00666542	0.00911045	0.00731872	0.0100012	20.5	Boltigen	9.3	11.6	90.6	0	0.9		
141	Därstetten	604278	167393	1053	01.06.2019	R.h.	0	158	110	0	0	0	0	0	0	no	no	0.0157042	0.015992099	0.00394368	0.00401599	0.004202	0.00427812	66.3	Boltigen	9.3	11.6	90.6	0	0.9		
142	Därstetten	603998	167445	1034	01.06.2019	R.h.	2	219	110	0	0	0	0	0	0	no	no	0.00845661	0.00823013	0.0020226	0.0020226	0.00242145	0.00235754	179.5	Boltigen	9.3	11.6	90.6	0	0.9		
143	Därstetten	604421	167362	1029	01.06.2019	R.h.	NA	278	110	0	0	0	0	0	0	no	yes	0.00381319	0.027375899	0.000977351	0.00695743	0.00143562	0.00783998	24.7	Boltigen	9.3	11.6	90.6	0	0.9	NoData-> BL shut down	
144	Därstetten	604280	167586	1075	01.06.2019	R.h.	0	98	110	0	0.5	0.5	0.5	0	0.3	yes	no	0.023440201	0.0230226	0.00583221	0.00574008	0.006013	0.00591883	101.1	Boltigen	9.3	11.6	90.6	0	0.9		
145	Därstetten	604636	167691	1032	01.06.2019	R.h.	4	465	110	0	0	0	0	0	0	no	yes	0.000459346	0.00057242	0.000112593	0.000140318	0.00014723	0.00018331	409.8	Boltigen	9.3	11.6	90.6	0	0.9		
146	Därstetten	603780	167647	1056	01.06.2019	R.h.	0	436	110	81	30	40	32	31	42.8	yes	no	0.00151535	0.00169426	0.000384319	0.000434222	0.000462994	0.000511379	434.3	Boltigen	9.3	11.6	90.6	0	0.9		
147	Därstetten	604492	166996	1061	01.06.2019	R.h.	3	609	110	0	0	0	0	0	0	yes	yes	0.116623998	0.078406103	0.00972363	0.0146004	0.019447301	0.021526299	1.6	Boltigen	9.3	11.6	90.6	0	0.9		
148	Amsoldingen	610714	175181	3314	31.05.2019	R.h.	1	53	60	1	1	1	1	1	1	yes	yes	0.139109999	0.105435997	0.035592198	0.0270366	0.036140699	0.0274218	46.7	Thun	2.6	13.3	77.8	0	0.9		
149	Amsoldingen	610717	175091	1031	31.05.2019	R.h.	2	61	60	0.5	0.5	0	0	0	0	2	yes	yes	0.058017202	0.059165299	0.0146624	0.0149551	0.0147122	0.0150056	27.1	Thun	2.6	13.3	77.8	0	0.9	
150	Amsoldingen	610149	175364	1057	31.05.2019	R.h.	3	576	60	0	0	0	0	0	0	no	yes	0.020013001	0.071045399	0.00481491	0.0169021	0.00532244	0.018623	577.7	Thun	2.6	13.3	77.8	0	0.9		
151	Amsoldingen	610753	175226	1061	31.05.2019	R.h.	4	113	60	0	0	0	0	0	0	no	yes	0.0363678	0.0459309	0.00937679	0.0118416											

site-ID	Community	x-Koord	y-Koord	Bat-logger	Recording Date	Species	Bat Activity	Distance site to roost [m]	Roost size [individuals]	Lux1	Lux2	Lux3	Lux4	Lux5	Lux_mean	light	corridor	Corridor value current_adv 5	Corridor value current_adv 15	Corridor value current_subavg 5	Corridor value current_subavg 15	Corridor value current_submax 5	Corridor value current_submax 15	Distance Site to LCP [m]	Weather Station	Distance Stat. to Roost [km]	Temperature [°C]	Humidity [%]	Precipitation [mm]	Wind speed [m/s]	Comment
196	Mühlau	672167	231500	1063	06.06.2019	M.m.	43	127	528	0.5	0.5	0.5	0.5	0.5	0.5	0.3	no	0.00166193	0.017163699	0.003886093	0.00388603	0.00723367	0.007163641	130.5	Cham	7.3	10.9	85.3	0	2.1	
197	Mühlau	672633	231699	1057	06.06.2019	M.m.	2	634	528	0	0	0	0	0	0	0	no	0.000458323	0.0303319	0.000160866	0.00698794	0.000884114	0.042731799	18.5	Cham	7.3	10.9	85.3	0	2.1	
198	Mühlau	672023	231378	1075	06.06.2019	M.m.	2	77	528	5	7	6	2	2	4.4	yes	yes	0.081456497	0.079772301	0.020881001	0.0204744	0.0226155	0.022235099	9.9	Cham	7.3	10.9	85.3	0	2.1	
199	Mühlau	671598	230948	1031	06.06.2019	M.m.	0	676	528	0	0	0	0	0	0	0	no	yes	0.188334003	0.152246997	0.051714201	0.041834202	0.086602798	0.0699986	16.1	Cham	7.3	10.9	85.3	0	2.1
200	Mühlau	671953	231380	1029	06.06.2019	M.m.	3	120	528	4.5	4	2	6	9	5.1	yes	yes	0.002661	0.170708001	0.000728098	0.0448539	0.000893566	0.052359988	2.5	Cham	7.3	10.9	85.3	0	2.1	
201	Mühlau	671743	231242	1249	06.06.2019	M.m.	4	371	528	0	0	0	0.5	0	0.1	no	yes	0.000192047	0.000192498	0.000333307	0.000337197	0.000515884	0.000519439	32.5	Cham	7.3	10.9	85.3	0	2.1	
202	Mühlau	672246	231440	1048	06.06.2019	M.m.	9	196	528	0	0	0	0	0	0	0	no	no	0.00929148	0.00926916	0.00208905	0.0020826	0.0054245	0.0053708	191.6	Cham	7.3	10.9	85.3	0	2.1
203	Mühlau	672425	231391	1032	06.06.2019	M.m.	3	380	528	0	0	0	0	0	0	0	no	no	0.0143341	0.0134049	0.00291333	0.00281614	0.0123048	0.012058	39.6	Cham	7.3	10.9	85.3	0	2.1
204	Mühlau	671584	231322	1056	06.06.2019	M.m.	0	483	528	1	0	1	3	2	1.4	no	no	0.0140241	0.0142115	0.00368747	0.00373686	0.00617414	0.00625711	9.2	Cham	7.3	10.9	85.3	0	2.1	
205	Mühlau	671827	231688	1053	06.06.2019	M.m.	3	326	528	0.5	0	0.5	0.5	0	0.3	yes	no	0.00940815	0.00941278	0.00261578	0.00261795	0.00367432	0.00367395	325.6	Cham	7.3	10.9	85.3	0	2.1	
206	Mühlau	672044	231254	1061	06.06.2019	M.m.	0	196	528	1	1	2.5	1	1	1.3	yes	no	0.00662337	0.00675595	0.00242038	0.00241196	0.00269656	0.00275888	82.7	Cham	7.3	10.9	85.3	0	2.1	
207	Mühlau	672128	231627	1036	06.06.2019	M.m.	0	193	528	1	1	1	1	1	1	yes	no	0.00638761	0.00644444	0.00195553	0.00198163	0.0043942	0.00442238	196.7	Cham	7.3	10.9	85.3	0	2.1	
208	Mühlau	671894	231588	1037	06.06.2019	M.m.	0	208	528	3	1	5	3	2	2.8	yes	no	0.00801336	0.00804077	0.00226457	0.00227328	0.00279001	0.00279753	208.1	Cham	7.3	10.9	85.3	0	2.1	
209	Mühlau	672538	231611	1073	06.06.2019	M.m.	1	514	528	0	0	0	0	0	0	yes	yes	0.00273104	0.00276431	0.000621711	0.000629217	0.00193297	0.00195649	37.7	Cham	7.3	10.9	85.3	0	2.1	
210	Mühlau	671856	231350	1074	06.06.2019	M.m.	5	218	528	0	0	0	0	0	0	yes	yes	0.277741998	0.216479003	0.0736138	0.057359599	0.0892803	0.069886804	2.5	Cham	7.3	10.9	85.3	0	2.1	
211	Mühlau	671413	231754	3314	06.06.2019	M.m.	1	706	528	0	0	0	0	0	0	no	yes	1.82413E-05	0.0066316	4.94641E-06	0.00182751	8.16858E-06	0.00294284	372.6	Cham	7.3	10.9	85.3	0	2.1	
212	Wegenstetten	637381	260960	1029	16.07.2019	M.m.	7	57	200	1	1	2	3	1	1.6	yes	yes	0.351514012	0.329396009	0.137303993	0.106339999	0.137786001	0.107329997	0.5	Rünenberg	8.3	18.8	51.1	0	0.6	
213	Wegenstetten	637292	260894	1249	16.07.2019	M.m.	2	168	200	1	1	1	1	1	1	yes	yes	0.047515102	0.048588298	0.0107804	0.0111167	0.0109777	0.0113188	60.5	Rünenberg	8.3	18.8	51.1	0	0.6	
214	Wegenstetten	637495	260594	1061	16.07.2019	M.m.	43	406	200	0	0	0	0	0	0	no	yes	0.172597006	0.078547403	0.0405868	0.018468799	0.065358803	0.029682601	0.5	Rünenberg	8.3	18.8	51.1	0	0.6	
215	Wegenstetten	637393	260780	1048	16.07.2019	M.m.	64	217	200	0	0	0	0	0	0	no	yes	0.0163367	0.0171795	0.00390026	0.00409938	0.00553246	0.00583346	14.1	Rünenberg	8.3	18.8	51.1	0	0.6	
216	Wegenstetten	637155	261083	1031	16.07.2019	M.m.	0	286	200	0	0	0	0	0	0	no	yes	0.041475099	0.039152499	0.0103006	0.00981641	0.0134179	0.0127826	0.0	Rünenberg	8.3	18.8	51.1	0	0.6	
217	Wegenstetten	637150	261341	1063	16.07.2019	M.m.	3	444	200	1	1	1	1	1	1	yes	yes	0.101496004	0.187608007	0.029035	0.053853501	0.0440052	0.082684398	1.4	Rünenberg	8.3	18.8	51.1	0	0.6	
218	Wegenstetten	637213	261428	1036	16.07.2019	M.m.	1	484	200	0	0	0	0	0	0	no	yes	0.00725878	0.00738412	0.00231145	0.00235568	0.00343853	0.00350594	16.3	Rünenberg	8.3	18.8	51.1	0	0.6	
219	Wegenstetten	637538	261132	1032	16.07.2019	M.m.	2	177	200	1	0	1	2	5	1.8	yes	yes	0.0172826	0.016543699	0.00436416	0.00420356	0.00483657	0.00476211	182.8	Rünenberg	8.3	18.8	51.1	0	0.6	
220	Wegenstetten	637414	261091	1037	16.07.2019	M.m.	0	98	200	9	4	4	12	23	10.4	yes	no	0.0226241	0.0224723	0.00579161	0.00579161	0.0057532	0.00632677	101.9	Rünenberg	8.3	18.8	51.1	0	0.6	
221	Wegenstetten	637504	260980	3314	16.07.2019	M.m.	3	78	200	0	0	0.5	0	0	0.1	no	no	0.0249616	0.025005201	0.0060855	0.00607912	0.00698333	0.00699578	81.1	Rünenberg	8.3	18.8	51.1	0	0.6	
222	Wegenstetten	637191	260786	1075	16.07.2019	M.m.	0	315	200	2	1	2	5	3	2.6	yes	no	0.0114936	0.0113039	0.0026808	0.00272038	0.00307128	0.0031542	168.0	Rünenberg	8.3	18.8	51.1	0	0.6	
223	Wegenstetten	637752	261208	1073	16.07.2019	M.m.	0	389	200	0	0	0	0	0	0	no	no	0.0038993	0.00389967	0.00105668	0.00105005	0.0015175	0.00150534	394.5	Rünenberg	8.3	18.8	51.1	0	0.6	
224	Wegenstetten	637554	260821	1074	16.07.2019	M.m.	4	215	200	0	0	0	0	0	0	no	no	0.00897264	0.00886841	0.00215184	0.00212959	0.0030343	0.002996	171.6	Rünenberg	8.3	18.8	51.1	0	0.6	
225	Wegenstetten	637614	261007	1057	16.07.2019	M.m.	4	187	200	0	0	0	0	0	0	no	no	0.00984233	0.00980043	0.00235355	0.00234593	0.00301771	0.00300992	191.3	Rünenberg	8.3	18.8	51.1	0	0.6	
226	Wegenstetten	637050	260869	1056	16.07.2019	M.m.	1	397	200	3	1	0	7	1	2.4	yes	no	0.00629796	0.00627529	0.00191636	0.00192633	0.00230582	0.00230048	207.9	Rünenberg	8.3	18.8	51.1	0	0.6	
227	Wegenstetten	637354	261206	1053	16.07.2019	M.m.	1	224	200	1	1	1	1	2	1.2	yes	no	0.016218601	0.016514299	0.00428313	0.00436219	0.00510822	0.00520585	176.2	Rünenberg	8.3	18.8	51.1	0	0.6	
228	Buttisholz	650164	216902	1053	05.07.2019	M.m.	55	50	569	0	0	0	0	0	0	no	yes	0.054822698	0.055429999	0.0131997	0.0131997	0.0133399	0.0133399	11.2	Egolzwil	11.2	20.6	59.1	0	0.6	
229	Buttisholz	650223	216998	1031	05.07.2019	M.m.	24	87	569	0	0	0	0	0	0	no	yes	0.057004198	0.0576705	0.0152597	0.0154742	0.0152597	0.0154742	17.5	Egolzwil	11.2	20.6	59.1	0	0.6	
230	Buttisholz	650140	216993	1074	05.07.2019	M.m.	9	157	569	0	0	0	0	0	0	no	yes	0.0240294	0.0229422	0.00427941	0.00433269	0.00427941	0.00433269	162.1	Egolzwil	11.2	20.6	59.1	0	0.6	
231	Buttisholz	650122	216834	1057	05.07.2019	M.m.	16	119	569	0	0	0	0	0	0	no	yes	0.025428399	0.0325955	0.00527138	0.00685923	0.00527138	0.00685923	117.1	Egolzwil	11.2	20.6	59.1	0	0.6	
232	Buttisholz	650354	217192	1061	05.07.2019	M.m.	61	317	569	0	0	0	0	0	0	no	yes	0.0204053	0.021233501	0.00602153	0.00627447	0.00602153	0.00627447	11.3	Egolzwil	11.2	20.6	59.1	0		

site ID	Community	x-Koord	y-Koord	Bat-logger	Recording Date	Bat Species	Bat Activity	Distance to roost [m]	Roost size		Corridor value					Corridor	Distance Site to LCP [m]	Weather Station	Distance to Roost [km]	Temperature [°C]	Humidity [%]	Precipitation [mm]	Wind speed [m/s]	Comment							
									Individuals	Roost size	current_adv 5	current_adv 15	current_subavg 5	current_subavg 15	current_submax 5										current_submax 15	Lux1	Lux2	Lux3	Lux4	Lux5	Lux_mean
276	Giswil	654480	186913	1032	13.06.2019	R.h.	0	259	400	0	0	0	0	0	0	no	yes	0.0179535	0.0188703	0.00451589	0.00474561	0.0045918	0.00482997	262.6	Giswil	3.3	13.8	86.3	0	1.4	
277	Giswil	654657	186897	1029	13.06.2019	R.h.	1	159	400	0	0	0	0	0	0	no	yes	0.030609701	0.0286352	0.00769745	0.0071988	0.00782245	0.0073138	162.0	Giswil	3.3	13.8	86.3	0	1.4	
278	Giswil	654851	186862	1063	13.06.2019	R.h.	20	241	400	0	0	0	0	0	0	no	yes	0.027107099	0.0228508	0.00689518	0.00580907	0.00708406	0.00586295	68.1	Giswil	3.3	13.8	86.3	0	1.4	
279	Giswil	654386	187263	1053	13.06.2019	R.h.	8	379	400	0	0	0	0	0	0	no	yes	0.00821557	0.0166761	0.0021167	0.00430526	0.00240783	0.00531104	282.9	Giswil	3.3	13.8	86.3	0	1.4	
280	Giswil	654668	187085	1074	13.06.2019	R.h.	2	47	400	1	1	1	1	1	1	no	yes	0.078404501	0.072125897	0.019533001	0.017927101	0.0195641	0.017958401	47.4	Giswil	3.3	13.8	86.3	0	1.4	
281	Giswil	654681	187006	1037	13.06.2019	R.h.	0	48	400	1	1	1	1	1	1	no	yes	0.065344602	0.066509597	0.016298199	0.016584599	0.0164128	0.0167011	51.2	Giswil	3.3	13.8	86.3	0	1.4	
282	Giswil	654822	187067	1249	13.06.2019	R.h.	1	123	400	0.5	0	0	0.5	0.5	0.3	no	yes	0.046381202	0.0398046	0.0115464	0.00990899	0.011768	0.0100994	46.0	Giswil	3.3	13.8	86.3	0	1.4	
283	Giswil	654806	187107	1056	13.06.2019	R.h.	1	120	400	0	0	0	0	0	0	no	yes	0.0381651	0.037795901	0.00948874	0.00939701	0.00969454	0.00960148	6.4	Giswil	3.3	13.8	86.3	0	1.4	
284	Giswil	654591	187277	1031	13.06.2019	R.h.	1	252	400	0	0	0	0	0	0	no	no	0.00913645	0.00872072	0.00229552	0.0021936	0.00238116	0.00227334	114.6	Giswil	3.3	13.8	86.3	0	1.4	
285	Giswil	654356	187066	1073	13.06.2019	R.h.	2	344	400	0	0	0	0	0	0	no	no	0.00521484	0.00592286	0.00131882	0.00149777	0.00135323	0.00153637	346.8	Giswil	3.3	13.8	86.3	0	1.4	
286	Giswil	654547	186735	1075	13.06.2019	R.h.	0	350	400	0	0	0	0	0	0	no	no	0.0046379	0.0047118	0.00117862	0.00119696	0.0012035	0.00122183	168.3	Giswil	3.3	13.8	86.3	0	1.4	
287	Giswil	654967	187029	1036	13.06.2019	R.h.	2	268	400	0	0	0	0	0	0	no	no	0.00554224	0.0056646	0.00154284	0.00155735	0.00169398	0.00169605	84.2	Giswil	3.3	13.8	86.3	0	1.4	
288	Giswil	654985	186943	1048	13.06.2019	R.h.	1	304	400	0	0	0	0	0	0	no	no	0.00713362	0.00780743	0.00191793	0.00208457	0.00214833	0.00231336	30.4	Giswil	3.3	13.8	86.3	0	1.4	
289	Giswil	654826	187188	3314	13.06.2019	R.h.	23	187	400	0	0	0	0	0	0	no	no	0.027102301	0.027355799	0.00667753	0.0060338	0.00691403	0.00727386	6.5	Giswil	3.3	13.8	86.3	0	1.4	
290	Giswil	654469	187024	1057	13.06.2019	R.h.	0	232	400	0	0	0	0	0	0	no	no	0.00760616	0.00776254	0.00191099	0.00195085	0.0019318	0.0019727	235.2	Giswil	3.3	13.8	86.3	0	1.4	
291	Giswil	654411	187204	1061	13.06.2019	R.h.	3	327	400	0	0	0	0	0	0	no	no	0.00978755	0.00926808	0.00250135	0.00236684	0.00266451	0.00249794	294.7	Giswil	3.3	13.8	86.3	0	1.4	
292	Beggingen	682434	291313	1075	11.07.2019	M.m.	6	84	630	0	0.5	0.5	0	0	0.2	no	yes	0.251944005	0.224160001	0.063923702	0.065863301	0.065123402	0.057922799	3.5	Hallau	9.2	13.7	91.2	0	0.3	
293	Beggingen	682548	291168	1048	11.07.2019	M.m.	32	227	630	1	0.5	0.5	1	1	0.8	yes	yes	0.074662603	0.056938201	0.01871201	0.0150038	0.020161601	0.0153581	19.3	Hallau	9.2	13.7	91.2	0	0.3	
294	Beggingen	682205	291170	1031	11.07.2019	M.m.	12	189	630	0	0	0	0	0	0	no	yes	0.00936872	0.0185706	0.0027256	0.00276095	0.00282476	0.00286181	31.6	Hallau	9.2	13.7	91.2	0	0.3	
295	Beggingen	682601	291037	1037	11.07.2019	M.m.	7	351	630	0	0	0	0	0	0	no	yes	0.0272955	0.080631901	0.007168	0.015887201	0.00737645	0.0163853	15.5	Hallau	9.2	13.7	91.2	0	0.3	
296	Beggingen	682535	290938	1061	11.07.2019	M.m.	3	392	630	1	0.5	0.5	1	0.5	0.7	yes	yes	0.035232101	0.0414485	0.009031	0.0099929	0.00926347	0.010255	69.6	Hallau	9.2	13.7	91.2	0	0.3	
297	Beggingen	682684	291464	1074	11.07.2019	M.m.	14	375	630	0	0	0	0	0	0	no	yes	0.00220251	0.019132299	0.000700755	0.00477712	0.000730009	0.00489382	231.7	Hallau	9.2	13.7	91.2	0	0.3	
298	Beggingen	682077	291178	1029	11.07.2019	M.m.	2	297	630	1	1	2	1	2	1.4	yes	yes	0.096808702	0.113023966	0.0250593	0.0290263	0.0261587	0.0303976	6.4	Hallau	9.2	13.7	91.2	0	0.3	
299	Beggingen	682277	291312	1249	11.07.2019	M.m.	6	81	630	0	0.5	0.5	0	0	0.2	no	yes	0.0878148	0.084667496	0.021661701	0.0208993	0.021897299	0.021134101	75.7	Hallau	9.2	13.7	91.2	0	0.3	
300	Beggingen	682187	291465	1063	11.07.2019	M.m.	4	245	630	0	0	0	0	0	0	no	no	0.00616904	0.00647327	0.00125619	0.0013144	0.00127833	0.00133537	226.1	Hallau	9.2	13.7	91.2	0	0.3	
301	Beggingen	682436	291460	1036	11.07.2019	M.m.	3	192	630	0	0	0	0	0	0	no	no	0.00384581	0.00385527	0.000792682	0.000795323	0.00080763	0.000810323	135.2	Hallau	9.2	13.7	91.2	0	0.3	
302	Beggingen	682259	291112	1056	11.07.2019	M.m.	5	198	630	0	0	0	0	0	0	no	no	0.00668015	0.00663158	0.00172672	0.00171412	0.00173749	0.00172502	54.6	Hallau	9.2	13.7	91.2	0	0.3	
303	Beggingen	682252	291248	1032	11.07.2019	M.m.	0	109	630	1	1	1	1	0	0.8	yes	no	0.0111222	0.0109764	0.00286651	0.00282554	0.00291634	0.00287606	55.1	Hallau	9.2	13.7	91.2	0	0.3	
304	Beggingen	681916	291295	3314	11.07.2019	M.m.	0	438	630	0	0	0	0	1	0.2	yes	no	0.00529078	0.00538242	0.0014476	0.00146082	0.00151803	0.00153368	118.8	Hallau	9.2	13.7	91.2	0	0.3	
305	Beggingen	682404	290897	1073	11.07.2019	M.m.	1	392	630	0	0	0	0	0	0	no	no	0.00413246	0.00413465	0.00107797	0.00107854	0.00108989	0.00109047	157.7	Hallau	9.2	13.7	91.2	0	0.3	
306	Beggingen	682290	291343	1053	11.07.2019	M.m.	1	86	630	1	1	1	1	3	1.4	yes	no	0.0144995	0.0142334	0.00379865	0.00383569	0.00390854	0.00394467	72.4	Hallau	9.2	13.7	91.2	0	0.3	
307	Beggingen	682054	291007	1057	11.07.2019	M.m.	9	410	630	1	1	1	1	1	0.8	yes	no	0.00882035	0.00858564	0.00230541	0.0022431	0.00240597	0.0023354	176.8	Hallau	9.2	13.7	91.2	0	0.3	
308	Flawil	733428	252728	1037	20.07.2019	M.m.	2	71	275	1	1	1	5	9	3.4	yes	yes	0.051743001	0.052145399	0.0127898	0.0129032	0.0129374	0.0130316	67.8	Bischofszell	9.8	20	89.5	0	0.8	
309	Flawil	733568	252663	1053	20.07.2019	M.m.	14	94	275	0	0	0	0	0	0	no	yes	0.056136299	0.0566145	0.0139407	0.0140601	0.0140576	0.0141772	96.9	Bischofszell	9.8	20	89.5	0	0.8	
310	Flawil	733216	252876	1074	20.07.2019	M.m.	3	328	275	1	1	1	2	2	1.4	yes	yes	0.0105375	0.015965501	0.00247048	0.00372779	0.00266908	0.00404473	290.3	Bischofszell	9.8	20	89.5	0	0.8	
311	Flawil	733559	252513	1036	20.07.2019	M.m.	39	182	275	0	0	0	0	0	0	no	yes	0.0256109	0.092813604	0.027184799	0.025423599	0.033135299	0.0308521	6.5	Bischofszell	9.8	20	89.5	0	0.8	
312	Flawil	733423	252941	1061	20.07.2019	M.m.	3	271	275	0	0	0	0	0	0	no	yes	0.0265834	0.0269539	0.00626556	0.00635289	0.00672355	0.00681766	193.7	Bischofszell	9.8	20	89.5	0	0.8	
313	Flawil	733403	252365	1073	20.07.2019	M.m.	2	318	275	3	3	5	3	2	3.2	yes	yes	0.00351712	0.00965945	0.011821	0.00972116	0.025599699	0.0269384	191.1	Bischofszell	9.8	20	89.5	0	0.8	
314	Flawil	733618	252852	3314	20.07.2019	M.m.	1	228	275	0	0	0	0	0	0	no	yes	0.100033998	0.084406301	0.025125301	0.021164799	0.025395	0.021362901	212.4	Bischofszell	9.8	20	89.5	0	0.8	
315	Flawil	733833	252818	1249	20.07.2019	M.m.	1	386	275	0	0	0	0	0	0	no	yes	0.00414227	0.084037697	0.000605611	0.0177618	0.00119773	0.0248843	14.1	Bischofszell	9.8	20	89.5	0	0.8	
316	Flawil	733654	252641	1032	20.07.2019	M.m.	7	182	275	0	0	0	0	0	0	no	no	0.0153351	0.0155551	0.00394102	0.00401814	0.0039733									

site-ID	Community	x-Koord	y-Koord	Bat-logger	Recording Date	Species	Bat Activity	Distance to roost [m]	Roost size [individuals]	Lux1	Lux2	Lux3	Lux4	Lux5	Lux_mean	light	corridor	Corridor value current_adv 5	Corridor value current_adv 15	Corridor value current_subavg 5	Corridor value current_subavg 15	Corridor value current_submax 5	Corridor value current_submax 15	Distance Site to LCP [m]	Weather Station	Distance to Roost [km]	Temperature [°C]	Humidity [%]	Precipitation [mm]	Wind speed [m/s]	Comment
356	Uors	733380	173632	3314	26.07.2019	R.h.	7	46	234	0	0	0	0	0	0	no	yes	0.126379997	0.119418003	0.031645101	0.0299049	0.031648099	0.0299071	27.1	Vais	8.1	15.9	78.8	0	0.4	
357	Uors	733385	173654	1061	26.07.2019	R.h.	8	49	234	0	0	0	0	0	0	no	yes	0.130123004	0.127959996	0.032682901	0.032127898	0.032683101	0.032127898	6.4	Vais	8.1	15.9	78.8	0	0.4	
358	Uors	733364	173613	1063	26.07.2019	R.h.	1	62	234	0	0	0	0	0	0	no	yes	0.077752702	0.082999296	0.019323201	0.0205868	0.0193389	0.0206396	51.5	Vais	8.1	15.9	78.8	0	0.4	
359	Uors	733456	173658	1032	26.07.2019	R.h.	0	45	234	23	10	28	12	21	18.8	yes	yes	0.064424902	0.065712303	0.016099401	0.016417401	0.0161027	0.0164207	42.8	Vais	8.1	15.9	78.8	0	0.4	
360	Uors	733376	173782	1037	26.07.2019	R.h.	144	164	234	0	0	0	0	0	0	no	yes	0.0059277	0.065462798	0.00148841	0.016406201	0.00148886	0.016426001	26.7	Vais	8.1	15.9	78.8	0	0.4	
361	Uors	733335	173834	1036	26.07.2019	R.h.	24	228	234	0	0	0	0	0	0	no	yes	0.00310856	0.084368899	0.000779357	0.0211384	0.000779602	0.021154899	21.9	Vais	8.1	15.9	78.8	0	0.4	
362	Uors	733309	173570	1249	26.07.2019	R.h.	1	128	234	0	0	0	0	0	0	no	yes	0.00396728	0.0517013	0.024531599	0.0206326	0.049063299	0.040685602	78.5	Vais	8.1	15.9	78.8	0	0.4	
363	Uors	733410	173725	1031	26.07.2019	R.h.	3	101	234	0.5	0.5	0.5	0	0	0	no	yes	0.031860299	0.0320214	0.0078814	0.00870147	0.00788365	0.00870396	58.0	Vais	8.1	15.9	78.8	0	0.4	
364	Uors	733467	173783	1075	26.07.2019	R.h.	0	163	234	0	0	0.5	0	0.5	0.2	no	no	0.00634361	0.00638909	0.00158721	0.00159948	0.0015877	0.00159998	116.1	Vais	8.1	15.9	78.8	0	0.4	
365	Uors	733563	173775	1048	26.07.2019	R.h.	0	204	234	7	6	4	7	10	6.8	yes	no	0.00778152	0.00722024	0.00183183	0.00178637	0.00183243	0.00178695	198.2	Vais	8.1	15.9	78.8	0	0.4	
366	Uors	733479	173490	1056	26.07.2019	R.h.	1	145	234	0.5	0	0.5	0.5	0.5	0.4	no	no	0.0130101	0.0130542	0.00309136	0.0031294	0.00309525	0.003133	89.1	Vais	8.1	15.9	78.8	0	0.4	
367	Uors	733550	173447	1029	26.07.2019	R.h.	3	218	234	0	0	0	0	0	0	no	no	0.00732518	0.00669815	0.00182589	0.00166955	0.00182761	0.00167113	105.4	Vais	8.1	15.9	78.8	0	0.4	
368	Uors	733496	174014	1053	26.07.2019	R.h.	1	395	234	0	0	0	0	0	0	no	no	0.000895059	0.000895039	0.000212841	0.000212849	0.000212909	0.000212917	121.6	Vais	8.1	15.9	78.8	0	0.4	
369	Uors	733718	173898	1073	26.07.2019	R.h.	1	400	234	0	0	0	0	0	0	no	no	0.00125941	0.0011664	0.000330179	0.000306759	0.000330288	0.00030686	365.4	Vais	8.1	15.9	78.8	0	0.4	
370	Uors	733376	173575	1074	26.07.2019	R.h.	0	70	234	0	0	0	0	0	0	no	no	0.038130298	0.038036101	0.00863949	0.00862702	0.00864227	0.00863016	68.7	Vais	8.1	15.9	78.8	0	0.4	
371	Uors	733471	173561	1057	26.07.2019	R.h.	2	79	234	1	0.5	0	1	0.5	0.6	yes	no	0.031008599	0.029631499	0.00771343	0.00737129	0.00771445	0.00737214	82.1	Vais	8.1	15.9	78.8	0	0.4	
372	Waltensburg	728210	182037	1031	25.06.2019	R.h.	9	95	105	0.5	0.5	0	0	0.5	0.3	no	yes	0.153818995	0.153289005	0.038490999	0.031748898	0.0387692	0.039979398	42.5	Ilanz	7.4	19.3	75.3	0	noData	
373	Waltensburg	728282	182053	1053	25.06.2019	R.h.	5	21	105	1	1	1	2	2	1.4	yes	yes	0.090466097	0.088178203	0.022642599	0.0189212	0.022654399	0.0225062	24.0	Ilanz	7.4	19.3	75.3	0	noData	
374	Waltensburg	728330	181780	1063	25.06.2019	R.h.	0	275	105	0	0	0	0	0	0	no	yes	0.00621011	0.0069317	0.0015478	0.00172764	0.00155218	0.00173255	236.6	Ilanz	7.4	19.3	75.3	0	noData	
375	Waltensburg	728226	181971	1037	25.06.2019	R.h.	0	113	105	1	0.5	1	0.5	1	0.8	no	yes	0.057695601	0.062399201	0.0143507	0.014358	0.0155206	0.0155306	41.2	Ilanz	7.4	19.3	75.3	0	noData	
376	Waltensburg	728395	182167	1048	25.06.2019	R.h.	2	146	105	0	0	0	0	0	0	no	yes	0.000752345	0.058974098	9.1856E-05	0.0104921	0.000183712	0.020907501	23.3	Ilanz	7.4	19.3	75.3	0	noData	
377	Waltensburg	728193	181868	1057	25.06.2019	R.h.	1	216	105	1	0.5	0.5	0.5	0	0.5	no	yes	0.012748	0.0116883	0.00317616	0.00290692	0.00318341	0.00291357	147.1	Ilanz	7.4	19.3	75.3	0	noData	
378	Waltensburg	728456	181694	1061	25.06.2019	R.h.	0	391	105	0	0	0	0	0	0	no	yes	0.000703515	0.00942791	0.000175087	0.000175087	0.000175967	0.00235816	369.6	Ilanz	7.4	19.3	75.3	0	noData	
379	Waltensburg	728304	181986	1073	25.06.2019	R.h.	0	68	105	1	0.5	1	1	2	1.1	yes	yes	0.0368011	0.0391666	0.00918612	0.00977557	0.00919958	0.00978932	54.1	Ilanz	7.4	19.3	75.3	0	noData	
380	Waltensburg	727937	181713	1029	25.06.2019	R.h.	1	500	105	0	0	0	0	0	0	no	no	0.00112977	0.00108758	0.00028143	0.000270921	0.000283096	0.000272525	428.2	Ilanz	7.4	19.3	75.3	0	noData	
381	Waltensburg	728045	181807	1249	25.06.2019	R.h.	1	357	105	0.5	0.5	0.5	0.5	0.5	0.5	no	no	0.00312606	0.00348997	0.000778366	0.000868994	0.000782559	0.000873498	285.1	Ilanz	7.4	19.3	75.3	0	noData	
382	Waltensburg	728110	182137	1075	25.06.2019	R.h.	0	210	105	0	0	0	0	0	0	no	no	0.00036641	0.000369862	9.09939E-05	9.18424E-05	9.1912E-05	9.28066E-05	163.2	Ilanz	7.4	19.3	75.3	0	noData	
383	Waltensburg	728754	182057	1032	25.06.2019	R.h.	0	450	105	0	0	0	0	0	0	no	no	0.000216358	0.000215859	5.41948E-05	5.41948E-05	5.41948E-05	5.46918E-05	355.0	Ilanz	7.4	19.3	75.3	0	noData	
384	Waltensburg	728011	181875	1074	25.06.2019	R.h.	0	342	105	7	4	5	7	15	7.6	yes	no	0.00190562	0.00208477	0.000474266	0.00051885	0.000476798	0.000521667	273.1	Ilanz	7.4	19.3	75.3	0	noData	
385	Waltensburg	728543	182178	1036	25.06.2019	R.h.	0	270	105	1	1	1	2	2	1.4	yes	no	0.000761245	0.000798671	0.00018994	0.000198713	0.000189764	0.000199096	120.2	Ilanz	7.4	19.3	75.3	0	noData	
386	Waltensburg	728414	182120	1056	25.06.2019	R.h.	0	129	105	1	0.5	1	1	1	0.9	yes	no	0.00513024	0.0052278	0.00127922	0.00130356	0.00128386	0.00130382	70.0	Ilanz	7.4	19.3	75.3	0	noData	
387	Waltensburg	728492	181947	3314	25.06.2019	R.h.	0	217	105	0	0	0	0	0	0	no	no	0.00249431	0.00250305	0.000622196	0.000624325	0.000624538	0.000626595	245.8	Ilanz	7.4	19.3	75.3	0	noData	
388	Castiel	764975	189797	1056	24.06.2019	R.h.	1	53	67	0.5	0	0	0	0	0	no	yes	0.088200301	0.090960398	0.0221755	0.0206035	0.0221854	0.0236244	5.7	Chur	6.5	21.5	67.5	0	1.9	close by street lamp not working
389	Castiel	764988	189632	1029	24.06.2019	R.h.	0	119	67	0	0	0	0	0	0	no	yes	0.00843062	0.0149321	0.0021415	0.00376488	0.00214599	0.0037727	121.4	Chur	6.5	21.5	67.5	0	1.9	
390	Castiel	765003	189562	1249	24.06.2019	R.h.	0	188	67	0	0	0	0	0	0	no	yes	0.00133277	0.00138408	0.000353808	0.000367442	0.000354913	0.000368589	140.5	Chur	6.5	21.5	67.5	0	1.9	
391	Castiel	765042	189834	1048	24.06.2019	R.h.	0	94	67	1	0.5	1	1	1	0.9	yes	yes	0.036563098	0.0386995	0.00802698	0.00734798	0.0095636	0.00877558	50.5	Chur	6.5	21.5	67.5	0	1.9	
392	Castiel	765101	189812	1036	24.06.2019	R.h.	0	119	67	8	2	9	2	53	14																

## Appendix II

The screenshot displays the BATLOGGER M BATPARS Editor software interface. The window title is "BATLOGGER M BATPARS Editor". The main area is divided into several sections:

- Schedule:**
  - Run for x days: 1
  - Interval (min): 0
  - Time frame T1 Start: Sunset, -00:15
  - Time frame T1 Stop: Sunrise, 00:15
  - T1: (@23.09.2019) 19:00 - 07:15
  - Estimated operation time: ≈ 1.0 nights à 12.25 hours (≈ 1.0 nights à 12.25 hours with Strongbox)
  - Time frame T2 Start: Fixed, 00:00
  - Time frame T2 Stop: Fixed, 00:00
  - T2: n/a
- Trigger:**
  - Pre-Trigger time (ms): 500
  - Auto Trigger max time (ms): 10000
  - Record:  automatically
  - Mode: Period
  - ProdVal: 8
  - Post-Trigger time (ms): 1000
  - Manual Trigger max time (ms): 20000
  - Post-Trigger ignore (s): 0
  - DivVal: 20
- Audio:**
  - Volume: 4
  - Monitoring (Mixer)\*: Off
  - Microphone Testmode\*: Manual
  - Playback Mode: Mixer
  - Playback Speed: 10
  - Squelch (Noise limiter) (s): 0
- Location / GPS / Time:**
  - GPS: Enabled
  - Choose manual Location: ...
  - Coord. Format: WGS84
  - Time Mode: Manual
  - Position Update Interval (s): 10
  - Man. Loc. Latitude [WGS84 \*]: 47.2616
  - Man. Loc. Longitude [WGS84 \*]: 8.4559
  - Timezone: UTC (GMT) 2

At the bottom, there is a "Load from profile:" dropdown, a copyright notice "©2017 Elekon AG, v2.5.1.31", and "Save" and "Close" buttons.

Figure 10: Setting of the Batlogger M for bat activity recording

## Appendix III

Table 15: Filter queries applied to verify *M. myotis* calls

Level on BatScope	Sequence	Sequence	Sequence	Calls	Sequence	Calls	Calls	Calls	Calls	Sequence	Calls	
Filter	Auto_Class 1st Taxon	Auto_Class 2nd Taxon	Auto_Class 3rd Taxon	MLS	Taxon all	FreqPeakFIL	95% CI-Test	#Agreeing Classifier	Confidence	Status	Call	Result
1				MMY			pass		$\geq 0.75$			MY
2				MMY		< 20	fail		< 0.2			disable
3					not MMY	> 45	pass		$\geq 0.5$			disable
4	MMY			MMY			pass					MMY
5	N.leisleri or Eptesicus sp. or Vespertilio sp.	MMY	MMY	MMY		$\geq 30$						MMY
6	E. nilssonii			MMY			pass	$\geq 4$		enable	selected	MMY
7	E. serotinus			MMY			pass	$\geq 4$		enable	selected	MMY
8	N. leisleri			MMY			pass	$\geq 4$		enable	selected	MMY
9		MMY		MMY			pass		$(\geq 0.75)$	enable		MMY
10			MMY	MMY			pass		$(\geq 0.75)$	enable		MMY
11				N.leisleri		$\geq 30$	fail		$(\leq 0.5)$	enable		check for MMY
12				E.nilssonii		$\geq 30$	fail		$(\leq 0.5)$	enable		check for MMY
13				E.serotinus		$\geq 30$	fail		$(\leq 0.5)$	enable		check for MMY
14	M. daubentonii	MMY								enable		check for MMY
15	M. daubentonii		MMY							enable		check for MMY
16	M. bechsteinii	MMY								enable		check for MMY
17	M. bechsteinii		MMY							enable		check for MMY

## Appendix IV

1) Correlation coefficient matrix of explanatory variables for *M. myotis*

2) Correlation coefficient matrix of explanatory variables for *R. hipposideros*

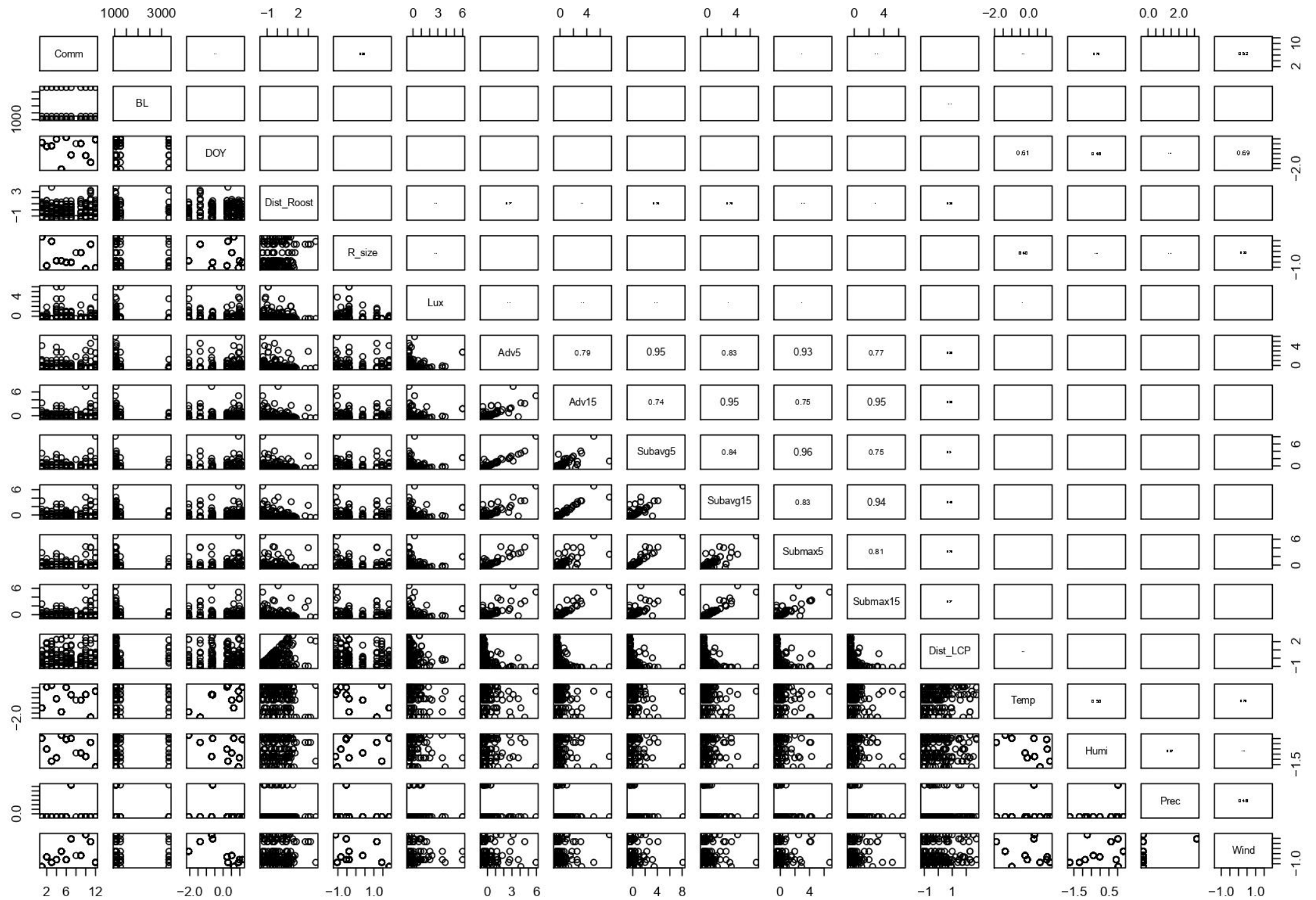


Figure 11: Correlation coefficient matrix of explanatory variables for *M. myotis*

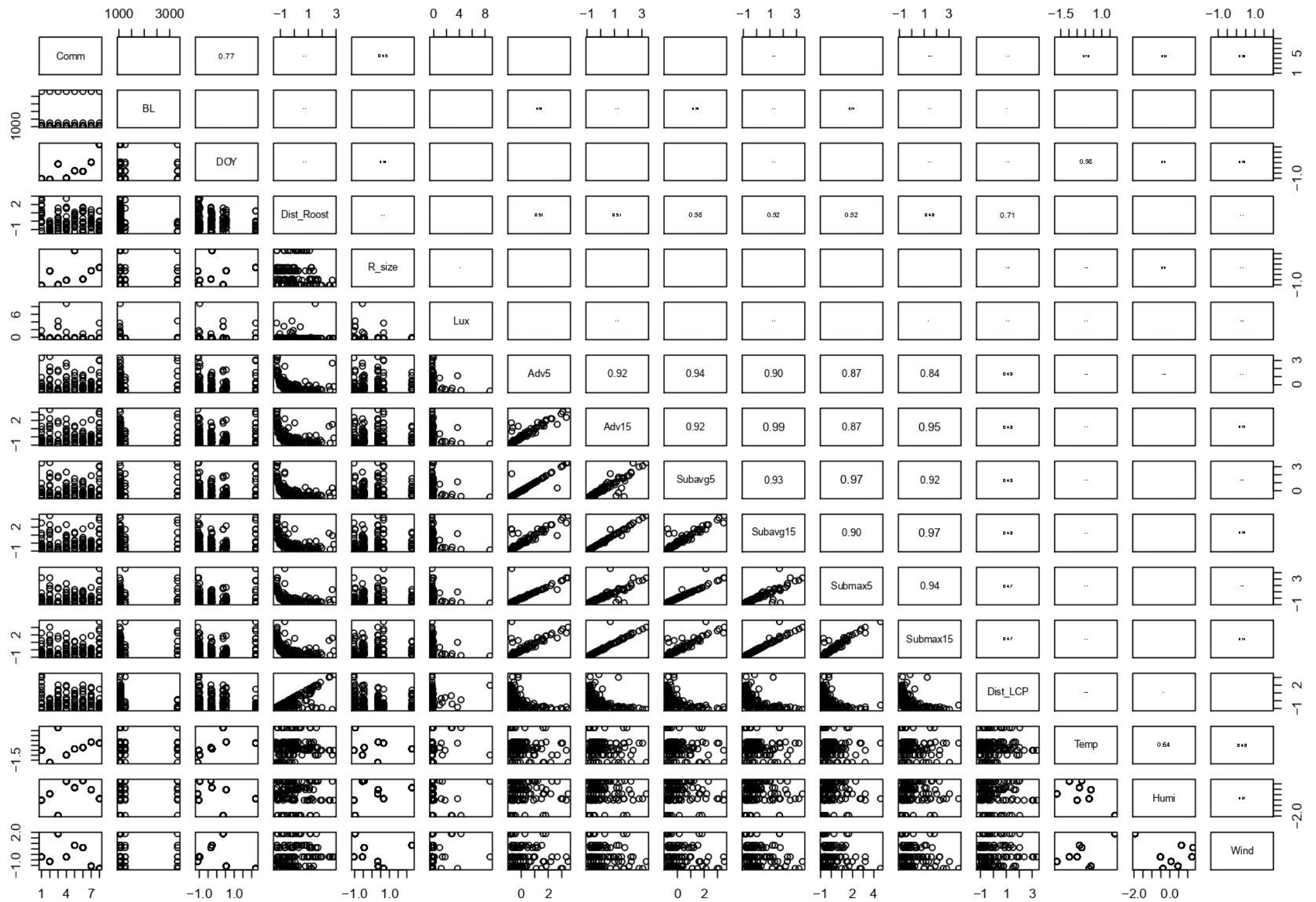


Figure 12: Correlation coefficient matrix of explanatory variables for *R. hipposideros*

## Appendix V

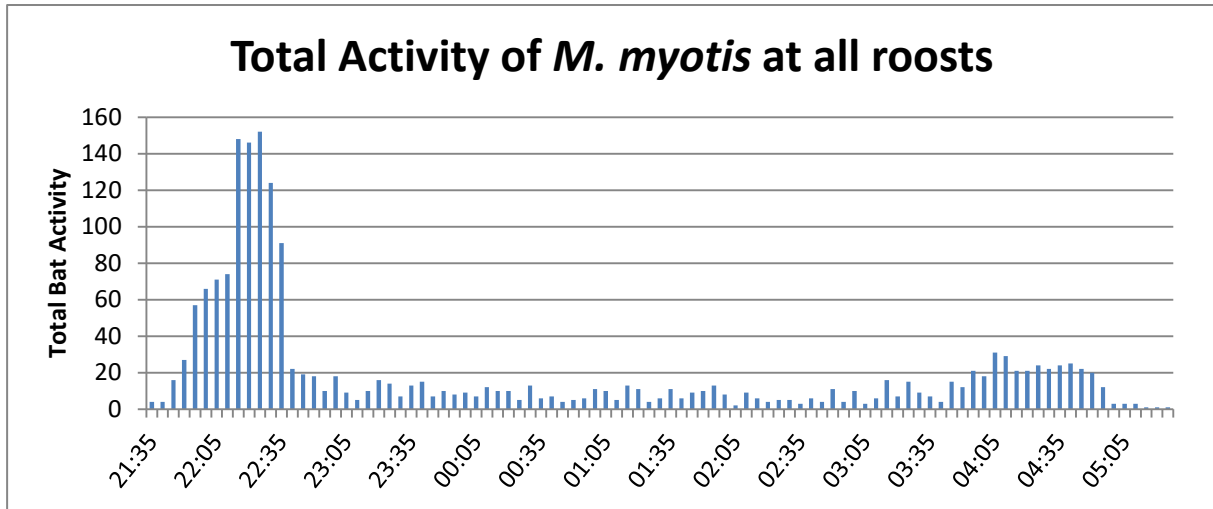


Figure 13: Distribution of total activity of *M. myotis* at all *M. myotis* study sites

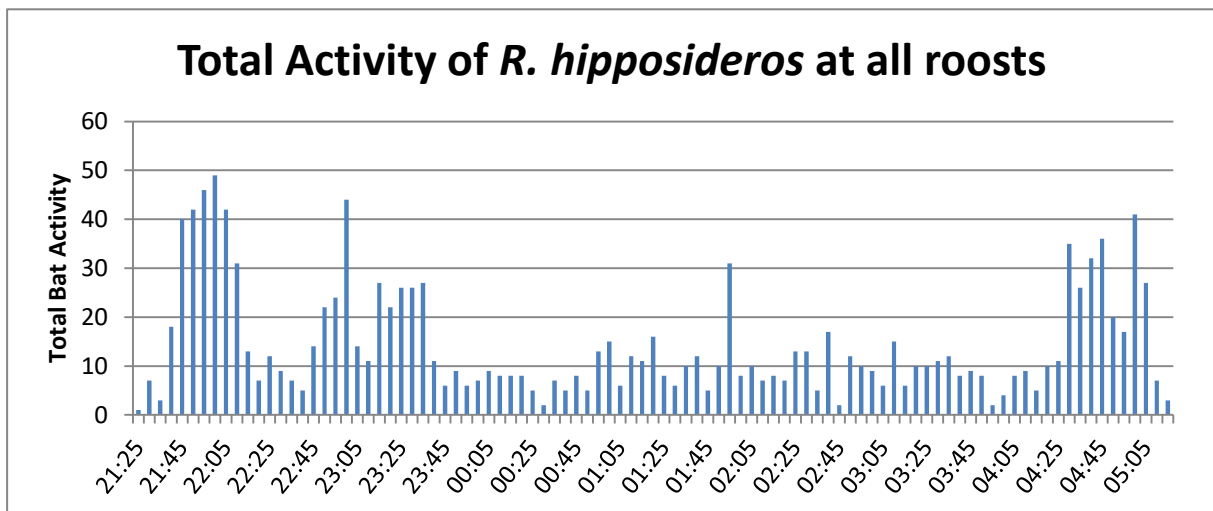


Figure 14: Distribution of total activity of *R. hipposideros* at all *R. hipposideros* study sites.

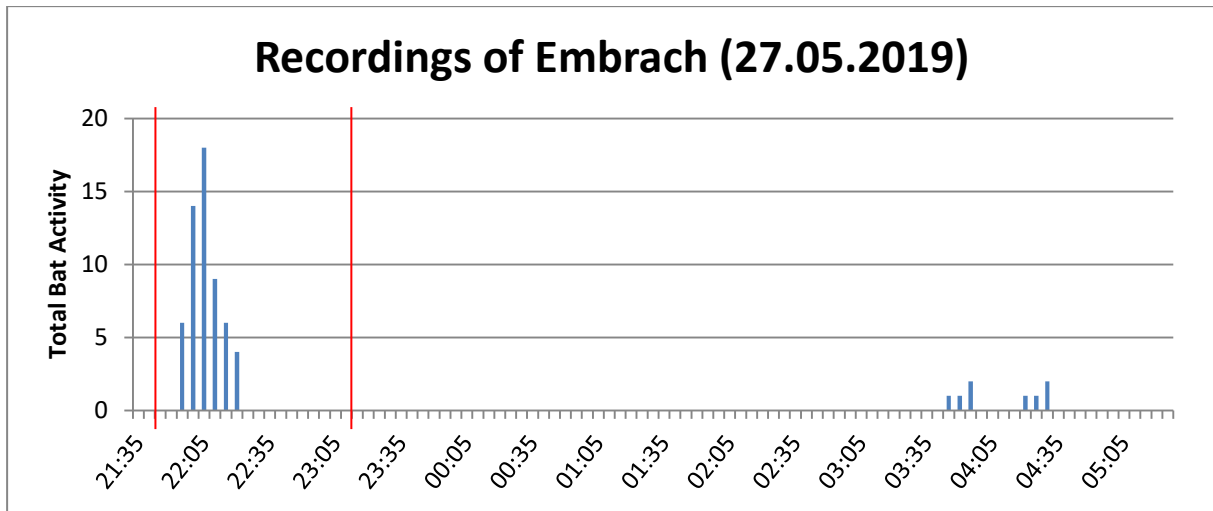


Figure 15: Distribution of total activity of *M. myotis* in Embrach during the first recording. Start and end time of 'fly-out' period in red.

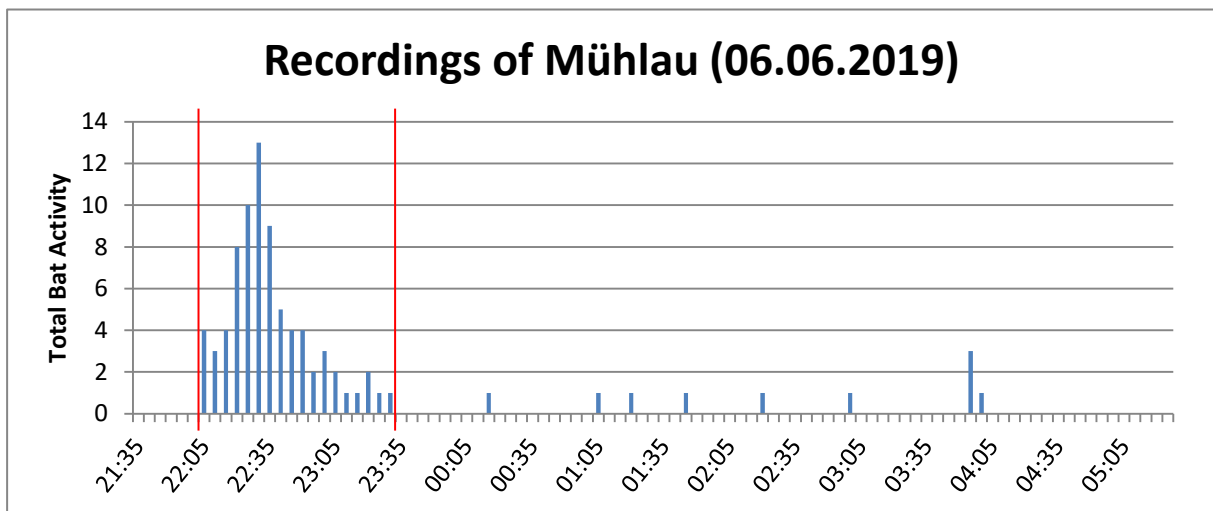


Figure 16: Distribution of total activity of *M. myotis* in Embrach. Start and end time of 'fly-out' period in red.

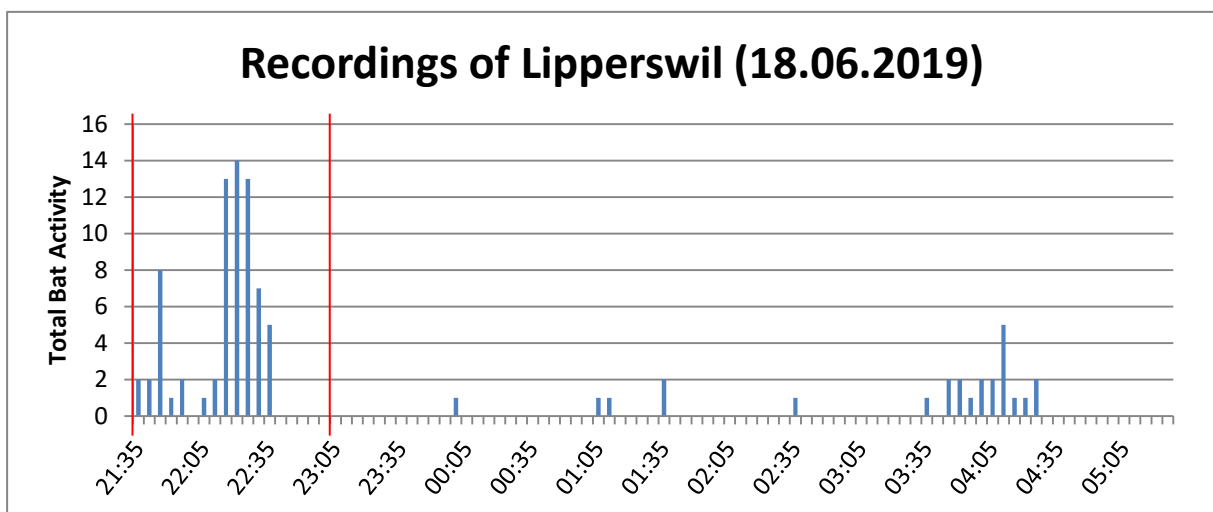


Figure 17: Distribution of total activity of *M. myotis* in Lipperswil. Start and end time of 'fly-out' period in red.

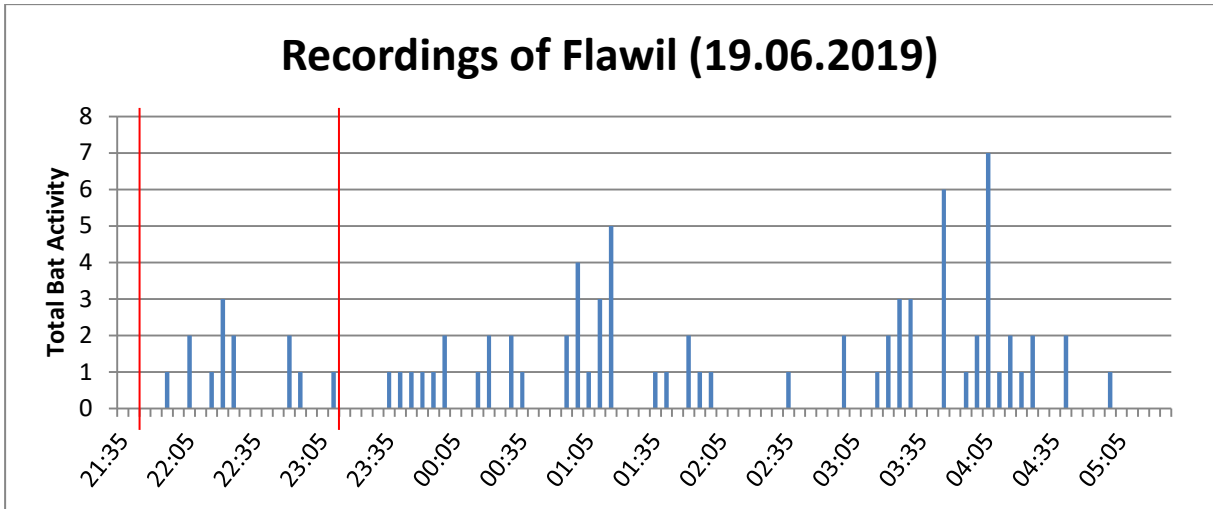


Figure 18: Distribution of total activity of *M. myotis* in Flawil during the first recording. Start and end time of 'fly-out' period in red.

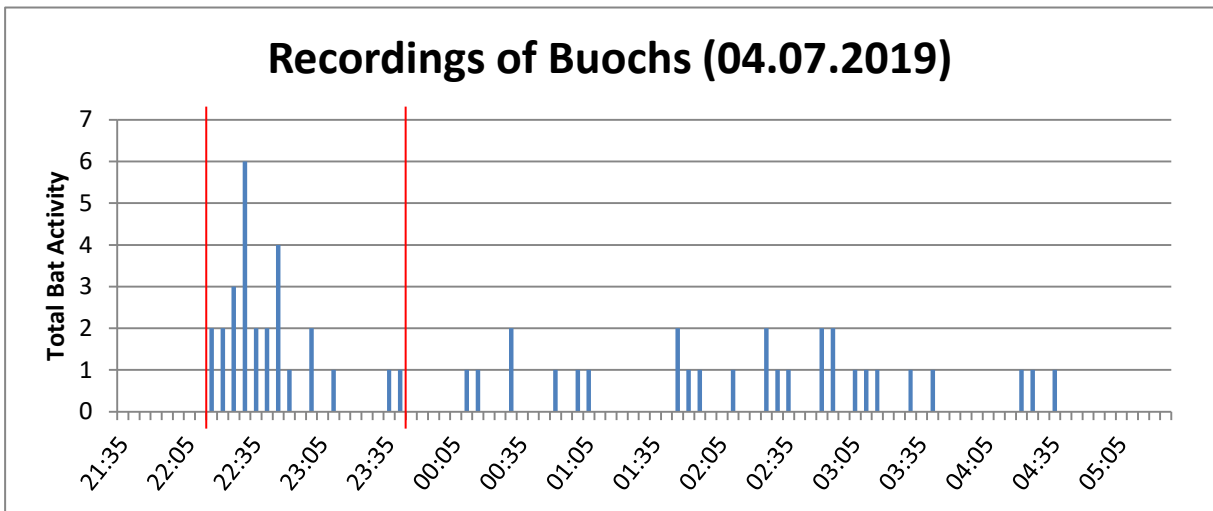


Figure 19: Distribution of total activity of *M. myotis* in Buochs. Start and end time of 'fly-out' period in red.

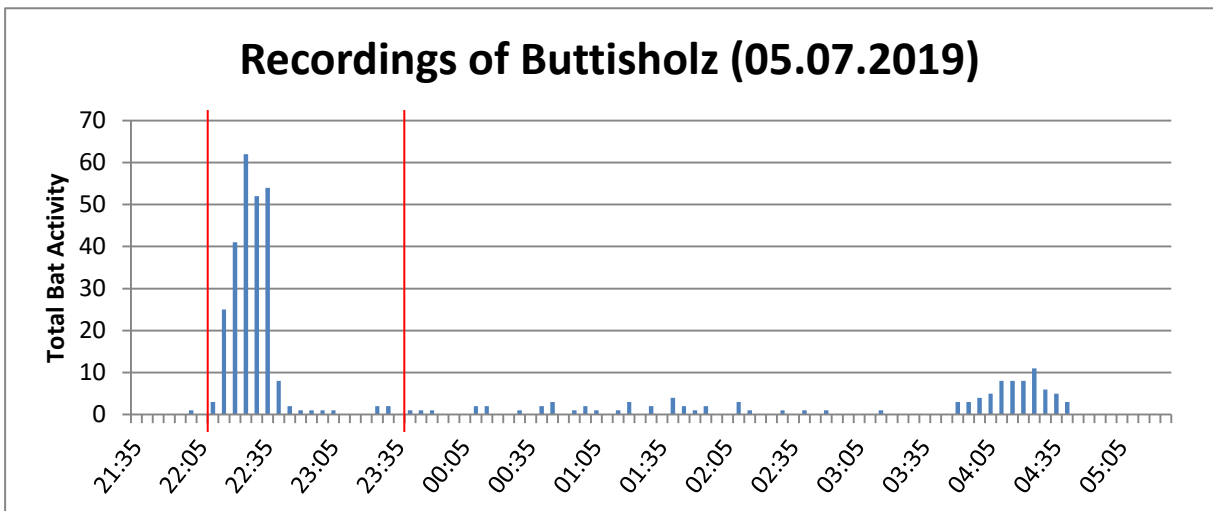


Figure 20: Distribution of total activity of *M. myotis* in Buttisholz. Start and end time of 'fly-out' period in red.

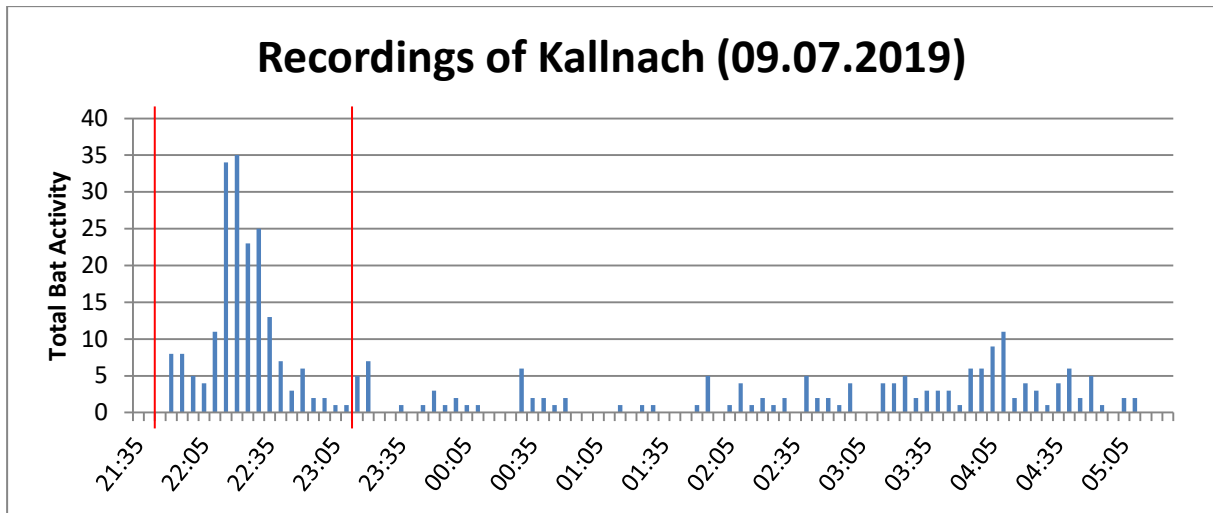


Figure 21: Distribution of total activity of *M. myotis* in Kallnach. Start and end time of 'fly-out' period in red.

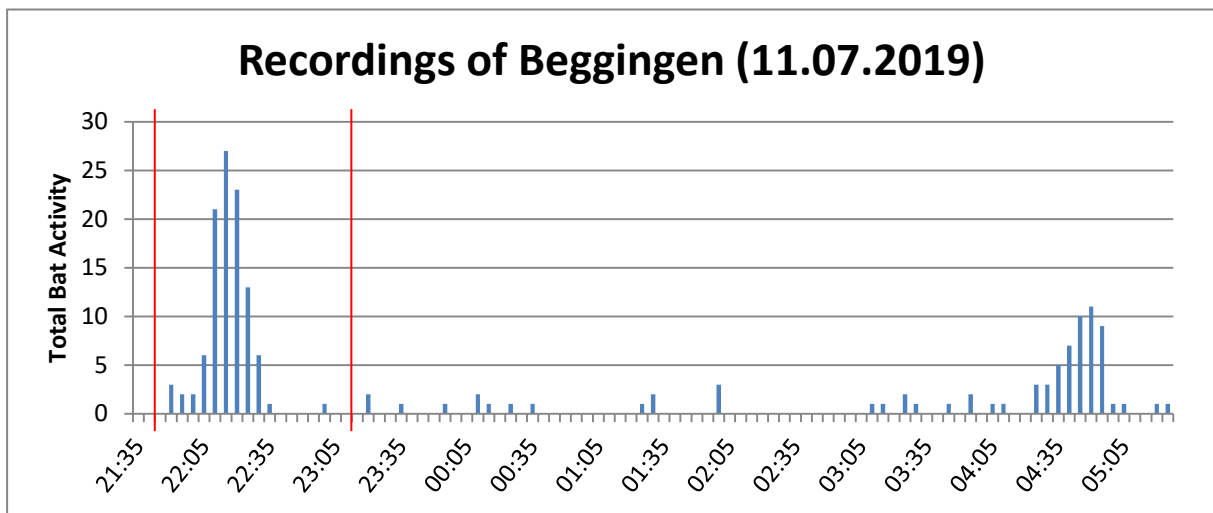


Figure 22: Distribution of total activity of *M. myotis* in Beggingen. Start and end time of 'fly-out' period in red.

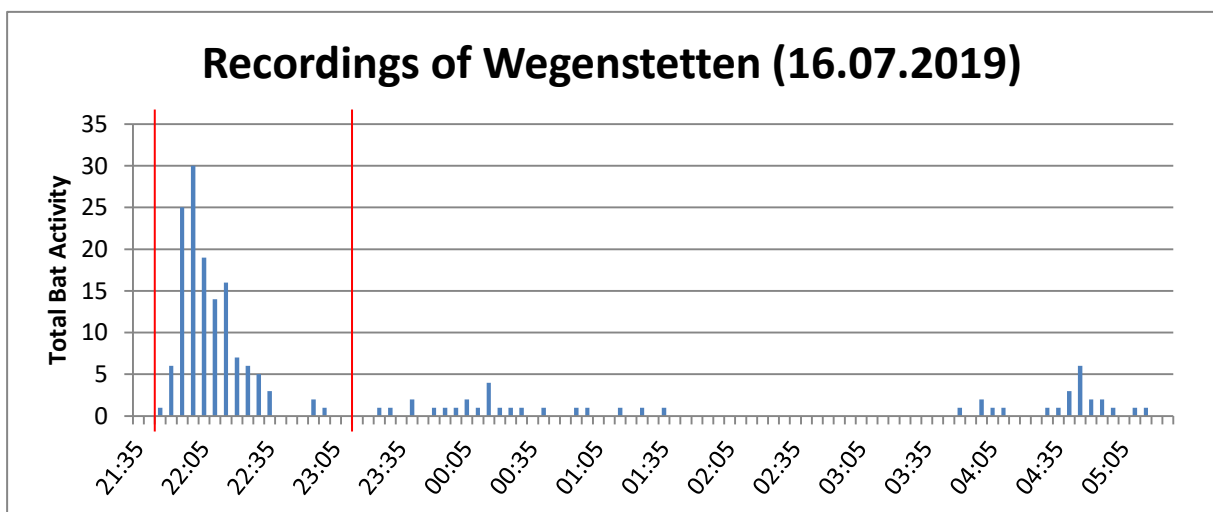


Figure 23: Distribution of total activity of *M. myotis* in Wegenstetten. Start and end time of 'fly-out' period in red.

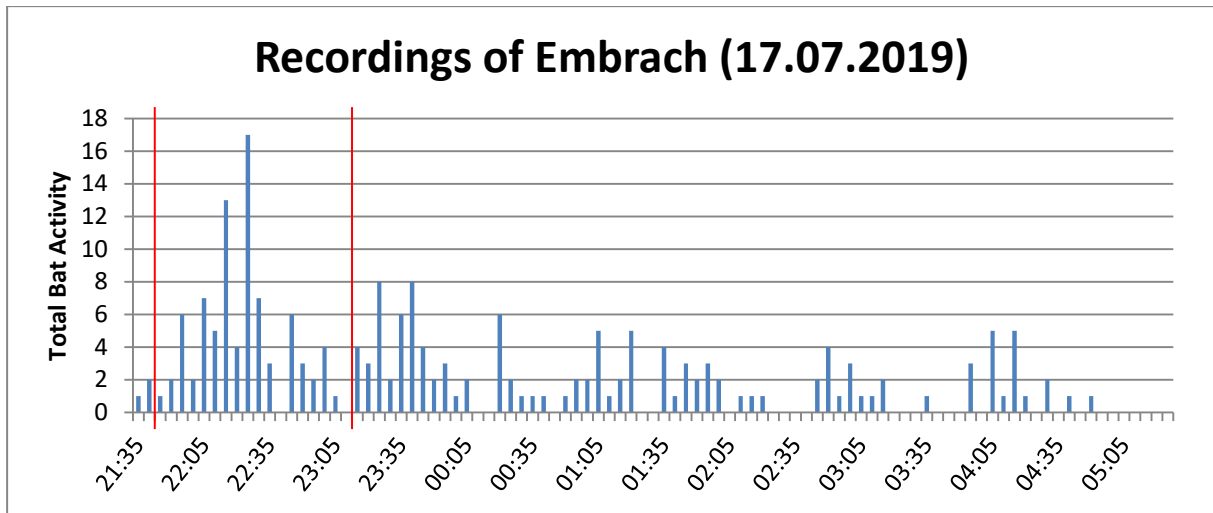


Figure 24: Distribution of total activity of *M. myotis* in Embrach during the second recording. Start and end time of 'fly-out' period in red.

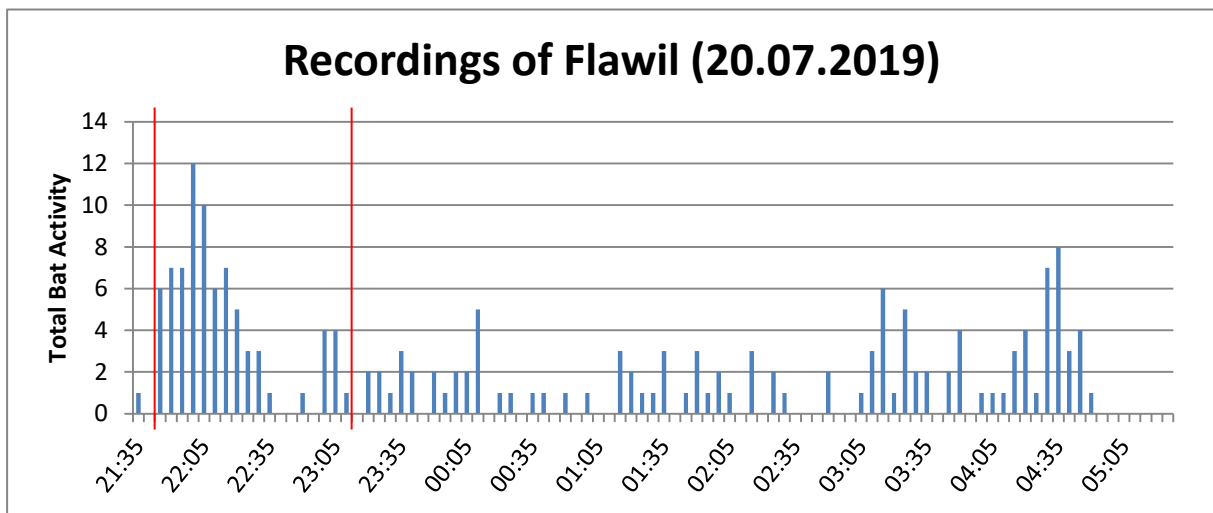


Figure 25: Distribution of total activity of *M. myotis* in Flawil during the second recording. Start and end time of 'fly-out' period in red.

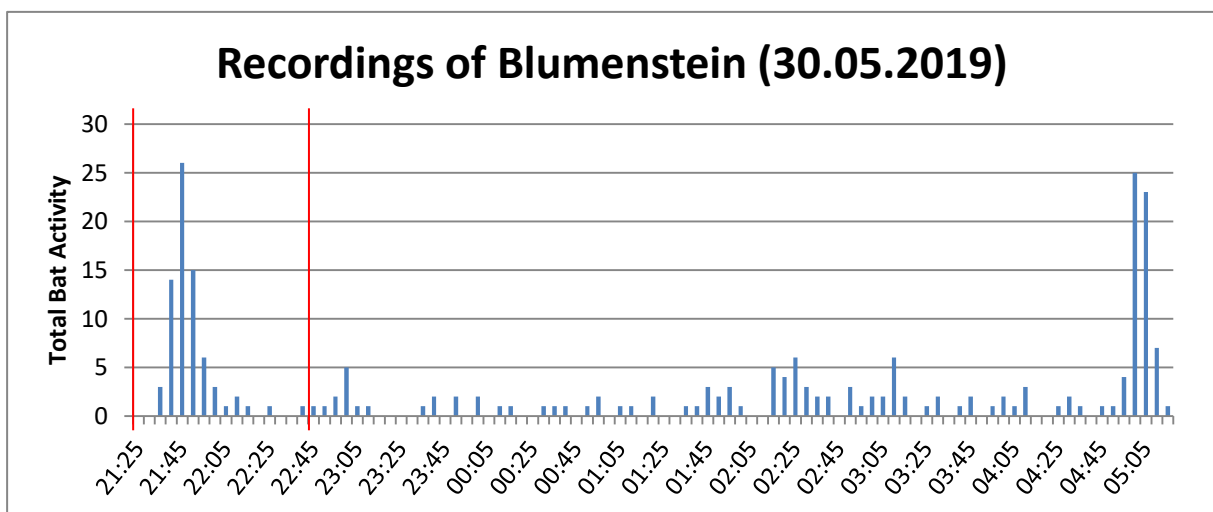


Figure 26: Distribution of total activity of *R. hipposideros* in Blumenstein. Start and end time of 'fly-out' period in red.

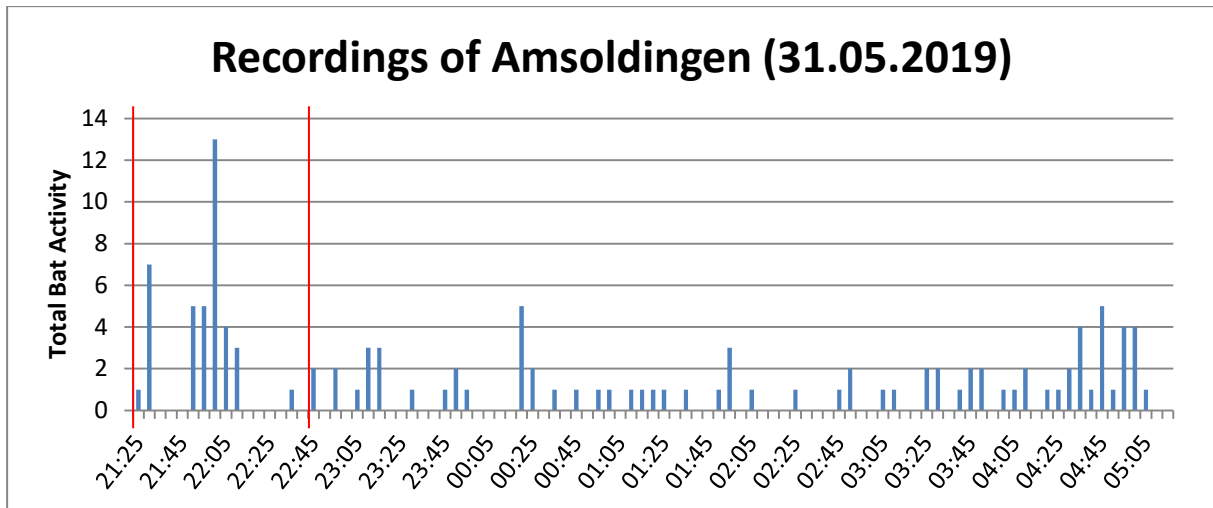


Figure 27: Distribution of total activity of *R. hipposideros* in Amsoldingen. Start and end time of 'fly-out' period in red.

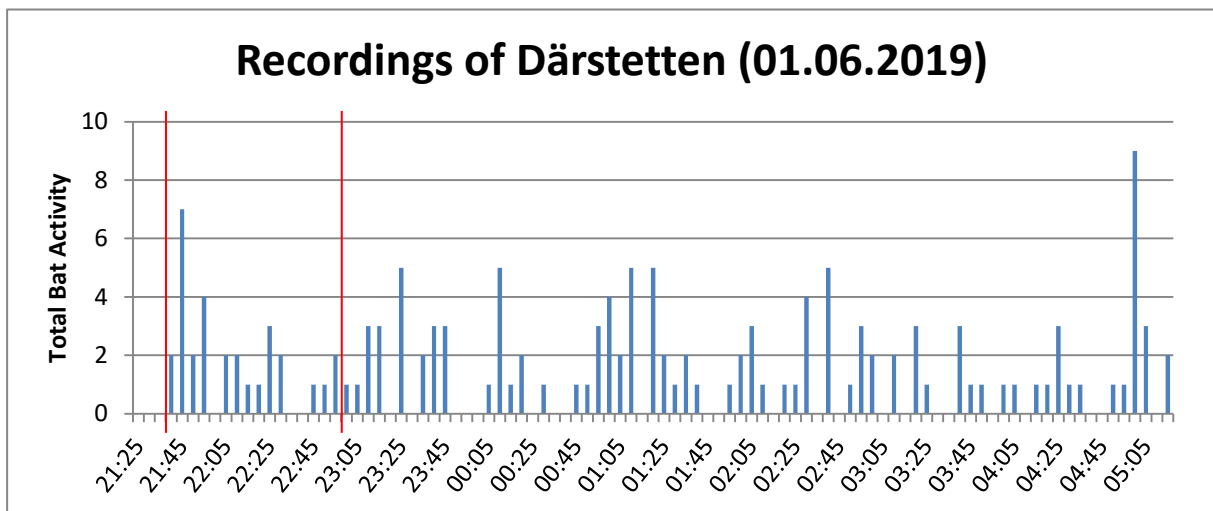


Figure 28: Distribution of total activity of *R. hipposideros* in Därstetten. Start and end time of 'fly-out' period in red.

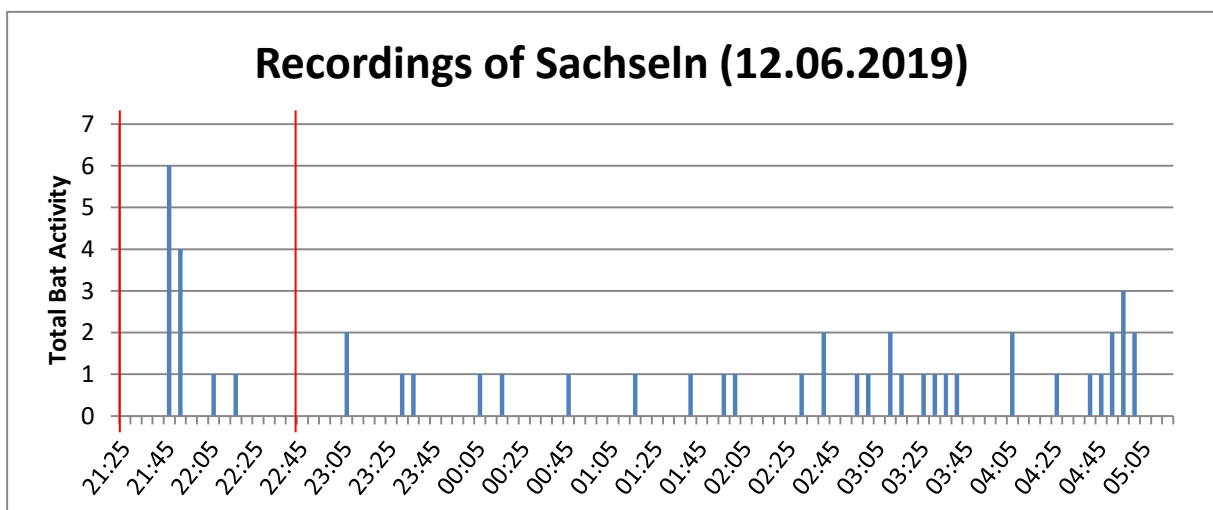


Figure 29: Distribution of total activity of *R. hipposideros* in Sachseln. Start and end time of 'fly-out' period in red.

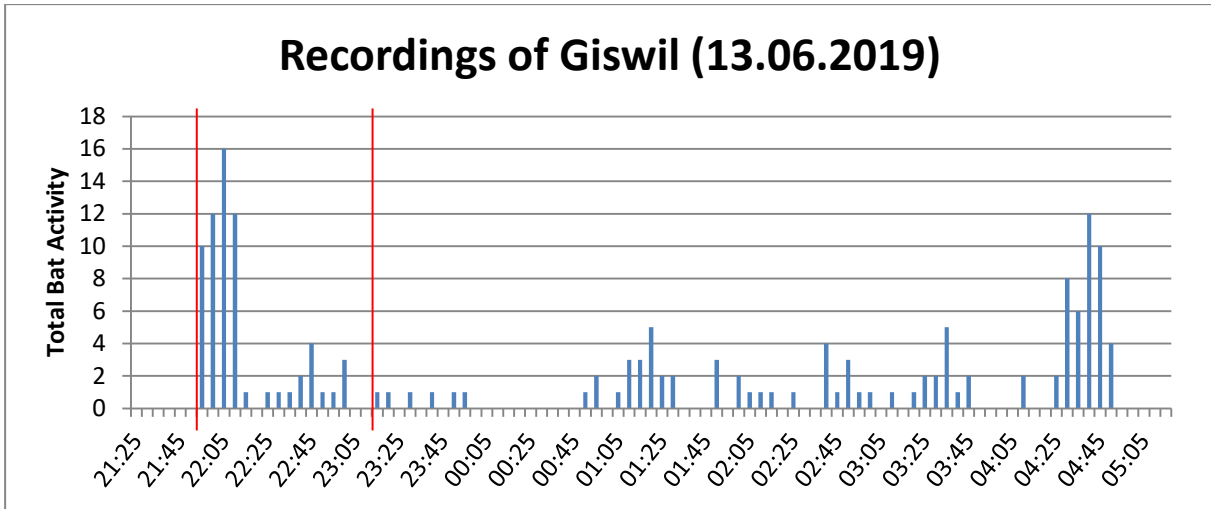


Figure 30: Distribution of total activity of *R. hipposideros* in Giswil. Start and end time of 'fly-out' period in red.

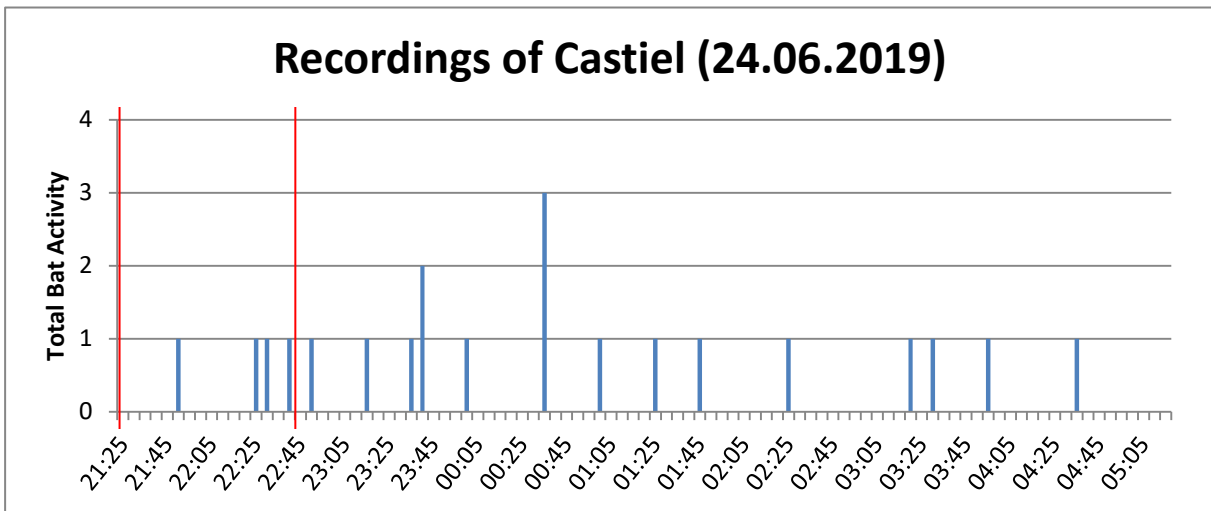


Figure 31: Distribution of total activity of *R. hipposideros* in Castiel. Start and end time of 'fly-out' period in red.

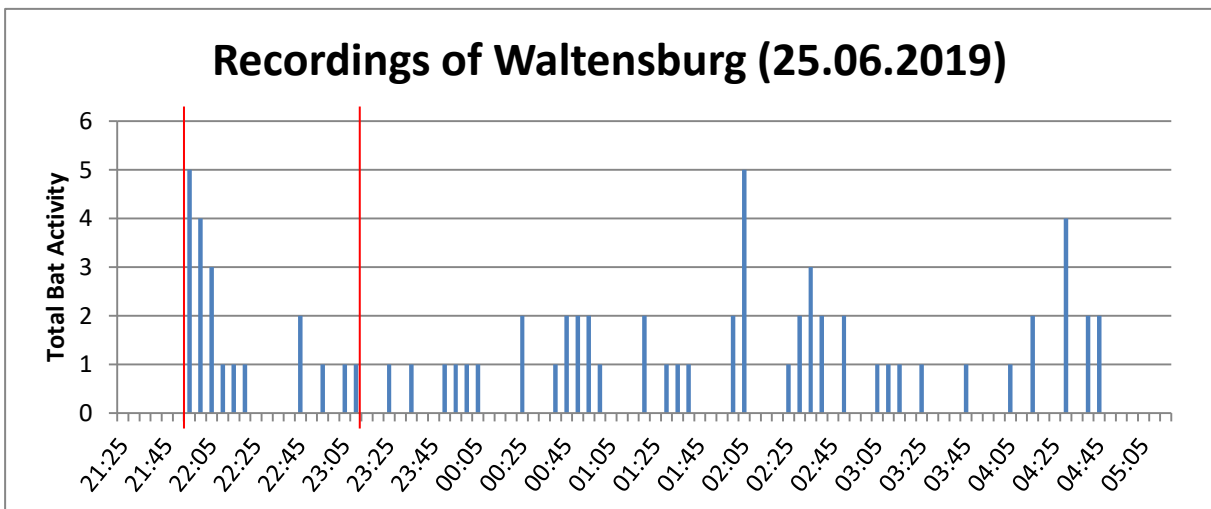


Figure 32: Distribution of total activity of *R. hipposideros* in Waltensburg. Start and end time of 'fly-out' period in red.

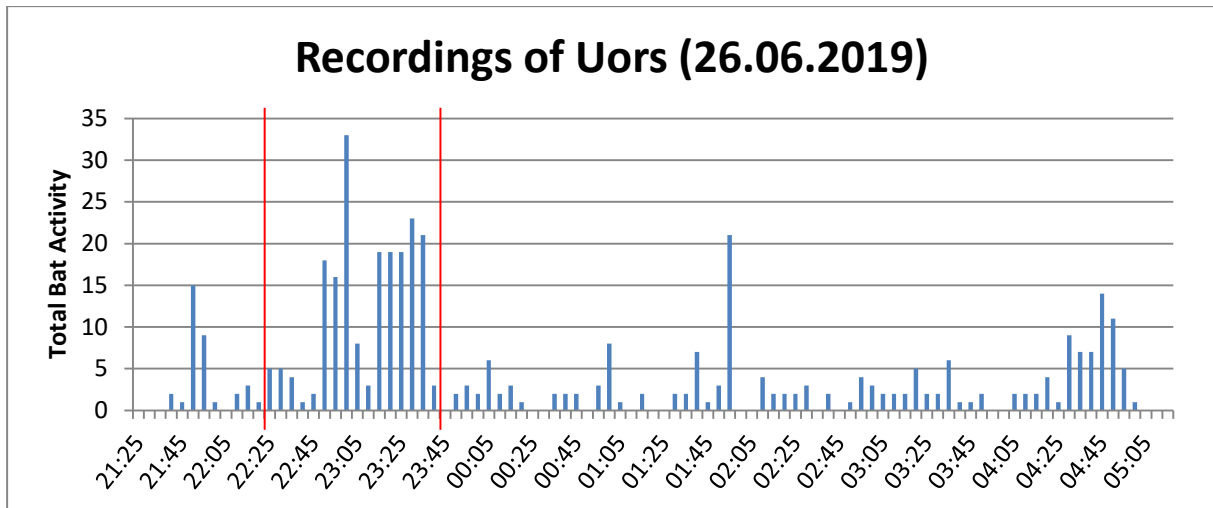


Figure 33: Distribution of total activity of *R. hipposideros* in Uors. Start and end time of 'fly-out' period in red.

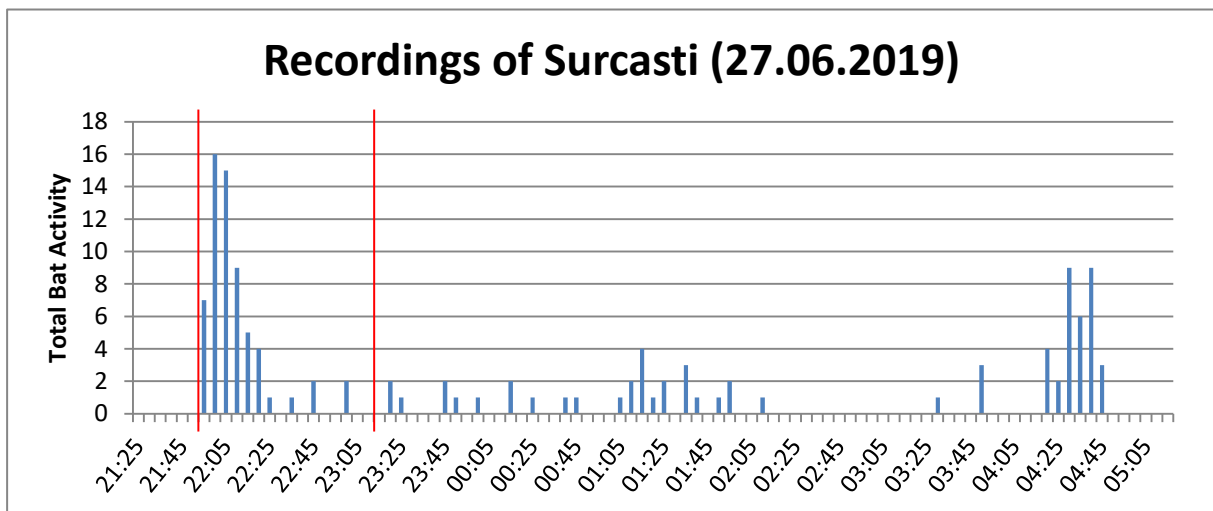


Figure 34: Distribution of total activity of *R. hipposideros* in Surcasti. Start and end time of 'fly-out' period in red.

## Appendix VI

Table 16: Full model ranking list for *M. myotis* data with Adv15 variable included.

rank	Adv15	Dist_LCP	Dist_Roost	Lux	df	logLik	AICc	delta	weight
1	-	-0.406	-0.205	-0.397	9	-849.938	1718.973	0.000	0.530
2	-0.052	-0.428	-0.216	-0.399	10	-848.930	1719.209	0.237	0.470
3	-	-0.478	-	-0.383	8	-867.068	1751.009	32.036	5.85e-8
4	-0.011	-0.483	-	-0.383	9	-867.020	1753.138	34.165	2.02e-8
5	-	-0.400	-0.196	-	8	-876.329	1769.531	50.558	5.56e-12
6	-0.054	-0.423	-0.207	-	9	-875.264	1769.627	50.654	5.30e-12
7	-	-0.469	-	-	7	-891.846	1798.366	79.393	3.05e-18
8	-0.015	-0.476	-	-	8	-891.755	1800.383	81.410	1.11e-18
9	0.079	-	-0.307	-0.392	9	-896.803	1812.704	93.731	2.35e-21
10	-	-	-0.335	-0.394	8	-899.344	1815.560	96.587	5.63e-22
11	0.075	-	-0.298	-	8	-920.728	1858.329	139.356	2.90e-31
12	-	-	-0.323	-	7	-922.981	1860.636	141.664	9.16e-32
13	0.164	-	-	-0.364	8	-937.123	1891.119	172.146	2.20e-38
14	-	-	-	-0.362	7	-950.651	1915.976	197.003	8.81e-44
15	0.158	-	-	-	7	-957.988	1930.651	211.678	5.74e-47
16	-	-	-	-	6	-970.250	1953.003	234.030	8.03e-52

Table 17: Full model ranking list for *M. myotis* data with Subavg15 variable included.

rank	Subavg15	Dist_LCP	Dist_Roost	Lux	df	logLik	AICc	delta	weight
1	-	-0.406	-0.205	-0.397	9	-849.938	1718.973	0.000	0.609
2	-0.043	-0.426	-0.214	-0.397	10	-849.255	1719.860	0.888	0.391
3	-	-0.478	-	-0.383	8	-867.068	1751.009	32.036	6.73e-8
4	0.001	-0.477	-	-0.383	9	-867.068	1753.233	34.260	2.21e-8
5	-	-0.400	-0.196	-	8	-876.329	1769.531	50.558	6.40e-12
6	-0.050	-0.422	-0.207	-	9	-875.457	1770.012	51.039	5.03e-12
7	-	-0.469	-	-	7	-891.846	1798.366	79.393	3.50e-18
8	-0.007	-0.472	-	-	8	-891.826	1800.525	81.552	1.19e-18
9	0.091	-	-0.301	-0.396	9	-895.869	1810.836	91.863	6.87e-21
10	-	-	-0.335	-0.394	8	-899.344	1815.560	96.587	6.47e-22
11	0.084	-	-0.293	-	8	-920.150	1857.173	138.201	5.95e-31
12	-	-	-0.323	-	7	-922.981	1860.636	141.664	1.05e-31
13	0.185	-	-	-0.373	8	-933.927	1884.727	165.754	6.19e-37
14	-	-	-	-0.362	7	-950.651	1915.976	197.003	1.01e-43
15	0.175	-	-	-	7	-955.632	1925.939	206.966	6.96e-46
16	-	-	-	-	6	-970.250	1953.003	234.030	9.24e-52

Table 18: Full model ranking list of *M. myotis* data with Submax15 variable included.

rank	Submax15	Dist_LCP	Dist_Roost	Lux	df	logLik	AICc	delta	weight
1	-	-0.406	-0.205	-0.397	9	-849.938	1718.973	0.000	0.586
2	-0.047	-0.428	-0.208	-0.397	10	-849.159	1719.668	0.695	0.414
3	-	-0.478	-	-0.383	8	-867.068	1751.009	32.036	6.48e-8
4	-0.035	-0.494	-	-0.383	9	-866.599	1752.296	33.324	3.40e-8
5	-	-0.400	-0.196	-	8	-876.329	1769.531	50.558	6.16e-12
6	-0.051	-0.423	-0.199	-	9	-875.416	1769.930	50.957	5.04e-12
7	-	-0.469	-	-	7	-891.846	1798.366	79.393	3.37e-18
8	-0.040	-0.488	-	-	8	-891.247	1799.366	80.394	2.05e-18
9	0.096	-	-0.313	-0.396	9	-895.616	1810.330	91.358	8.51e-21
10	-	-	-0.335	-0.394	8	-899.344	1815.560	96.587	6.23e-22
11	0.090	-	-0.303	-	8	-919.817	1856.507	137.534	7.99e-31
12	-	-	-0.323	-	7	-922.981	1860.636	141.664	1.01e-31
13	0.152	-	-	-0.368	8	-939.860	1896.592	177.620	1.58e-39
14	-	-	-	-0.362	7	-950.651	1915.976	197.003	9.76e-44
15	0.145	-	-	-	7	-960.673	1936.022	217.049	4.33e-48
16	-	-	-	-	6	-970.250	1953.003	234.030	8.89e-52

Table 19: Full model ranking list of *R. hipposideros* data with Adv15 variable included.

rank	Adv15	Dist_LCP	Dist_Roost	Lux	df	logLik	AICc	delta	weight
1	0.345	-0.737	0.407	-15.829	8	-586.655	1190.552	0.000	1.000
2	0.219	-0.629	-	-19.435	7	-603.242	1221.442	30.890	1.96e-7
3	-	-0.937	0.205	-20.264	7	-608.490	1231.938	41.386	1.03e-9
4	-	-0.832	-	-21.618	6	-613.657	1240.026	49.474	1.81e-11
5	0.455	-	0.155	-15.202	7	-632.628	1280.214	89.662	3.39e-20
6	0.398	-	-	-16.678	6	-635.235	1283.182	92.631	7.68e-21
7	0.464	-0.787	0.662	-	7	-640.052	1295.061	104.509	2.02e-23
8	-	-	-0.209	-21.828	6	-676.671	1366.053	175.502	7.77e-39
9	-	-	-	-20.390	5	-682.978	1376.460	185.909	4.27e-41
10	-	-1.136	0.428	-	6	-682.560	1377.831	187.279	2.15e-41
11	0.284	-0.580	-	-	6	-688.784	1390.280	199.728	4.26e-44
12	0.597	-	0.397	-	6	-690.006	1392.723	202.172	1.26e-44
13	-	-0.916	-	-	5	-706.602	1423.708	233.156	2.35e-51
14	0.455	-	-	-	5	-710.592	1431.687	241.136	4.35e-53
15	-	-	-	-	4	-777.650	1563.633	373.081	9.69e-82
16	-	-	-0.024	-	5	-777.561	1565.625	375.074	3.58e-82

**Table 20: Full model ranking list of *R. hipposideros* data with Subavg15 variable included.**

rank	Subavg15	Dist_LCP	Dist_Roost	Lux	df	logLik	AICc	delta	weight
1	0.322	-0.761	0.418	-15.826	8	-589.689	1196.620	0.000	1.000
2	0.181	-0.662	-	-19.694	7	-606.139	1227.235	30.615	2.25e-7
3	-	-0.937	0.205	-20.264	7	-608.490	1231.938	35.318	2.14e-8
4	-	-0.832	-	-21.618	6	-613.657	1240.026	43.406	3.75e-10
5	0.426	-	0.158	-15.235	7	-638.641	1292.239	95.619	1.72e-21
6	0.365	-	-	-16.764	6	-641.112	1294.935	98.315	4.48e-22
7	0.451	-0.809	0.688	-	7	-641.866	1298.689	102.069	6.86e-23
8	-	-	-0.209	-21.828	6	-676.671	1366.053	169.433	1.61e-37
9	-	-	-	-20.390	5	-682.978	1376.460	179.840	8.88e-40
10	-	-1.136	0.428	-	6	-682.560	1377.831	181.211	4.47e-40
11	0.249	-0.617	-	-	6	-692.002	1396.716	200.096	3.55e-44
12	0.578	-	0.415	-	6	-695.206	1403.124	206.504	1.44e-45
13	-	-0.916	-	-	5	-706.602	1423.708	227.088	4.88e-50
14	0.424	-	-	-	5	-716.309	1443.123	246.502	2.97e-54
15	-	-	-	-	4	-777.650	1563.633	367.013	2.01e-80
16	-	-	-0.024	-	5	-777.561	1565.625	369.005	7.44e-81

**Table 21: Full model ranking list of *R. hipposideros* data with Submax15 variable included.**

rank	Submax15	Dist_LCP	Dist_Roost	Lux	df	logLik	AICc	delta	weight
1	0.163	-0.854	0.301	-17.816	8	-602.754	1222.749	0.000	0.990
2	-	-0.937	0.205	-20.264	7	-608.490	1231.938	9.189	0.010
3	0.081	-0.765	-	-20.670	7	-612.043	1239.043	16.294	2.86e-4
4	-	-0.832	-	-21.618	6	-613.657	1240.026	17.278	1.75e-4
5	0.254	-	-	-17.428	6	-661.057	1334.827	112.078	4.55e-25
6	0.251	-	-0.011	-17.534	7	-661.045	1337.048	114.299	1.50e-25
7	0.295	-0.928	0.570	-	7	-662.217	1339.390	116.642	4.65e-26
8	-	-	-0.209	-21.828	6	-676.671	1366.053	143.305	7.54e-32
9	-	-	-	-20.390	5	-682.978	1376.460	153.712	4.14e-34
10	-	-1.136	0.428	-	6	-682.560	1377.831	155.082	2.09e-34
11	0.167	-0.737	-	-	6	-699.577	1411.866	189.117	8.49e-42
12	-	-0.916	-	-	5	-706.602	1423.708	200.959	2.28e-44
13	0.409	-	0.253	-	6	-728.529	1469.770	247.022	2.27e-54
14	0.338	-	-	-	5	-736.941	1484.386	261.637	1.52e-57
15	-	-	-	-	4	-777.650	1563.633	340.885	9.40e-75
16	-	-	-0.024	-	5	-777.561	1565.625	342.877	3.47e-75



## Eigenständigkeitserklärung

Die unterzeichnete Eigenständigkeitserklärung ist Bestandteil jeder während des Studiums verfassten Semester-, Bachelor- und Master-Arbeit oder anderen Abschlussarbeit (auch der jeweils elektronischen Version).

Die Dozentinnen und Dozenten können auch für andere bei ihnen verfasste schriftliche Arbeiten eine Eigenständigkeitserklärung verlangen.

Ich bestätige, die vorliegende Arbeit selbständig und in eigenen Worten verfasst zu haben. Davon ausgenommen sind sprachliche und inhaltliche Korrekturvorschläge durch die Betreuer und Betreuerinnen der Arbeit.

**Titel der Arbeit** (in Druckschrift):

Challenging the predictive power of flight corridor models for bats

**Verfasst von** (in Druckschrift):

*Bei Gruppenarbeiten sind die Namen aller Verfasserinnen und Verfasser erforderlich.*

**Name(n):**

Meier

**Vorname(n):**

Tina

Ich bestätige mit meiner Unterschrift:

- Ich habe keine im Merkblatt „Zitier-Knigge“ beschriebene Form des Plagiats begangen.
- Ich habe alle Methoden, Daten und Arbeitsabläufe wahrheitsgetreu dokumentiert.
- Ich habe keine Daten manipuliert.
- Ich habe alle Personen erwähnt, welche die Arbeit wesentlich unterstützt haben.

Ich nehme zur Kenntnis, dass die Arbeit mit elektronischen Hilfsmitteln auf Plagiate überprüft werden kann.

**Ort, Datum**

Zürich, 28.10.2019

**Unterschrift(en)**

T. Meier

*Bei Gruppenarbeiten sind die Namen aller Verfasserinnen und Verfasser erforderlich. Durch die Unterschriften bürgen sie gemeinsam für den gesamten Inhalt dieser schriftlichen Arbeit.*